Bi9393 Analytická cytometrie
Lekce 2

Karel Souček, Ph.D.

Oddělení cytokinetiky
Biofyzikální ústav AVČR, v.v.i
Královopolská 135
612 65 Brno

e-mail: ksoucek@ibp.cz
tel.: 541 517 166

Article

The NK cell receptor NKp46 recognizes ecto-calreticulin on ER-stressed cells

https://doi.org/10.1038/s41586-023-05912-0

Received: 13 August 2020

Accepted: 2 March 2023

Published online: 5 April 2023

Check for updates

Sumit Sen Santara[1,2,3,9], Dian-Jang Lee[1,2,9], Ângela Crespo[1,2], Jun Jacob Hu[1,4], Caitlin Walker[1,4], Xiyu Ma[1,2], Ying Zhang[1,2], Sourav Chowdhury[5], Karla F. Meza-Sosa[1,2,6], Mercedes Lewandrowski[1,2], Haiwei Zhang[1,2], Marjorie Rowe[1,2], Arthur McClelland[7], Hao Wu[1,4], Caroline Junqueira[1,2,8]✉ & Judy Lieberman[1,2]✉

Natural killer (NK) cells kill infected, transformed and stressed cells when an activating NK cell receptor is triggered[1]. Most NK cells and some innate lymphoid cells express the activating receptor NKp46, encoded by *NCR1*, the most evolutionarily ancient NK cell receptor[2,3]. Blockage of NKp46 inhibits NK killing of many cancer targets[4]. Although a few infectious NKp46 ligands have been identified, the endogenous NKp46 cell surface ligand is unknown. Here we show that NKp46 recognizes externalized calreticulin (ecto-CRT), which translocates from the endoplasmic reticulum (ER) to the cell membrane during ER stress. ER stress and ecto-CRT are hallmarks of chemotherapy-induced immunogenic cell death[5,6], flavivirus infection and senescence. NKp46 recognition of the P domain of ecto-CRT triggers NK cell signalling and NKp46 caps with ecto-CRT in NK immune synapses. NKp46-mediated killing is inhibited by knockout or knockdown of *CALR*, the gene encoding CRT, or CRT antibodies, and is enhanced by ectopic expression of glycosylphosphatidylinositol-anchored CRT. *NCR1*-deficient human (and *Ncr1*-deficient mouse) NK cells are impaired in the killing of ZIKV-infected, ER-stressed and senescent cells and ecto-CRT-expressing cancer cells. Importantly, NKp46 recognition of ecto-CRT controls mouse B16 melanoma and RAS-driven lung cancers and enhances tumour-infiltrating NK cell degranulation and cytokine secretion. Thus, NKp46 recognition of ecto-CRT as a danger-associated molecular pattern eliminates ER-stressed cells.

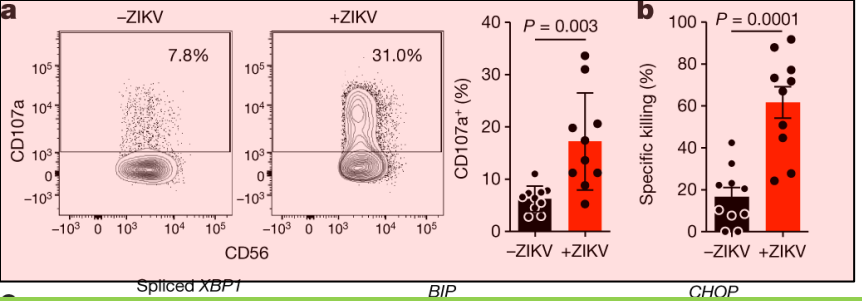

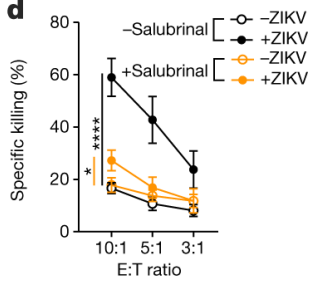

-CD56 is a single transmembrane glycoprotein also known as N-CAM (Neural Cell Adhesion Molecule), Leu-19, or NKH1. It is a member of the Ig superfamily. The 140 kD isoform is expressed on NK cells and NK-T cells. CD56 is also expressed in the brain (cerebellum and cortex) and at neuromuscular junctions.

-lysosomal-associated membrane protein-1 (LAMP-1 or CD107a) has been described as a marker of CD8+ T-cell degranulation following stimulation.

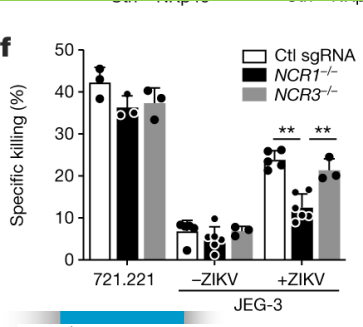

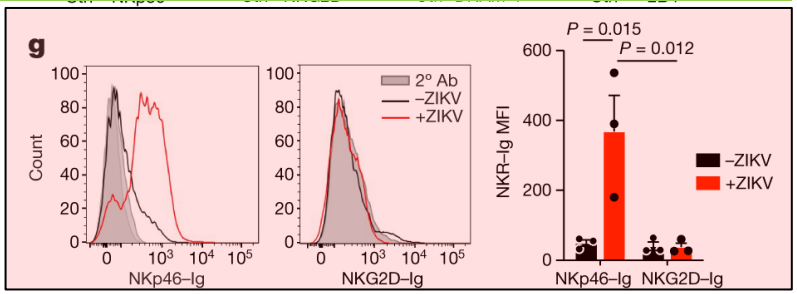

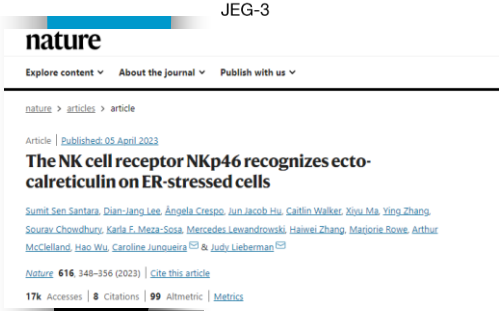
nature

Explore content · About the journal · Publish with us

nature > articles > article

Article | Published: 05 April 2023

The NK cell receptor NKp46 recognizes ecto-calreticulin on ER-stressed cells

Sumit Sen Santara, Dian-Jang Lee, Ángela Crespo, Jun Jacob Hu, Caitlin Walker, Xiyu Ma, Ying Zhang, Sourav Chowdhury, Karla F. Meza-Sosa, Mercedes Lewandrowski, Haiwei Zhang, Marjorie Rowe, Arthur McClelland, Hao Wu, Caroline Jungueira & Judy Lieberman

Nature **616**, 348–356 (2023) | Cite this article

17k Accesses | 8 Citations | 99 Altmetric | Metrics

a, Representative flow cytometry plots (left) and percentage of degranulating NK cells isolated from the blood of ten healthy donors (right), as measured by surface CD107a, in response to uninfected and ZIKV-infected JEG-3 cells (8 h coculture, E:T ratio 1:3). **b**, NK cell-specific killing of uninfected and ZIKV-infected JEG-3 cells. **c**, ER stress, as assessed by *XBP1* splicing (left) and increases in *BIP* (middle) and *CHOP* (right) mRNA, in JEG-3 cells that were uninfected or infected with ZIKV, HSV-2 or human cytomegalovirus (HCMV) for 1–2 days or treated with tunicamycin (Tu) for 1 day. Indicated samples were pretreated with the ER stress inhibitor salubrinal ($n = 3$ samples). mRNA levels, as assayed by quantitative PCR with reverse transcription (RT–qPCR), were normalized to *ACTB*. **d**, Effect of salubrinal pretreatment of target cells on NK cell killing of ZIKV-infected (top) and tunicamycin-treated (bottom) JEG-3 cells ($n = 6$ samples). **e**, Effect of NKR-blocking antibodies (Ab) on NK cell killing of uninfected or ZIKV-infected JEG-3 cells ($n = 3$–7 samples). Ctrl, control. **f**, Specific killing of the classical NK cell target 722.221 cells, or of uninfected or ZIKV-infected JEG-3 cells by human NK cell line YT cells knocked out for *NCR1* or *NCR3* or treated with control single-guide RNAs ($n = 3$–6 samples). **g**, Representative flow cytometry histogram (left) and mean fluorescence intensity (MFI) of NKR–Ig fusion protein (NKp46–Ig and NKG2D–Ig) binding to uninfected or ZIKV-infected JEG-3 cells (right) ($n = 3$ samples). **b**,**d**–**f**, Specific killing assessed by 8 h ^{51}Cr release assay using an E:T ratio of 10:1 unless otherwise indicated. Data are mean ± s.e.m. of at least three independent experiments or technical replicates. Statistics were performed using two-tailed, nonparametric, unpaired *t*-test (**a**,**b**), one-way analysis of variance (ANOVA) (**c**), two-way ANOVA (**e**–**g**) or area under the curve followed by one-way ANOVA (**d**). $^{*}P < 0.05$, $^{**}P < 0.01$, $^{***}P < 0.001$, $^{****}P < 0.0001$.

nature

Explore content ~ About the journal ~ Publish with us ~

nature > articles > article

Article | Published: 05 April 2023

The NK cell receptor NKp46 recognizes ecto-calreticulin on ER-stressed cells

Sumit Sen Santara, Dian-Jang Lee, Ángela Crespo, Jun Jacob Hu, Caitlin Walker, Xiyu Ma, Ying Zhang, Sourav Chowdhury, Karla F. Meza-Sosa, Mercedes Lewandrowski, Haiwei Zhang, Marjorie Rowe, Arthur McClelland, Hao Wu, Caroline Junqueira ✉ & Judy Lieberman ✉

Nature **616**, 348–356 (2023) | Cite this article

17k Accesses | 8 Citations | 99 Altmetric | Metrics

Flow cytometry

For surface staining, cells were stained for 30 min on ice in the dark with LIVE/DEAD-Violet stain (1:1,000) and then with primary antibodies for 15–30 min in PBS and 2% FCS (followed by secondary antibodies, when applicable, for 20 min). For protein–Ig staining, cells were incubated with 50 μg ml^{-1} fusion protein for 1 h at 4 °C and then stained with fluorescent-anti-human IgG for 1 h. Cells were fixed in 1% paraformaldehyde (Affymetrix) for 10 min before flow cytometry. Flow cytometry was assessed on gated live cells (Supplementary Fig. 1). For intracellular staining, cells were fixed and permeabilized using the CytoFix/CytoPerm kit. One of the treated samples was used for isotype staining, and MFI of staining with the isotype control antibody was subtracted from MFI of the specific antibody. Analysis was performed on a FACSCanto II (BD). BD FACSDiva 8.0 (BD) software was used for data collection, with analysis performed using FlowJo v.10.4.2 (TreeStar).

Supplementary Figure 1 | Flow cytometry gating strategy

a. Peripheral blood NK or YT NK cultured with JEG-3.

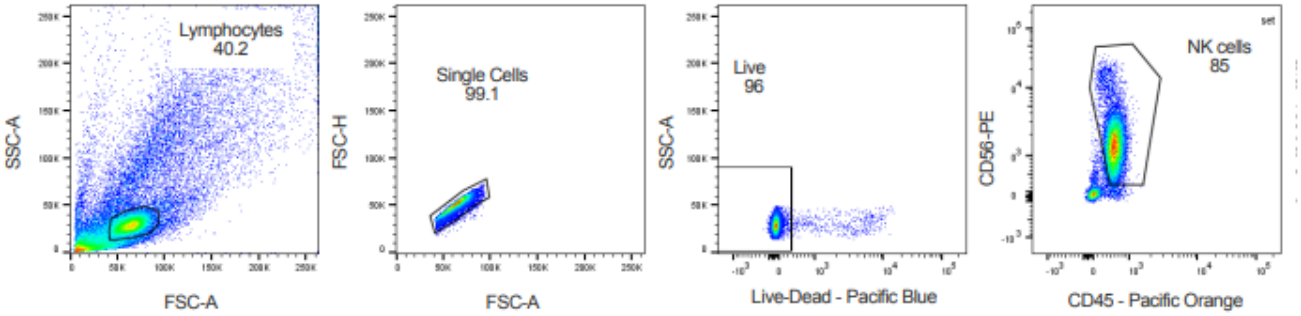

b. Tumor infiltrating lymphocytes (TILs) from tumor-bearing mice

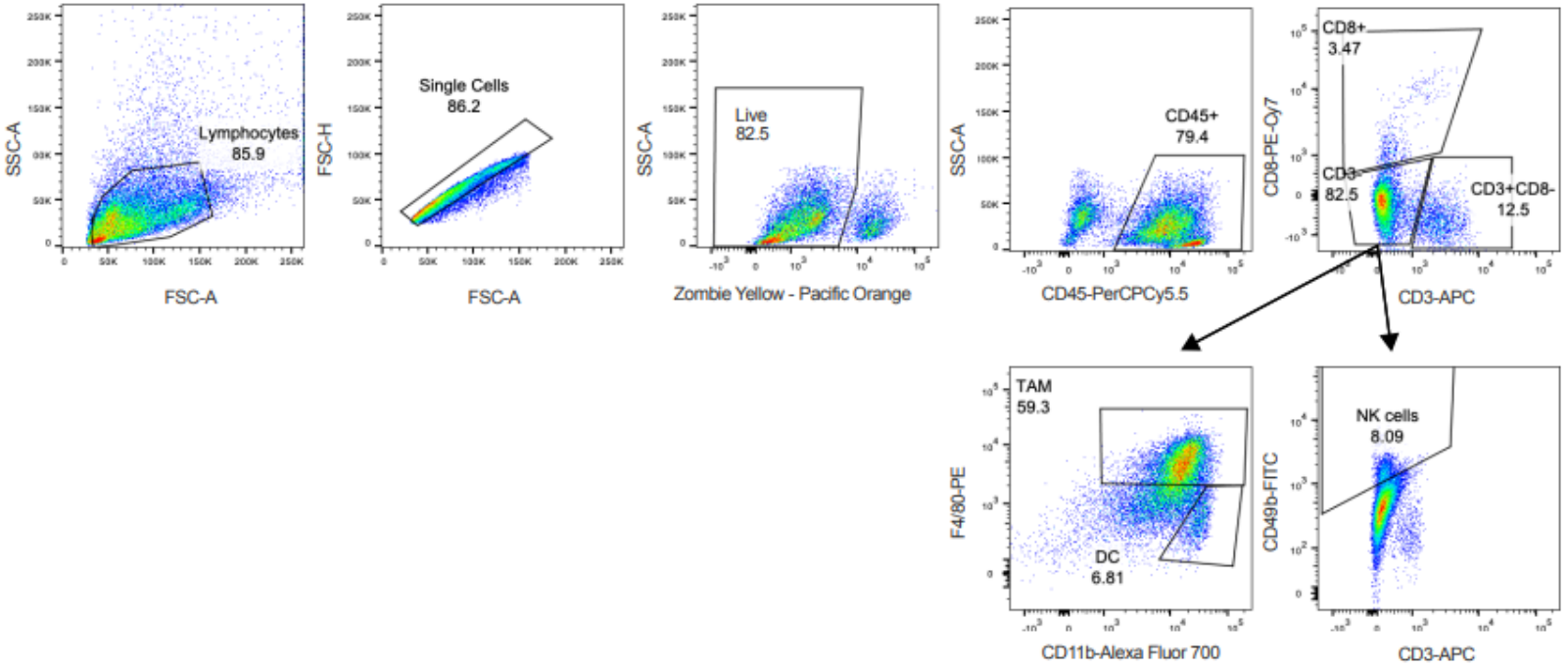

Comment

ILLUSTRATIONS BY DAVID PARKINS

Replication games: how to make reproducibility research more systematic

Abel Brodeur, Anna Dreber, Fernando Hoces de la Guardia & Edward Miguel

In some areas of social science, around half of studies can't be replicated. A new test-fast, fail-fast initiative aims to show what research is hot – and what's not.

In October last year, one of us (A.B.) decided to run an ad hoc workshop at a research centre in Oslo, to try to replicate papers from economics journals. Instead of the handful of locals who were expected to attend, 70 people from across Europe signed up. The message was clear: researchers want to replicate studies.

Replication is sorely needed. In areas of the social sciences, such as economics, philosophy and psychology, some studies suggest that between 35% and 70% of published results cannot be replicated when tested with new data[1–4]. Often, researchers cannot even reproduce results when using the same data and code as the original paper, because key information is missing.

Yet most journals will not publish a replication unless it refutes an impactful paper. In economics, less than 1% of papers published in the top 50 journals between 2010 and 2020 were some type of replication[5]. That suggests that many studies with errors are going undetected.

After the Oslo workshop, we decided to try to make replication efforts in our fields of economics and political science more systematic.

Reprodukovatelnost výsledků

Nature 533, 452–454 (26 May 2016)
doi:10.1038/533452a

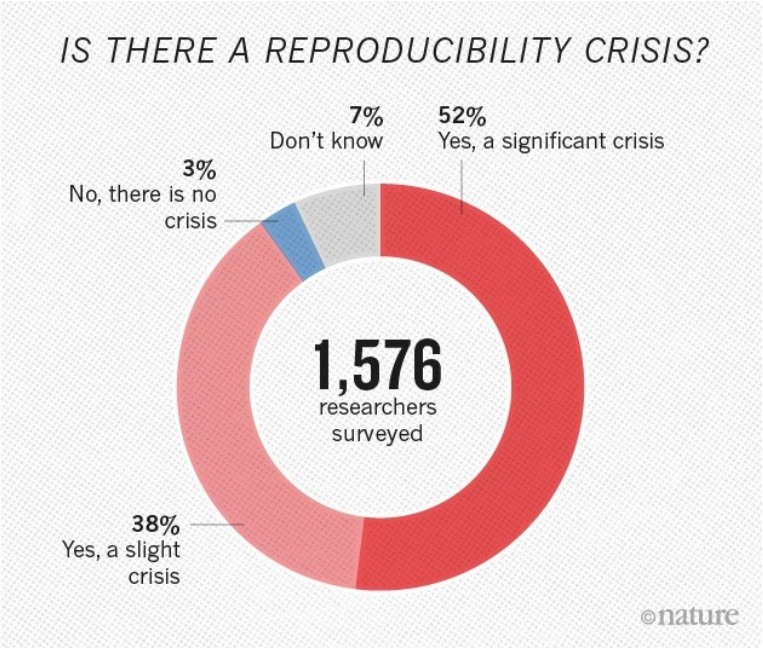

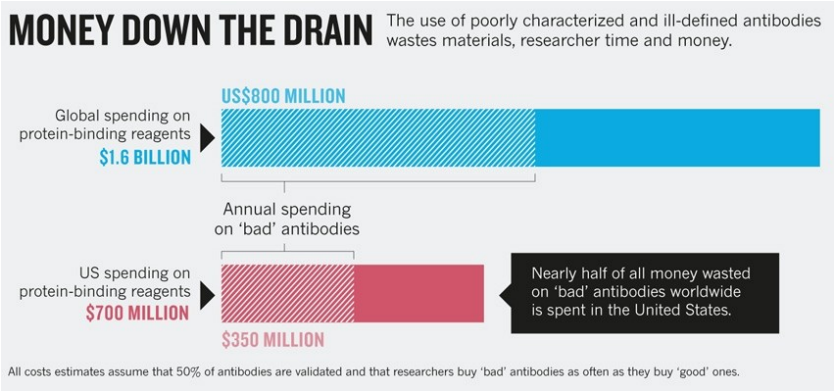

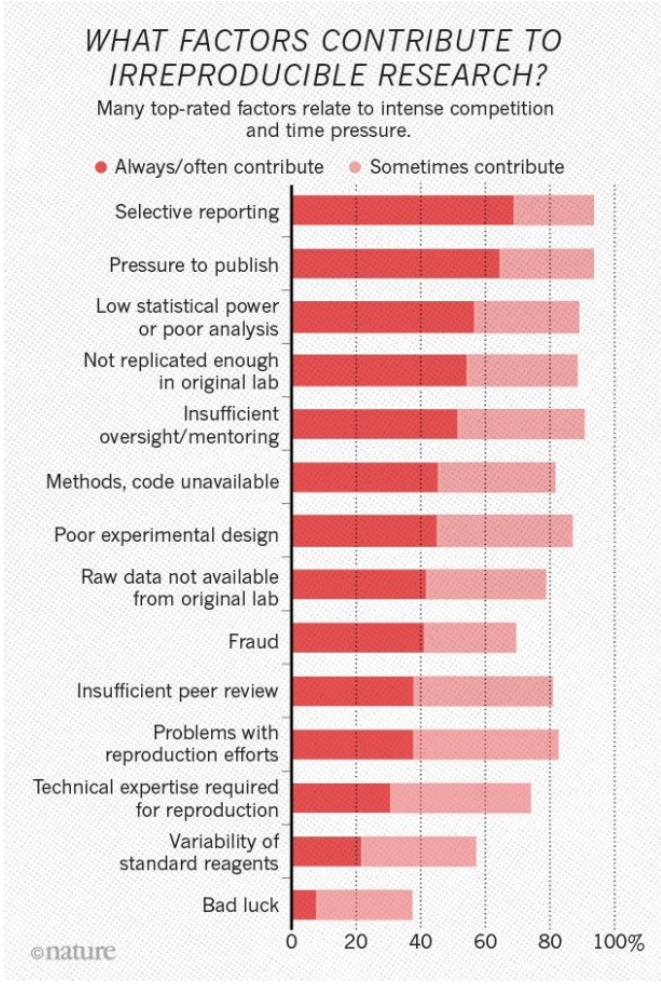

Circ Res. 2015 Jan 2;116(1):116-26. doi: 10.1161/CIRCRESAHA.114.303819.
Reproducibility in science: improving the standard for basic and preclinical research.
Begley CG[1], Ioannidis JP[2].

Nature. 2015 Feb 5;518(7537):27-9. doi: 10.1038/518027a.
Reproducibility: Standardize antibodies used in research.
Bradbury A[1], Plückthun A[2].

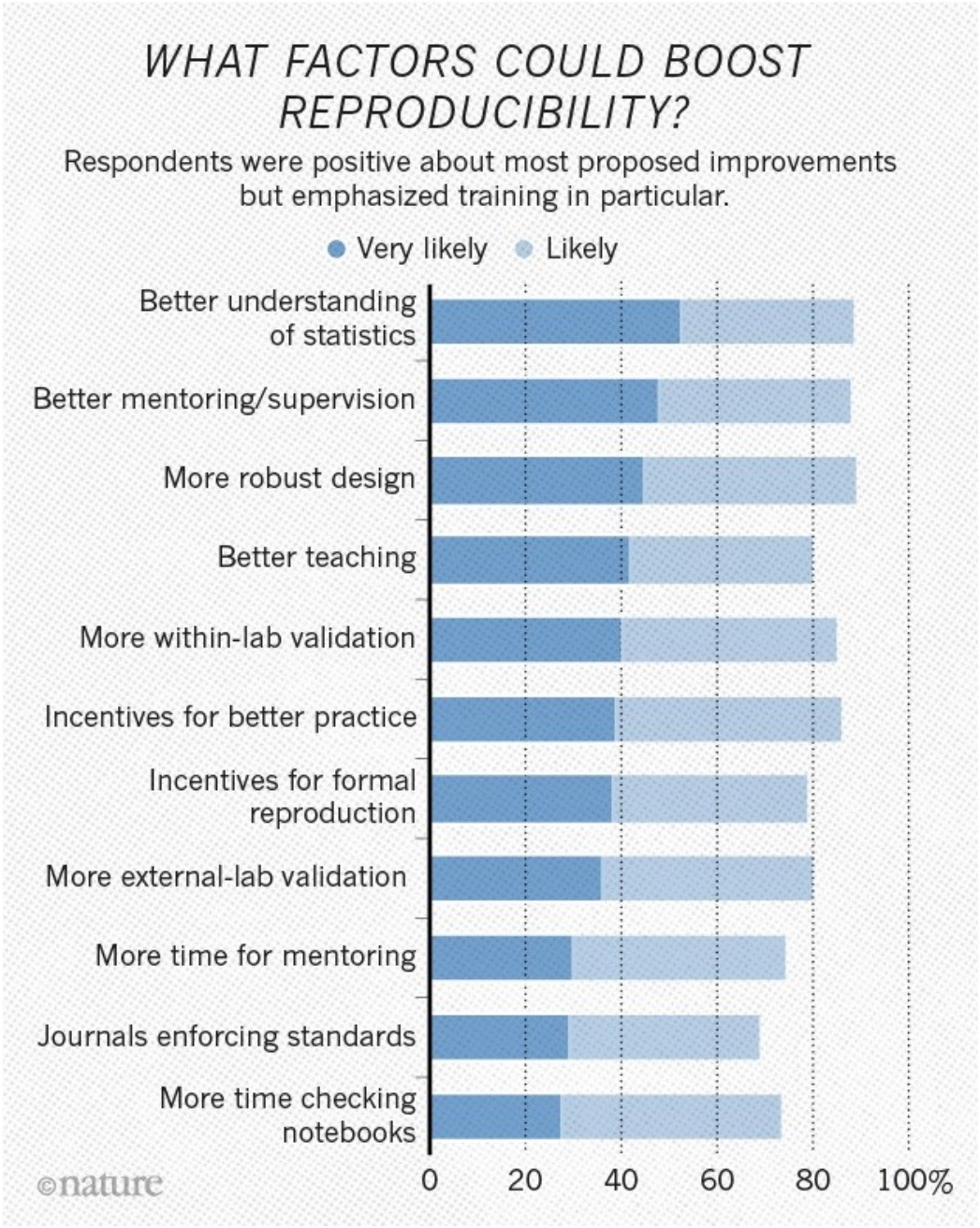
WHAT FACTORS COULD BOOST REPRODUCIBILITY?
Respondents were positive about most proposed improvements but emphasized training in particular.
Very likely
Likely
Better understanding of statistics
Better mentoring/supervision
More robust design
Better teaching
More within-lab validation
Incentives for better practice
Incentives for formal reproduction
More external-lab validation
More time for mentoring
Journals enforcing standards
More time checking notebooks
0
20
40
60
80
100%
©nature

Feature

ILLUSTRATION BY IÑIGO SALMÓN

HOW TO STOP DEEPFAKES FROM SINKING THE INTERNET

Deceptive videos and images created using generative AI could sway elections, crash stock markets and ruin reputations. Researchers are developing methods to limit their harm. **By Nicola Jones**

This June, in the political battle leading up to the 2024 US presidential primaries, a series of images were released showing Donald Trump embracing one of his former medical advisers, Anthony Fauci. In a few of the shots, Trump is captured awkwardly kissing the face of Fauci, a health official reviled by some US conservatives for promoting masking and vaccines during the COVID-19 pandemic.

"It was obvious" that they were fakes, says Hany Farid, a computer scientist at the University of California, Berkeley, and one of many specialists who examined the pictures. On close inspection of three of the photos, Trump's hair is strangely blurred, the text in the background is nonsensical, the arms and hands are unnaturally placed and the details of Trump's visible ear are not right. All are hallmarks – for now – of generative artificial intelligence (AI), also called synthetic AI.

Such deepfake images and videos, made by text-to-image generators powered by 'deep

"PEOPLE'S ABILITY TO REALLY KNOW WHERE THEY SHOULD PLACE THEIR TRUST IS FALLING AWAY."

Scammed science

What can researchers do to limit the impact of fake images on science?

Science isn't immune to the problem of AI-generated fakery. One concern is the integrity of biomedical images such as scans, microscopy images and western blots — a standard technique in which distinctive bands are created by proteins of various molecular weights as they spread across a gel. Fraudsters have long faked such images using Photoshop or other image-manipulation software, but that is often detectable by a trained eye or by computers that check for image duplication. Generating images entirely with AI presents a bigger detection problem.

Last year, Rongshan Yu and his colleagues at Xiamen University, China, created scientific images using synthetic AI to see how easily it can be done[7]. They trained one generative AI program to create new western blot images from a training data set of 3,000 images; and used another to insert features of oesophageal cancer into an image of a non-cancerous intestine. They then tested how convincing the western blots were by inviting three specialists to try to spot one fake in a set of four images; two of the experts performed worse than chance, and the third fared better by spotting a visual clue to do with the smoothness between the image and the background. A computer system did slightly better than the specialists.

In a larger study of 14,000 original western blot images and 24,000 synthetic ones, made using four different generators, Anderson Rocha at the University of Campinas, Brazil, and his colleagues found that AI detectors trained on large data sets achieved accuracies of more than 85% (ref. 8). "This is just the beginning, where we showed it's feasible. It's possible to do way more than that," Rocha says. He and his team have a paper under review that extends their methods beyond western blots, he says.

No one *Nature* spoke to could provide proof that AI is being used by academics to beef up their papers or funding applications, but experts say it's likely. Wael Abd-Almageed, an information scientist and computer engineer at the University of Southern California in Los Angeles, says he knows of specific cases in which academics have used AI to synthesize fakes, but declined to divulge details. Researchers investigating fake paper mills have said they have seen

"I don't k
paper that
illustrate th
Rocha, wh
Retraction
matter of ti

Publishe
chief editor
are certain
race betwe
tools, he sa
well-execu
all too easy
every level

Waterma
Pulverer ac
previously
prevent AI
and prever
says he pla
makers and
discuss the
provenanc

Beyond
tools again
encourage
science. At
could be th

"I don't know any case yet of a retracted paper that used synthetic creation to illustrate the results in that paper," says Rocha, who is working with the blog Retraction Watch on this issue. "But it's just a matter of time, I guess."

A proposal for validation of antibodies

Mathias Uhlen[1], Anita Bandrowski[2], Steven Carr[3], Aled Edwards[4], Jan Ellenberg[5], Emma Lundberg[1], David L Rimm[6], Henry Rodriguez[7], Tara Hiltke[7], Michael Snyder[8] & Tadashi Yamamoto[9]

We convened an *ad hoc* International Working Group for Antibody Validation in order to formulate the best approaches for validating antibodies used in common research applications and to provide guidelines that ensure antibody reproducibility. We recommend five conceptual 'pillars' for antibody validation to be used in an application-specific manner.

Table 1 | Proposed conceptual pillars for validation of antibodies

Validation strategy	Genetic	Orthogonal	Independent antibody	Tagged protein expression	IMS
Validation principle	The expression of the target protein is eliminated or significantly reduced by genome editing or RNA interference	Expression of the target protein is compared with an antibody-independent method	Expression of the target protein is compared using two antibodies with nonoverlapping epitopes	The target protein is expressed using a tag, preferably expressed at endogenous levels	The target protein is captured using an antibody and analyzed using MS
Validation criteria	Elimination or significant reduction in antibody labeling after gene disruption or mRNA knockdown	Significant correlation of protein levels detected by an antibody and an orthogonal method (e.g., MS)	Significant correlation of protein levels detected by two different antibodies recognizing independent regions of the same target protein	Significant correlation between antibody labeling and detection of the epitope tag	Target protein peptides among the most abundant detected by MS following immunocapture
Suitable for these applications	WB, IHC, ICC, FS, SA, IP/ChIP, RP	WB, IHC, ICC, FS, SA, RP	WB, IHC, ICC, FS, SA, IP/ChIP, RP	WB, IHC, ICC, FS	IP/ChIP

WB, western blot; IHC, immunohistochemistry; ICC, immunocytochemistry, including immunofluorescence microscopy; FS, flow sorting and analysis of cells; SA, sandwich assays, including ELISA; IP, immunoprecipitation; ChIP, chromatin immunoprecipitation; and RP, reverse-phase protein arrays.

CST Antibody Validation Principles

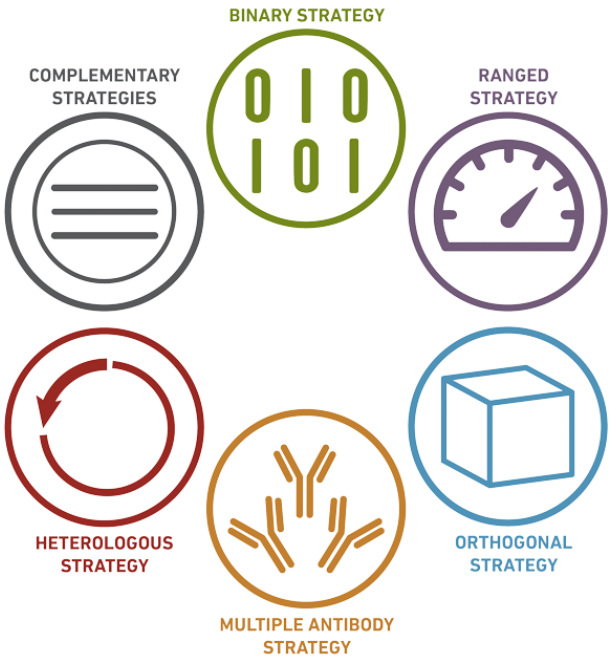

Hallmark Strategy	Description
	Binary Model: Antibody signal is measured in model systems with known presence/absence of target signal. Includes wild-type vs. genetic knockout, targeted induction or silencing.
	Ranged Expression: Antibody signal strength is measured in cell lines or tissues representing a known continuum of target expression levels. Includes siRNA and heterozygous knockout assays.
	Orthogonal Data: Antibody signal is correlated to target expression in model systems measured using antibody independent assays. Includes mass spectrometry and in situ hybridization.
	Multiple Antibodies: Antibody signal is compared to the signal observed using antibodies targeting nonoverlapping epitopes of the target. Includes IP, ChIP, and ChIP-seq.
	Heterologous Expression: Antibody signal is evaluated in cell lines following heterologous expression of native (or mutated) target protein.
	Complementary Assays: Antibody specificity may be validated using complementary assays. Includes competitive ELISA, peptide dot blots, peptide blocking, or protein arrays.

https://www.cellsignal.at/about-us/cst-antibody-validation-principles

Refine Results

Search Within

CLEAR ALL

Category

Research

- Cancer (1)
- Cell Biology (1)
- Fibrosis (4)
- Immunology and Immuno-Oncology (4)
- Metabolism (1)
- Neuroscience (4)
- All Research Areas

Application

- Flow Cytometry (Fixed/Permeabilized) (1)
- Flow Cytometry (Live) (1)
- IHC-paraffin (1)
- Immunofluorescence (Immunocytochemistry) (1)
- Western blot (3)

Products (4) | Content (1)

Sort By: Relevance

#	Product Name	Application	Reactivity	
98327	CD9 (E8L5J) Rabbit mAb	**WB** IP IHC **IF** **F** ChIP	M, R	COMPARE ADD
13403	CD9 (D3H4P) Rabbit mAb	**WB** IP **IHC** IF F ChIP	H	COMPARE ADD
13174	CD9 (D8O1A) Rabbit mAb	**WB** IP IHC IF F ChIP	H	COMPARE ADD
74220	Exosomal Marker Antibody Sampler Kit			ADD

Results per page: 30 60 100 200

Revision 3

Store at -20C

#98327

CD9 (E8L5J) Rabbit mAb

Cell Signaling TECHNOLOGY®

Orders: 877-616-CELL (2355)
orders@cellsignal.com

Support: 877-678-TECH (8324)

Web: info@cellsignal.com
www.cellsignal.com

3 Trask Lane | Danvers | Massachusetts | 01923 | USA

For Research Use Only. Not For Use In Diagnostic Procedures.

Applications:	Reactivity:	Sensitivity:	MW (kDa):	Source/Isotype:	UniProt ID:	Entrez-Gene Id:
WB, IF-IC, FC-FP, FC-L	M R	Endogenous	22-27	Rabbit IgG	P40240	12527

Product Usage Information

Application	Dilution
Western Blotting	1:1000
Immunofluorescence (Immunocytochemistry)	1:50
Flow Cytometry (Fixed/Permeabilized)	1:50 - 1:200
Flow Cytometry (Live)	1:50 - 1:200

Storage

Supplied in 10 mM sodium HEPES (pH 7.5), 150 mM NaCl, 100 µg/ml BSA, 50% glycerol and less than 0.02% sodium azide. Store at –20°C. *Do not aliquot the antibody.*

Specificity / Sensitivity

CD9 (E8L5J) Rabbit mAb recognizes endogenous levels of total CD9 protein.

Species Reactivity:
Mouse, Rat

Source / Purification

Monoclonal antibody is produced by immunizing animals with a synthetic peptide corresponding to residues surrounding Leu119 within the extracellular domain of mouse CD9 protein.

Background

The CD9 antigen belongs to the tetraspanin family of cell surface glycoproteins, and is characterized by four transmembrane domains, one short extracellular domain (ECL1), and one long extracellular domain (ECL2). Tetraspanins interact with a variety of cell surface proteins and intracellular signaling molecules in specialized tetraspanin-enriched microdomains (TEMs), where they mediate a range of processes including adhesion, motility, membrane organization, and signal transduction (1). Research studies demonstrate that CD9 expression on the egg is required for gamete fusion during fertilization (2-4). CD9 was also shown to play a role in dendritic cell migration, megakaryocyte differentiation, and homing of cord blood CD34+ hematopoietic progenitors to the bone marrow (5-7). In addition, downregulation of CD9 expression is associated with poor prognosis and progression of several types of cancer (8-10). Additional research identified CD9 as an abundant component of exosomes, and may play some role in the fusion of these secreted membrane vesicles with recipient cells (11).

1. Hemler, M.E. (2005) *Nat Rev Mol Cell Biol* 6, 801-11.
2. Le Naour, F. et al. (2000) *Science* 287, 319-21.
3. Miyado, K. et al. (2000) *Science* 287, 321-4.
4. Kaji, K. et al. (2000) *Nat Genet* 24, 279-82.
5. Mantegazza, A.R. et al. (2004) *Blood* 104, 1183-90.
6. Clay, D. et al. (2001) *Blood* 97, 1982-9.
7. Leung, K.T. et al. (2011) *Blood* 117, 1840-50.
8. Miyake, M. et al. (1995) *Cancer Res* 55, 4127-31.
9. Higashiyama, M. et al. (1995) *Cancer Res* 55, 6040-4.
10. Uchida, S. et al. (1999) *Br J Cancer* 79, 1168-73.
11. Théry, C. et al. (1999) *J Cell Biol* 147, 599-610.

Revision 3

#98327

CD9 (E8L5J) Rabbit mAb

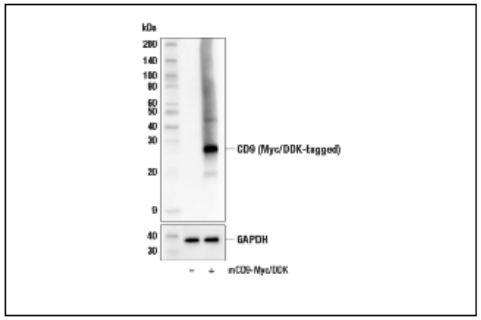

Western blot analysis of extracts from 293T cells, mock transfected (-) or transfected with a construct expressing Myc/DDK-tagged full-length mouse CD9 protein (mCD9-Myc/DDK; +), using CD9 (E8L5J) Rabbit mAb (upper) and GAPDH (D16H11) XP® Rabbit mAb #5174 (lower).

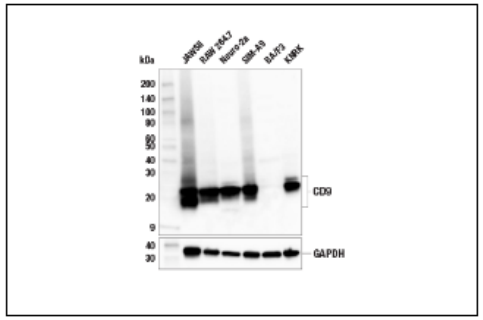

Western blot analysis of extracts from various cell lines using CD9 (E8L5J) Rabbit mAb (upper) and GAPDH (D16H11) XP® Rabbit mAb #5174 (lower). Absence of signal in BA/F3 cells is predicted from RNAseq data and confirms the specificity of the antibody.

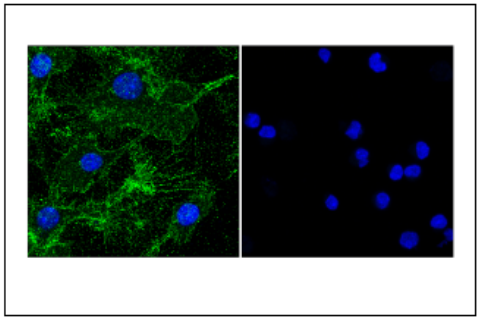

Confocal immunofluorescent analysis of RAW 264.7 cells (left, positive) or BA/F3 cells (right, negative) using CD9 (E8L5J) Rabbit mAb (green) and DAPI #4083 (blue).

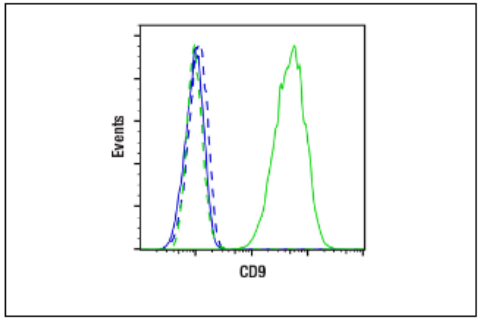

Flow cytometric analysis of live BA/F3 cells (blue, negative) and JAWSII cells (green, positive) using CD9 (E8L5J) Rabbit mAb (solid lines) or concentration-matched Rabbit (DA1E) mAb IgG XP® Isotype Control #3900 (dashed lines). Anti-rabbit IgG (H+L), F(ab')$_2$ Fragment (Alexa Fluor® 488 Conjugate) #4412 was used as a secondary antibody.

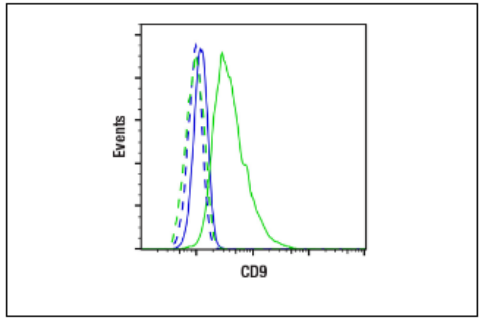

Flow cytometric analysis of fixed and permeabilized BA/F3 cells (blue, negative) and JAWSII cells (green, positive) using CD9 (E8L5J) Rabbit mAb (solid lines) or concentration-matched Rabbit (DA1E) mAb IgG XP® Isotype Control #3900 (dashed lines). Anti-rabbit IgG (H+L), F(ab')$_2$ Fragment (Alexa Fluor® 488 Conjugate) #4412 was used as a secondary antibody.

Comment

Reproducibility: expect less of the scientific paper

Olavo B. Amaral & Kleber Neves

Make science more reliable by placing the burden of replicability on the community, not on individual laboratories.

In 2018, we embarked on a journey to assess the reproducibility of biomedical research papers from Brazil. Thus began a multicentre collaboration of more than 60 laboratories to replicate 60 experiments from 2 decades of Brazilian publications[1]. We randomly selected experiments that used three common laboratory techniques: the MTT assay for cell viability, RT-PCR to measure specific messenger RNAs and the elevated plus maze to assess anxiety in rodents.

Each experiment will be repeated in three labs, and each lab has developed replication protocols based on the original article's written methods. The process of building, reviewing and preregistering these protocols has taken months of communication between the coordinating team and the labs performing replications. We had intense arguments around the meaning of positive and negative controls and the merits of different metrics to define replication success. We also spent many hours on mundane tasks, such as studying the nutritional content of different brands of bologna sausage to better emulate a cafeteria diet fed to rats in one experiment.

These are just some of the obstacles we

Dostupná technologie

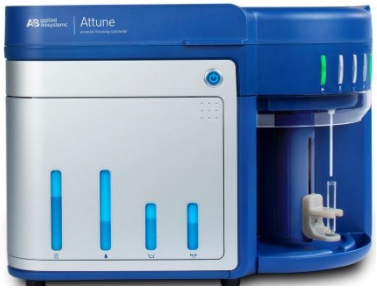

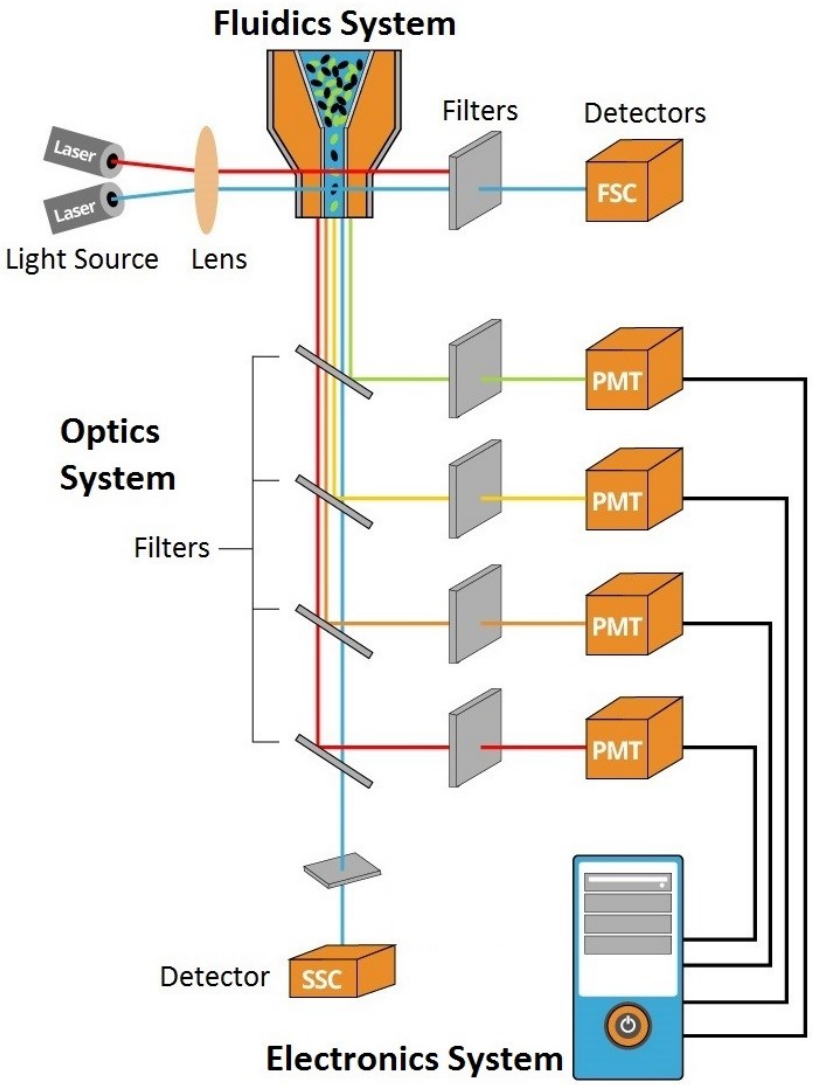

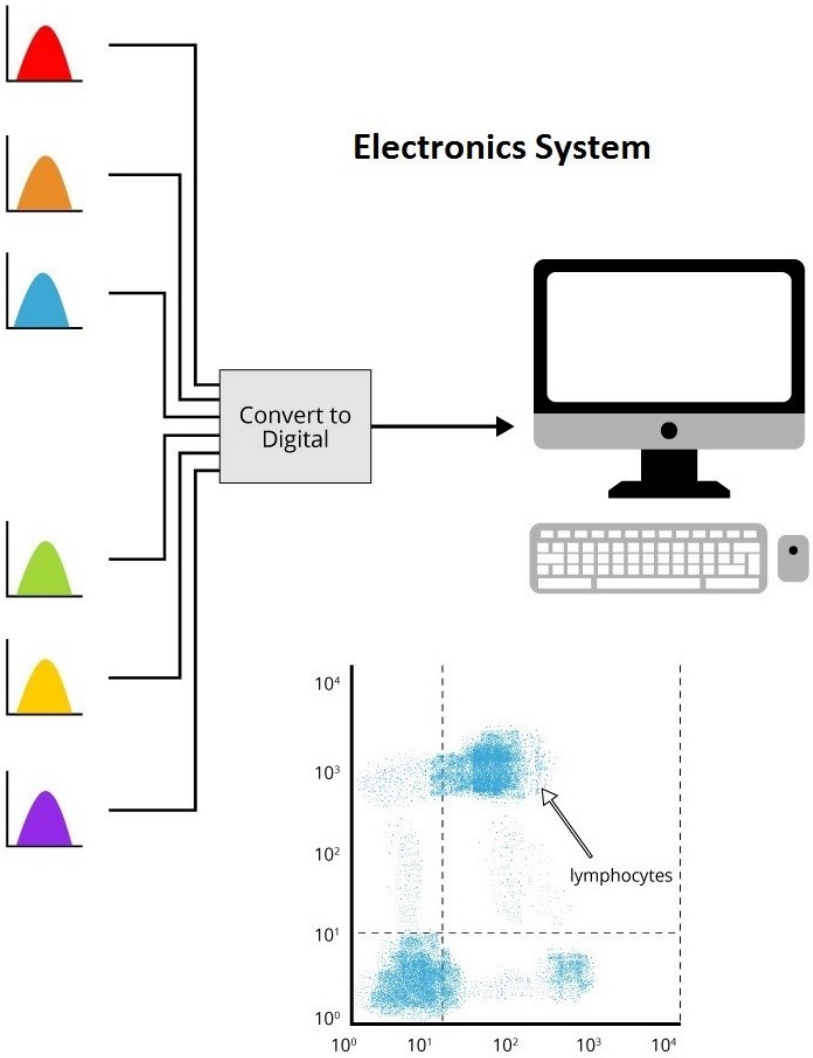

https://www.bosterbio.com/protocol-and-troubleshooting/flow-cytometry-principle

new automatic cell cloning assay (ACCA) for determination of clonogenic capacity of CSCs

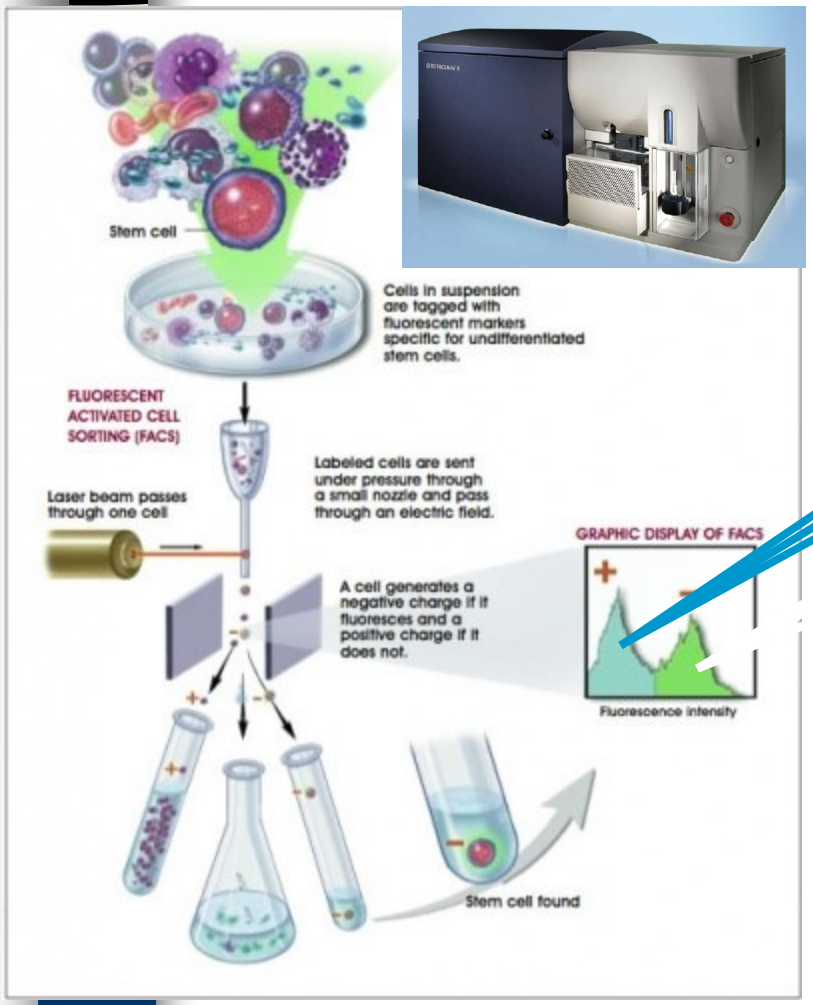

single cell/well
up to 384 well plate

re-culture after sorting (2D, 3D)

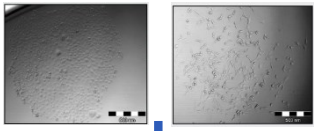

analysis: CyQuant, ATP, xCelligence, microscopy

Principy průtokové cytometrie a sortrování

- Světlo
- Fluorescence
- Zdroje excitace, optické systémy a způsoby detekce fluorescence
- Fluidní systémy

Pojmy

Fotometrie:

- **Světlo** – elektromagnetické záření viditelné lidským okem (400-750 nm, nejcitlivější ~ 550 nm). Při měření pod 400 nm (UV, IF) se jedná detekci záření (radiometrie).
- Energie záření se vyjadřuje v *joulech*
- Světelný tok (**radiant flux)** je udávána jako hodnota energie v čase ve *wattech* (1 watt= 1 joule/sekundu)
- foton – elementární částice. Popisuje je jejich vlnová délka, frekvence, energie a hybnost. Životnost fotonu je nekonečná (přesto vznikají a zanikají), existují pouze v pohybu. Má nulovou klidovou hmotnost, ale nenulovou energii, definovanou vztahem E = hv, kde **h** je Planckova konstanta a **v** frekvence. Neboť má energii, působí na něj gravitace dle obecné teorie relativity a on sám gravitačně působí na okolí. (http://cs.wikipedia.org/wiki/Foton)
- Energie fotonu je vyjádřena jako $E=h\nu$ a $E=hc/\lambda$ [ν-frequency (Hz), c – rychlost světla ($3x10^8$ m/s), λ-wavelength (nm), h-Planckova konstanta (6.63×10^{-34} J/s)]
- **Energie** je vyšší při kratších vlnových délkách a nižší při delších vlnových délkách.

Elektromagnetické spektrum

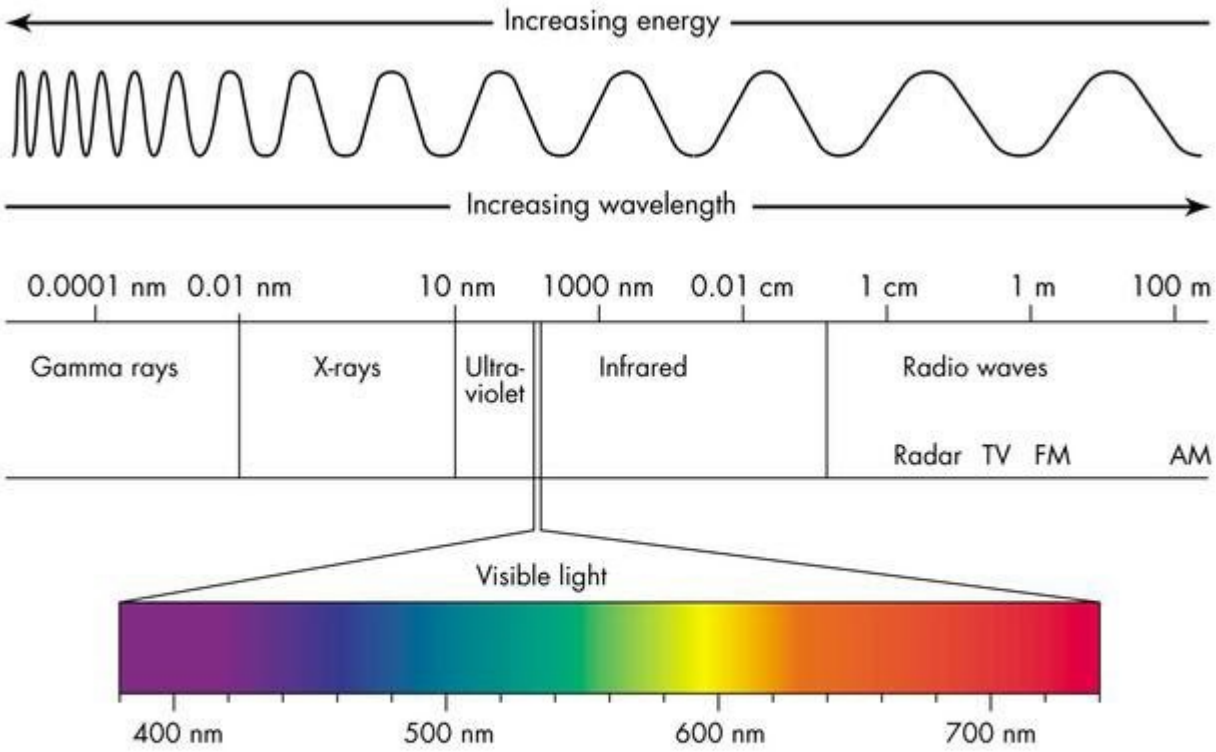

Rozptyl světla

- Hmota rozptyluje světlo vlnových délek které není schopna absorbovat
- Viditelné spektrum je 350-850 nm proto malé částice a molekuly (< 1/10 λ) spíše viditelné světlo rozptylují
- Pro malé částice byl popsán tzv. Rayleightův rozptyl (scatter) jehož intenzita je ~ stejná všemi směry
- Rozptyl větších částic charakterizuje tzv. Mieův rozptyl. Jeho množství je větší ve směru v jakém dopadá světlo na ozářenou částici ⇨ *na tomto principu je založeno měření velikosti částic pomocí průtokového cytometru*

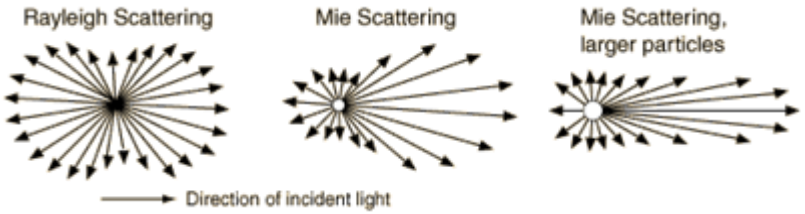

http://hyperphysics.phy-astr.gsu.edu/hbase/atmos/blusky.html

Shapiro p.106

Rayleightův a Mieův rozptyl

- Rayleightův rozptyl – molekuly a velmi malé částice neabsorbují, ale rozptylují světlo které má menší vlnovou délku než je jejich velikost (modré nebe - vzduch rozptyluje lépe kratší vlnové délky)
- Mieův rozptyl je charakteristický pro částice větší než je vlnová délka světla (bílá záře kolem slunečního kotouče, mlžné světlo)

http://hyperphysics.phy-astr.gsu.edu/hbase/atmos/blusky.html

Ohyb a rozklad světla

Krátké vlnové délky jsou
“ohnuty” více než dlouhé

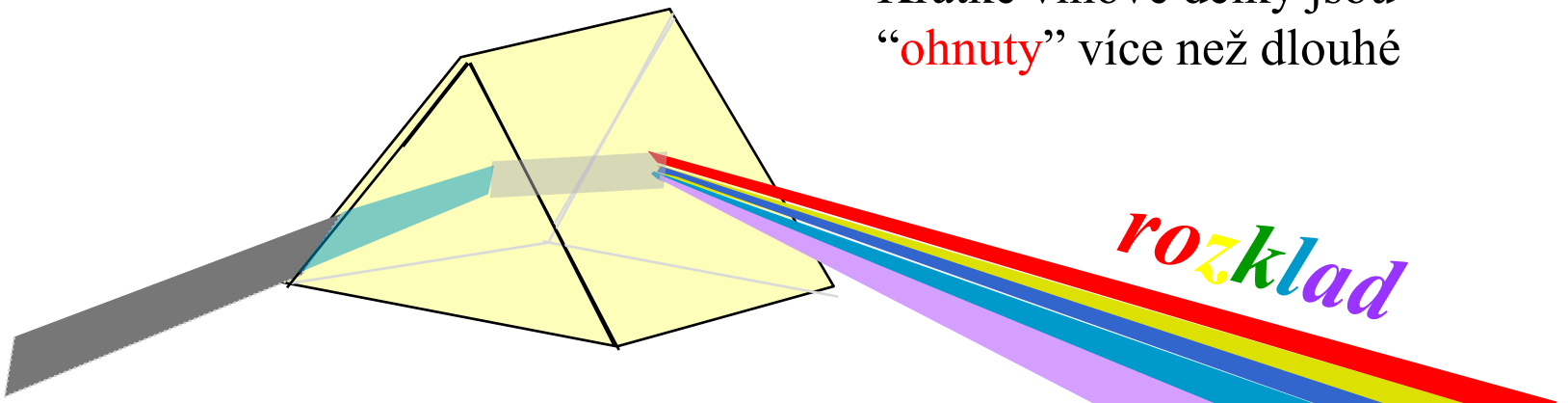

Fluorescence

https://en.wikipedia.org/wiki/Tonic_water

George Gabriel Stokes (1819 – 1903)

Anglický fyzik a matematik
působící na univerzitě v Cambridge

http://www.nndb.com/people/131/000097837/

1852 – popsal fluorescenci
Název vznikl z anglického slova *fluospar*
(fluorit, kazivec = nerost CaF_2)
- ke svému pozorování použil roztok chininu, jako zdroj světla sluneční paprsky, jako excitační filtr sloužilo tmavě modré okenní sklo a jako emisní filtr byla použita sklenice bílého vína

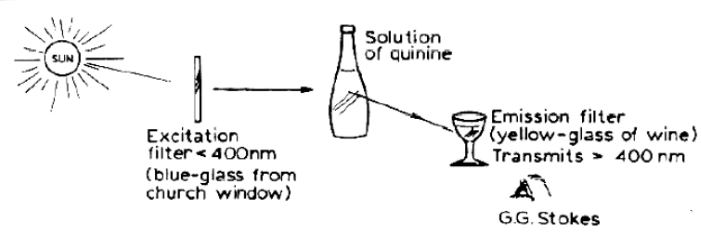

G. C. Stokes „*On the Change of Refrangibility of Light*“ Philosophical Transactions of the Royal Society of London, 1852, vol. 142, p. 463.)

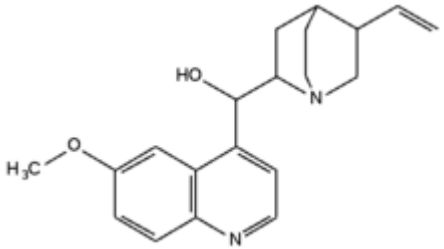

[463]

XXX. *On the Change of Refrangibility of Light.* *By* G. G. Stokes, *M.A., F.R.S., Fellow of Pembroke College, and Lucasian Professor of Mathematics in the University of Cambridge.*

Received May 11,—Read May 27, 1852.

Princip fluorescence

<u>Fluorescence</u> (patří mezi fotoluminiscenční záření, které je vyvoláno buď účinkem jiného dopadajícího záření, nebo účinkem dopadajících částic) je výsledek tří fázového u jevu některých chemickýc látek - **fluorochromů**, fluorescenčních barev.

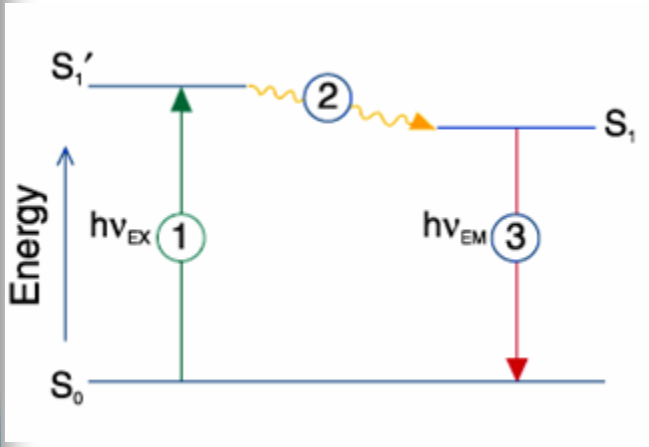

Jablonski diagram

Fáze 1: Excitace

- Záření z externího zdroje (např. laser) excituje fluorofor.
- Tím vzniká excitovaný stav (S1').

Fáze 2: Životnost vzrušeného stavu

- Vzrušený stav trvá chvíli (1–10^-9 sekundy).
- Fluorofor může procházet změnami a interakcemi.
- Ztrácí část energie, vzniká uvolněný excitovaný stav (S1).
- Některé molekuly nevrací energii formou fluorescenčního záření.
- To ovlivňuje fluorescenční kvantový výtěžek.

Fáze 3: Fluorescenční záření

- Fluorofor emituje foton a vrátí se do základního stavu (S0).
- Energie emitovaného fotonu (hvEM) je nižší a má delší vlnovou délku než excitační foton (hvEX).
- Rozdíl se nazývá Stokesův posun a je klíčový pro citlivost fluorescenčních technik.

Charakteristiky fluorescence

- **intenzita** – počet fotonů procházejících v daném směru jednotkovou plochou za jednotku času
- **spektrální složení** – spektrální hustota fotonového toku na jednotkový interval vlnových délek nebo frekvencí
- **polarizace** – směr kmitání elektrického vektoru elektromagnetické vlny
- **doba dohasínání** – je dána vnitřní dobou života excitovaného stavu, z něhož dochází k emisi; úzce souvisí s pochody vedoucími k nezářivé deaktivaci tohoto stavu
- **koherenční vlastnosti** – vztahy mezi fázemi světelných vln

Fluorescenční spektra

Fluorescenční proces je cyklický.
Kromě fluorochromu nevratně zničeného (photobleaching - „vysvícení“) může být opakovaně excitován.

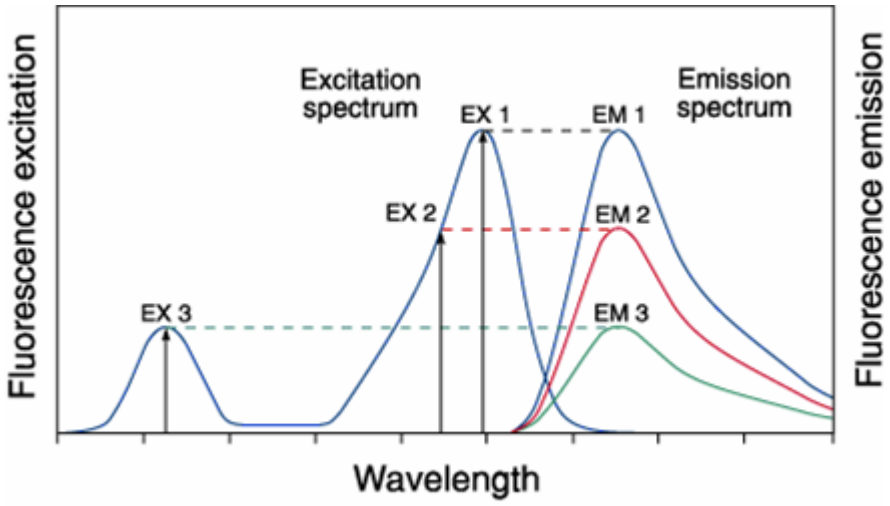

Excitation of a fluorophore at three different wavelengths (EX 1, EX 2, EX 3) does not change the emission profile but does produce variations in fluorescenceemission intensity (EM 1, EM 2, EM 3) that correspond to the amplitude of the excitation spectrum.

Fluorescenční barviva

- Fluorescenční barviva (fluorofory, fluorochromy) jsou chemické sloučeniny, které obsahují ve své molekule reaktivní skupinu, která je schopna reagovat s nukleofilními skupinami (NH_2, OH, SH).

- Obecně se fluorofory dělí na vnitřní (vlastní, intrinsic) a vnější (nevlastní, extrinsic).

Vnitřní fluorescence

- Vnitřní fluorescence buněk je dána přítomností vnitřních fluoroforů, mezi které patří proteiny, redukované formy NADH a NADPH, vitamin A, cytochromy, peroxidáza, hemoglobin, myoglobin či chlorofyl.

- Proteiny vyzařují fluorescenční záření v UV oblasti spektra. Hlavními fluorofory v proteinech jsou aromatické aminokyseliny (fenylalanin, tryptofan, tyrosin), jejichž absorpční i emisní pás leží mezi 240 a 300nm.

- Ostatní uvedené látky vyzařují ve viditelné oblasti spektra (modrá, žlutá či červená).

Vnější fluorescence

- Vnější fluorofory jsou používány mnohem častěji než vnitřní.
- Jsou přidávány ke studovanému vzorku a podle typu vazby jsou děleny na fluorescenční značky a fluorescenční sondy.

Fluorescenční značky

- Nejčastěji se používají k fluorescenčnímu značení proteinů, ke kterým se vážou kovalentní vazbou.

- Nejznámějšími fluorescenčními značkami jsou FITC (fluorescein-5-isothiokyanát) a TRITC (tetramethylrhodamin-5-isothiokyanát, tetramethylrhodamin-5-isothiokyanát).

Fluorescenční sondy

- vnější fluorofory, které se váží ke struktuře nekovalentní vazbou a často při tom mění své fluorescenční vlastnosti. Tyto fluorofory jsou používány ke studiu změn konformace bílkovin, tloušťky membrán, membránového potenciálu apod.

- K identifikaci a vizualizaci nukleových kyselin se používá řada fluorescenčních sond (např: akridinová oranž, ethidium bromid, DAPI a další).

- Nejznámější a také nejpoužívanější fluorescenční sondou pro vizualizaci veškeré jaderné DNA je DAPI. Chemicky se jedná o 4',6-Diamidino-2-fenylindol. Jeho absorpční maximum je při 345 nm, maximální fluorescence je při 455 nm (modrý fluorofor

- Dalším často používaným fluoroforem je akridinová oranž. Jedná se o fluorescenční sondu, jejíž absorpční a emisní pásma se liší podle substrátu, ke kterému je vázána DNA/RNA. Obě jmenované jsou většinou dodávány v podobě chloridových solí.

Detekce fluorescence

Vybavení pro fluorescenci

(1) zdroj excitace
(2) fluorochrom
(3) vlnové filtry pro izolaci emitovaných fotonů od excitovaných
(4) detektory pro registraci emitovaných fotonů

Fluorescenční přístroje

- spektrofluorometer měří průměrné vlastnosti objemu vzorku v kyvetě.
- fluorescenční mikroskop popisuje fluorescenci jako jev v prostorovém systému souřadnic
- flow cytometer měří fluorescenci v proudícím toku, umožňuje detekovat a kvantivikovat subpopulace uvnitř velkého vzorku

Fluorescenční signál

- spektrofluorometer je flexibilní, umožňuje měřit v kontinuálním spektru excitačních a emisních vlnových délek
- flow cytometr potřebuje fluorescenční značky excitovatelné
určitou vlnovou délkou.

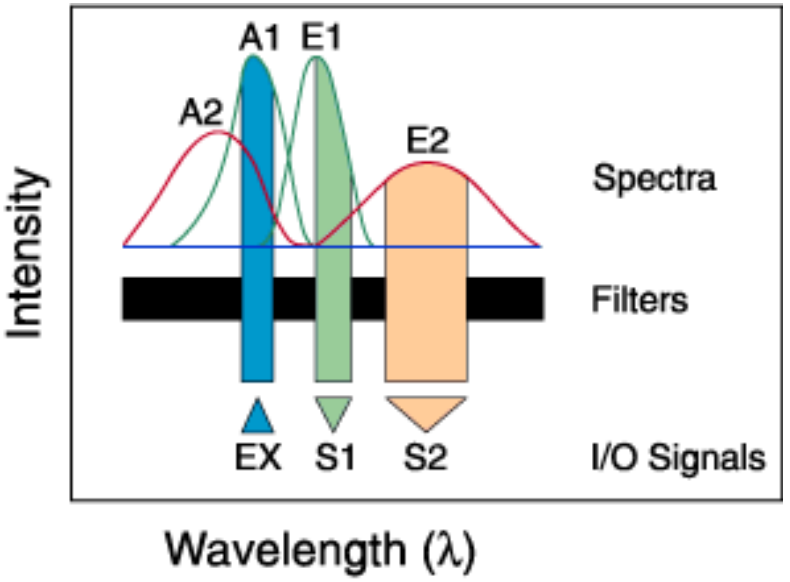

Fluorescence pozadí

- endogení složky - autofluorescence
- nenávazané nebo nespecificky vázané značky
= reagenční pozadí

Vícebarevné značení

- dvě a více značek, zároveň monitoruje různé funkce
- nutné: vhodně zvolit značky zdroj excitace a separační filtry

Fluorescence Output of Fluorophores
Comparing Different Dyes

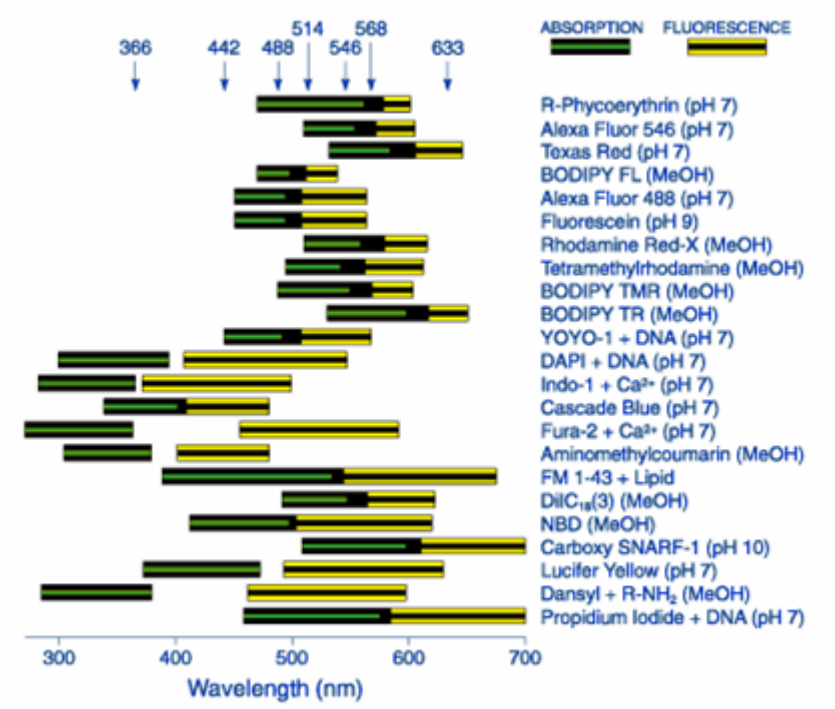

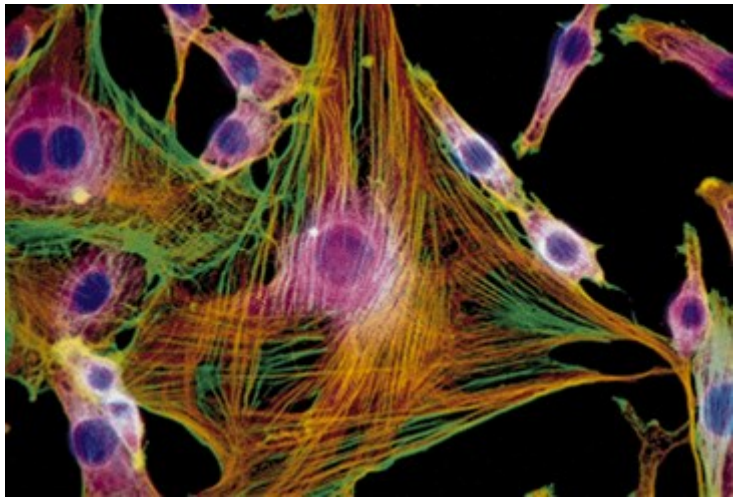

Mouse 3T3

F-actin ~
BODIPY FL phallacidin

anti-ß tubulin ~
Texas Red
goat anti–mouse IgG

DNA ~
DAPI

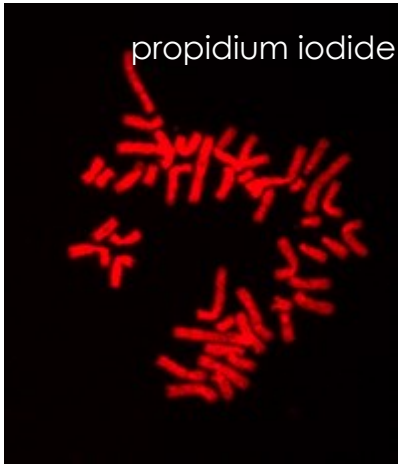

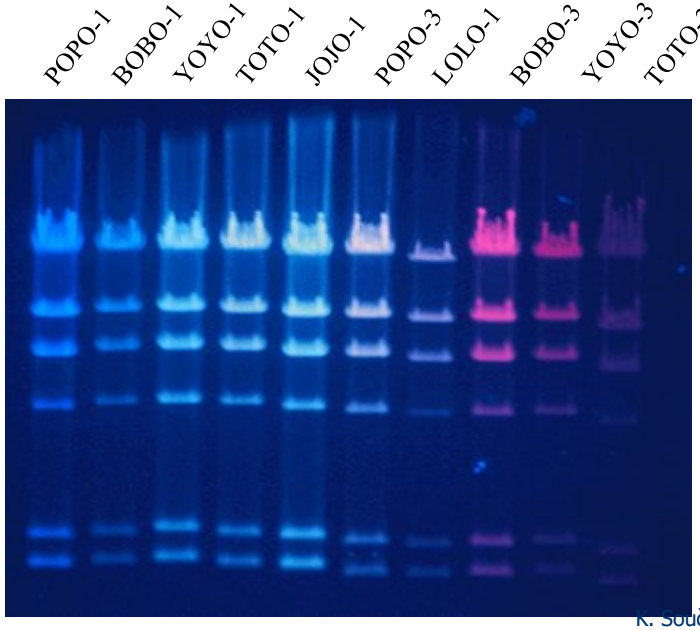

λ Hind III

Fluorochrome chart

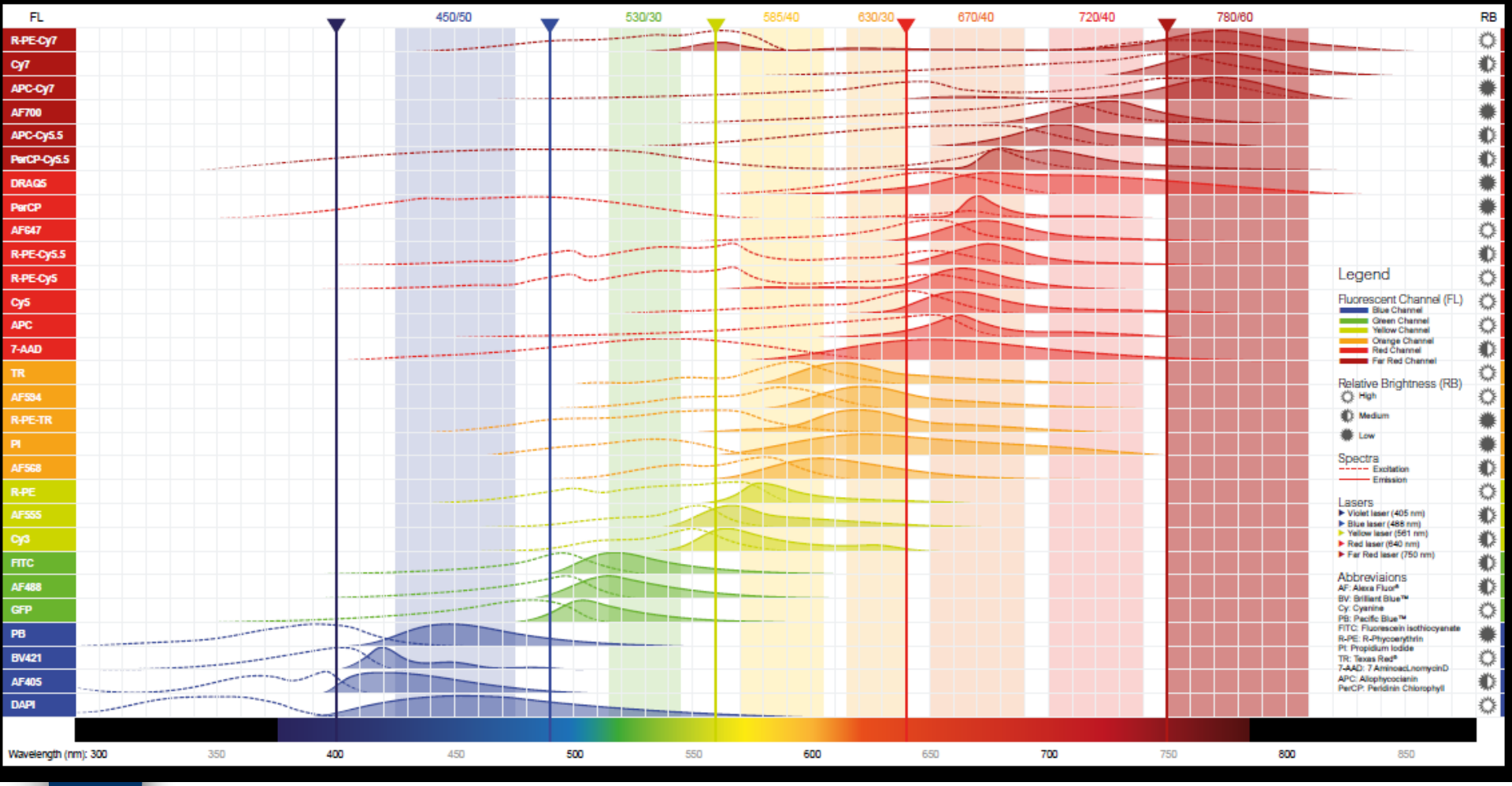

abcam®
discover more

Procesy interferující a detekcí fluorescence

- Quenching - „zhášení“ fluorescence pomocí polárních rozpouštědel, těžkých iontů.
- Bleaching – změna struktury fluorescenční molekuly vedoucí ke ztrátě fluorescence (působením světla a nebo chemickou interakcí.
- Photon saturation – stav kdy množství molekul v excitovaném stavu odpovídá množství molekul v bazální hladině

Photobleaching

- irreversible destruction or photobleaching of the excited fluorophore

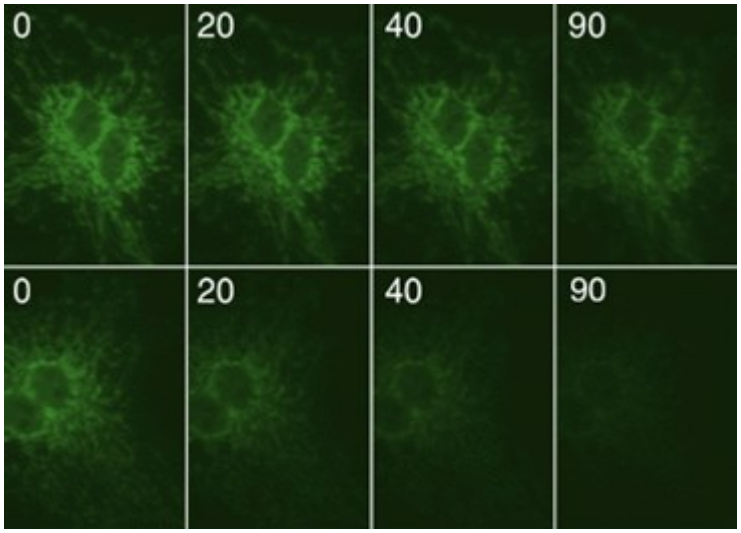

anti–human cytochrome oxidase subunit I

Oregon Green 514 goat anti–mouse IgG

fluorescein goat anti–mouse IgG

Molecular Probes

Základ průtokové cytometrie

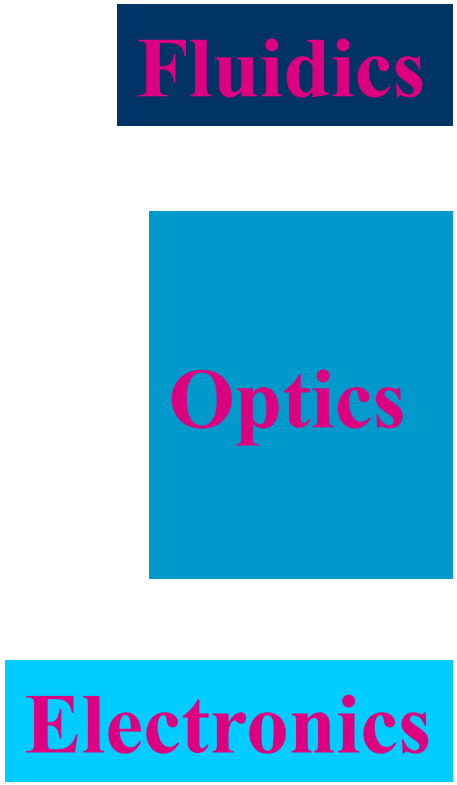

Buňky v suspenzi

protékají jednotlivě napříč

osvětlenou částí kde

rozptylují světlo a emitují fluorescenci,

která je detekována, filtrována a

převedena na digitální hodnoty

uložené do počítače

Optika - zdroj světla

- nutnost zaostřit zdroj světla na stejné místo, kde je zaostřen průtok buněk
- Lasery
  - produkují jednotlivou vlnovou délku světla (325, 488, ~630nm)
  - poskytují mW - W světla
  - mohou být “levné” - air-cooled , nebo drahé - water-cooled
  - poskytují koherentní světelný proud
- Obloukové lampy (Arc-lamps)
  - produkují směs vlnových délek, které musí být filtrovány
  - poskytují mW světla
  - levné - air-cooled
  - nekoherentní světelný proud

- optické kanály

- cesta světla z místa ozáření buněk k detektoru
- optické části separují určité vlnové délky

LASER(y)

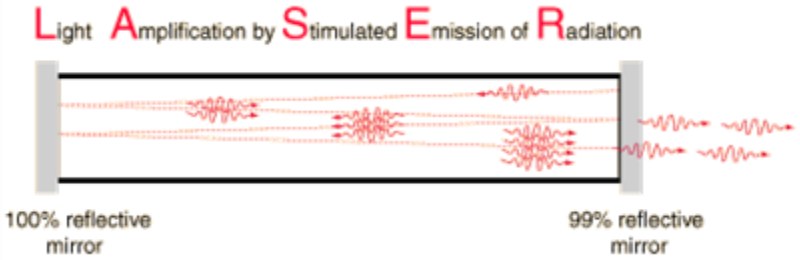

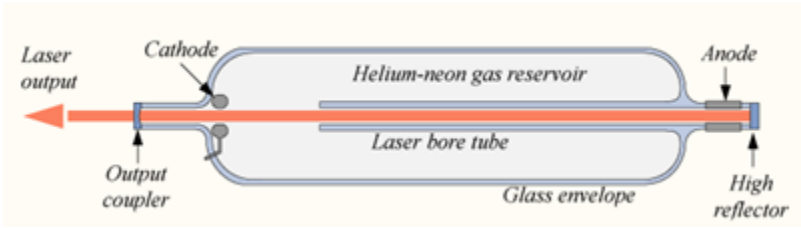

http://en.wikipedia.org/wiki/Helium-neon_laser

- koherentní (souvislý světelný tok)
- monochromatický
- soustředěný

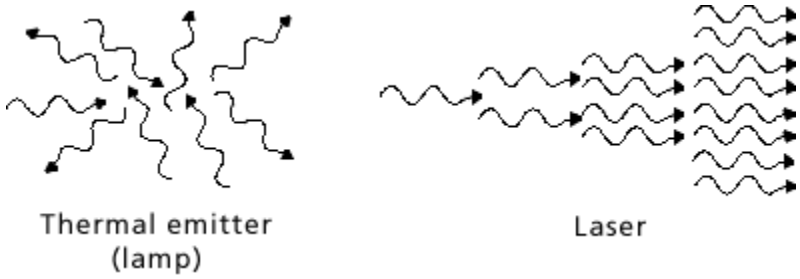

http://hyperphysics.phy-astr.gsu.edu/hbase/hframe.html

http://www.ilt.fraunhofer.de/eng/100053.html

COHERENT

LASER vs. Arc lamp

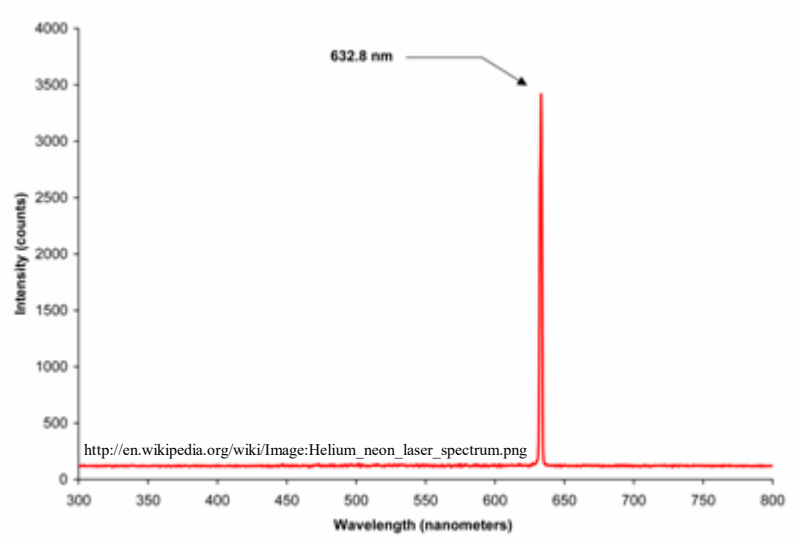

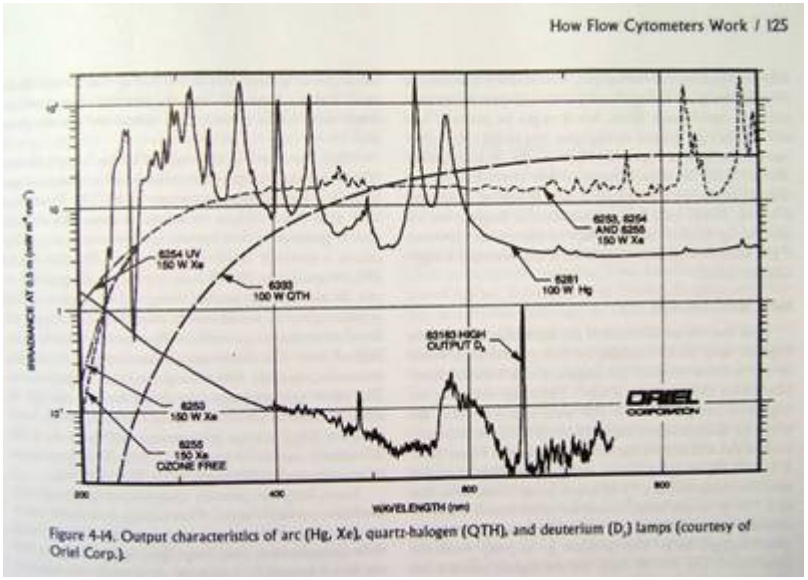

H.M. Shapiro, Practical Flow Cytometry, 4th ed.

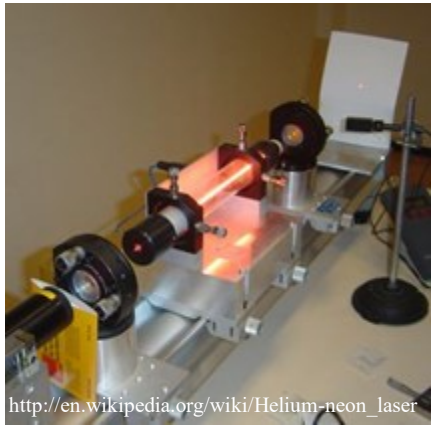

http://www.olympusmicro.com/primer/anatomy/sources.html

Optika - „Forward Scatter“ kanál

- část světla rozptýlená ve stejné ose jako je směr světelného paprsku
- intenzita „forward scatteru“ odpovídá velikosti, tvaru a optické homogenitě buněk

Forward Angle Light Scatter

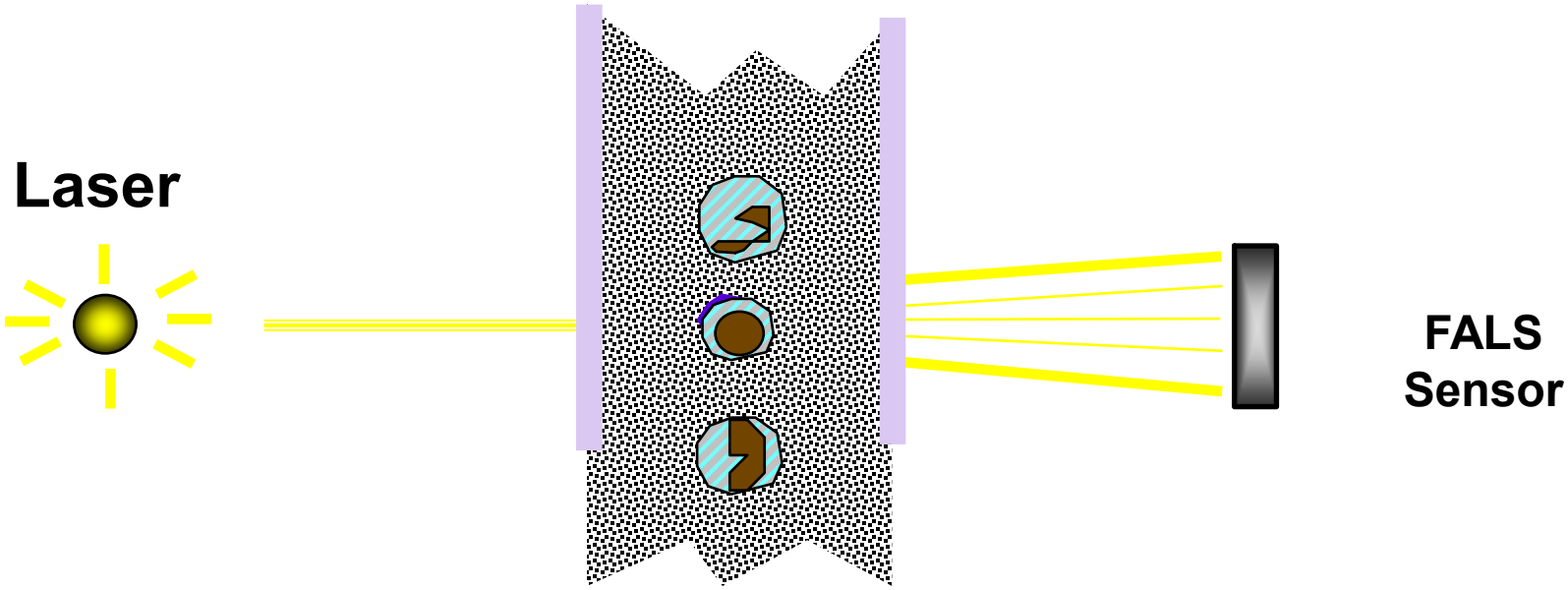

Optika - „Side Scatter“ kanál

- část světla rozptýlená kolmo do strany od osy směru světelného paprsku **side (90º) scatter channel**
- intenzita „side scatteru“ odpovídá **velikosti, tvaru a optické homogenitě** buněk

90 Degree Light Scatter

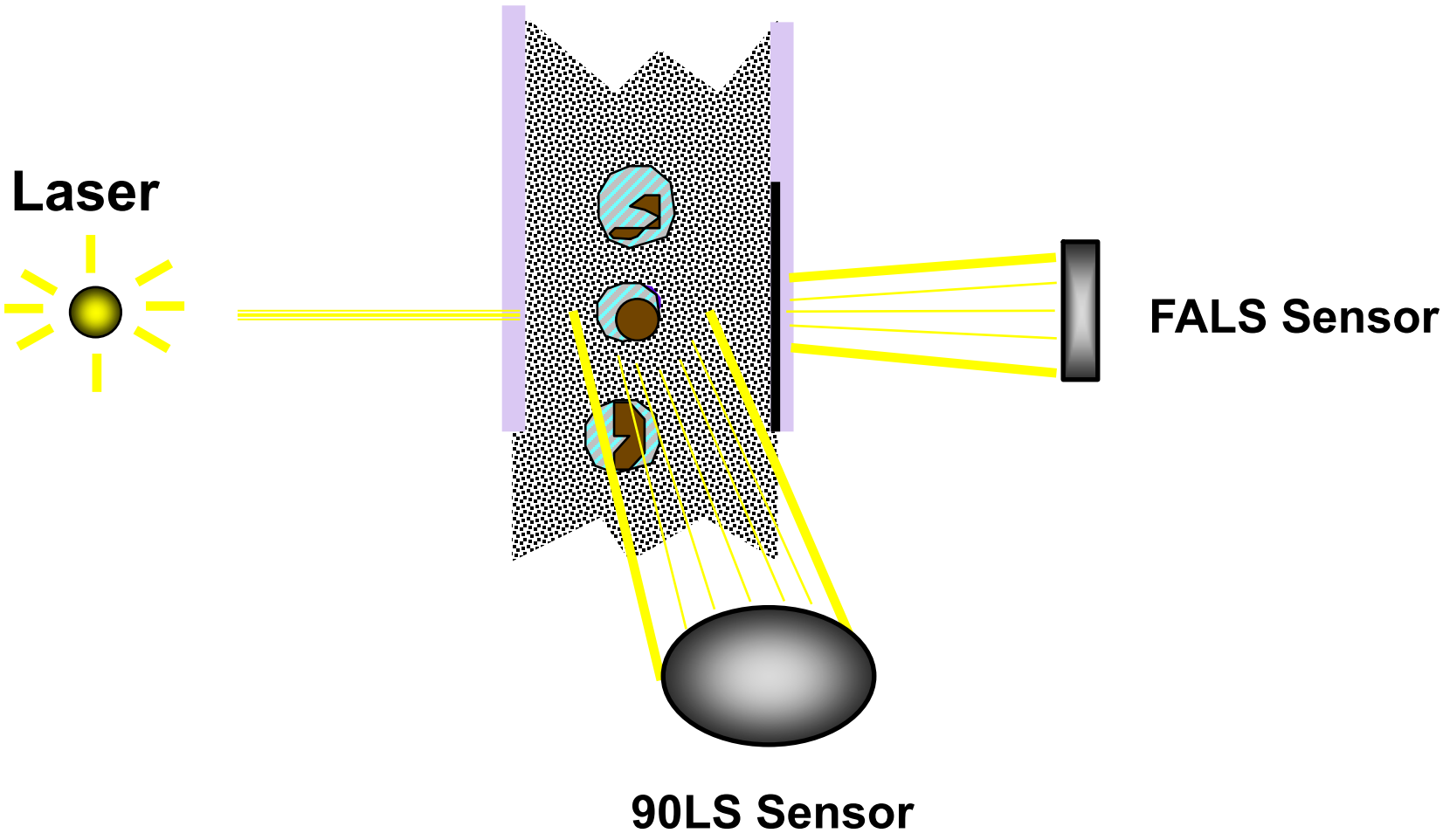

Optika - Light Scatter

- „Forward scatter“ zachycuje povrchové vlastnosti a velikost částic
- může být použit k rozlišení živých a mrtvých buněk
- „Side scatter“ odpovídá inkluzím uvnitř buněk
  - možno odlišit granulární a negranulární populaci

Optika - fluorescenční kanály

- fluorescence emitovaná z každého fluorochromu je detekována pomocí specifického **fluorescenčního kanálu**
- specifita detekce je kontrolována vlnovou selektivitou filtru a zrcadel

Fluorescence Detectors

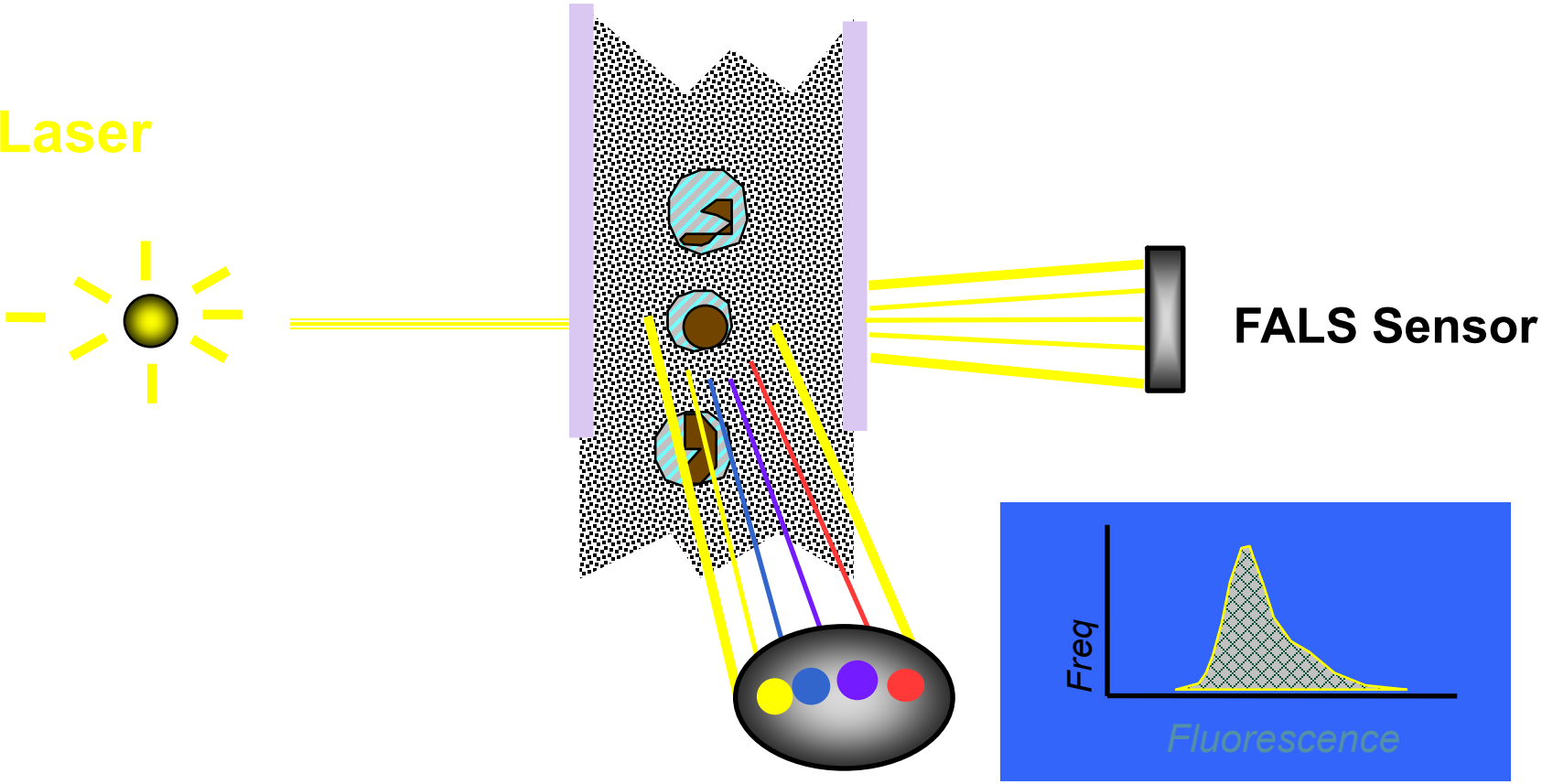

Fluorescence detector (PMT3, PMT4 etc.)

Optika - vlastnosti filtrů

- jsou konstruovány z materiálů absorbujících určitou vlnovou délku (a propouštějí jinou)
- přechod mezi absorbancí a transmisí není přesný; nutné specifikovat lom světla při konstrukci filtru

Optics - vlastnosti filtrů

- „Long pass“ filtr propouští vlnovou délku nad „řezanou“ délkou
- „Short pass“ filtr propouští vlnovou délku pod „řezanou“ délkou
- „Band pass“ filtr propouští vlnovou délku v úzkém rozmezí okolo specifické vlnové délky

Standard Long Pass Filters

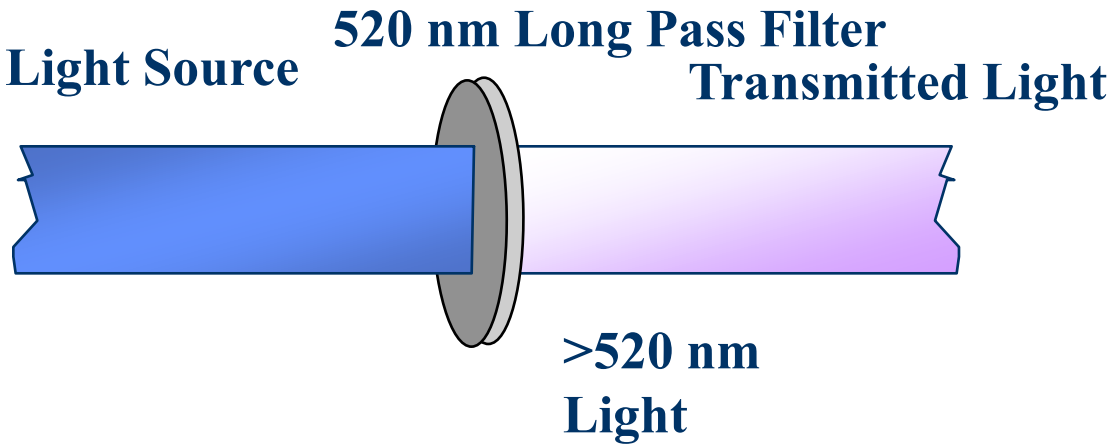

Standard Short Pass Filters

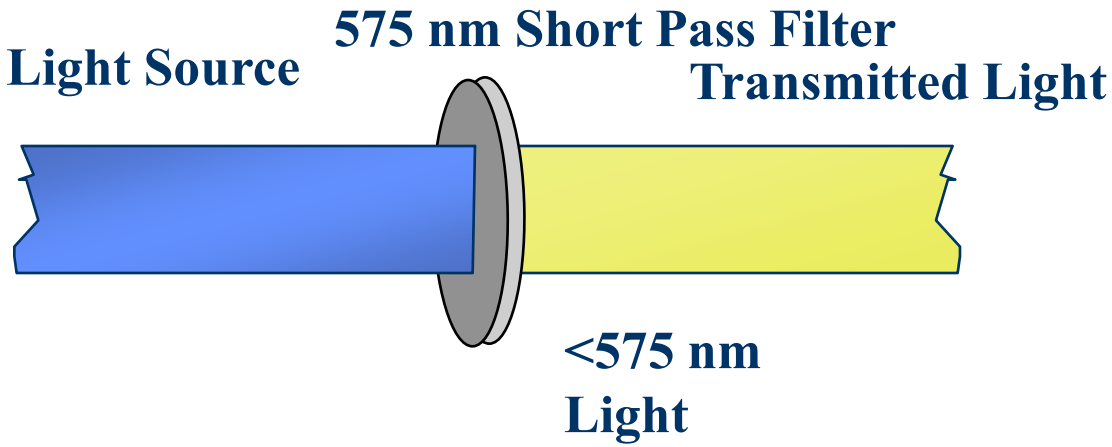

Standard Band Pass Filters

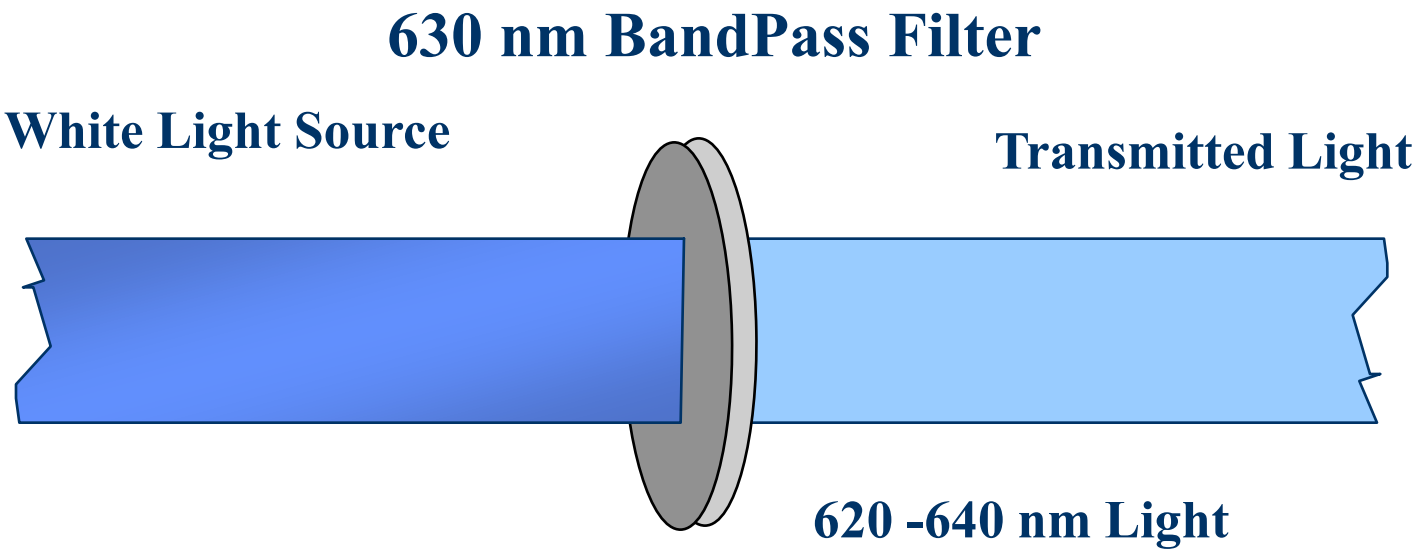

Optika - vlastnosti filtrů

- pokud je filtr umístěn v 45° úhlu ke zdroji světla, světlo, které má projít tak projde, ale blokované světlo je odraženo v 90° úhlu
- **dichroické filtry, dichroická zrcadla**

Dichroic Filter/Mirror

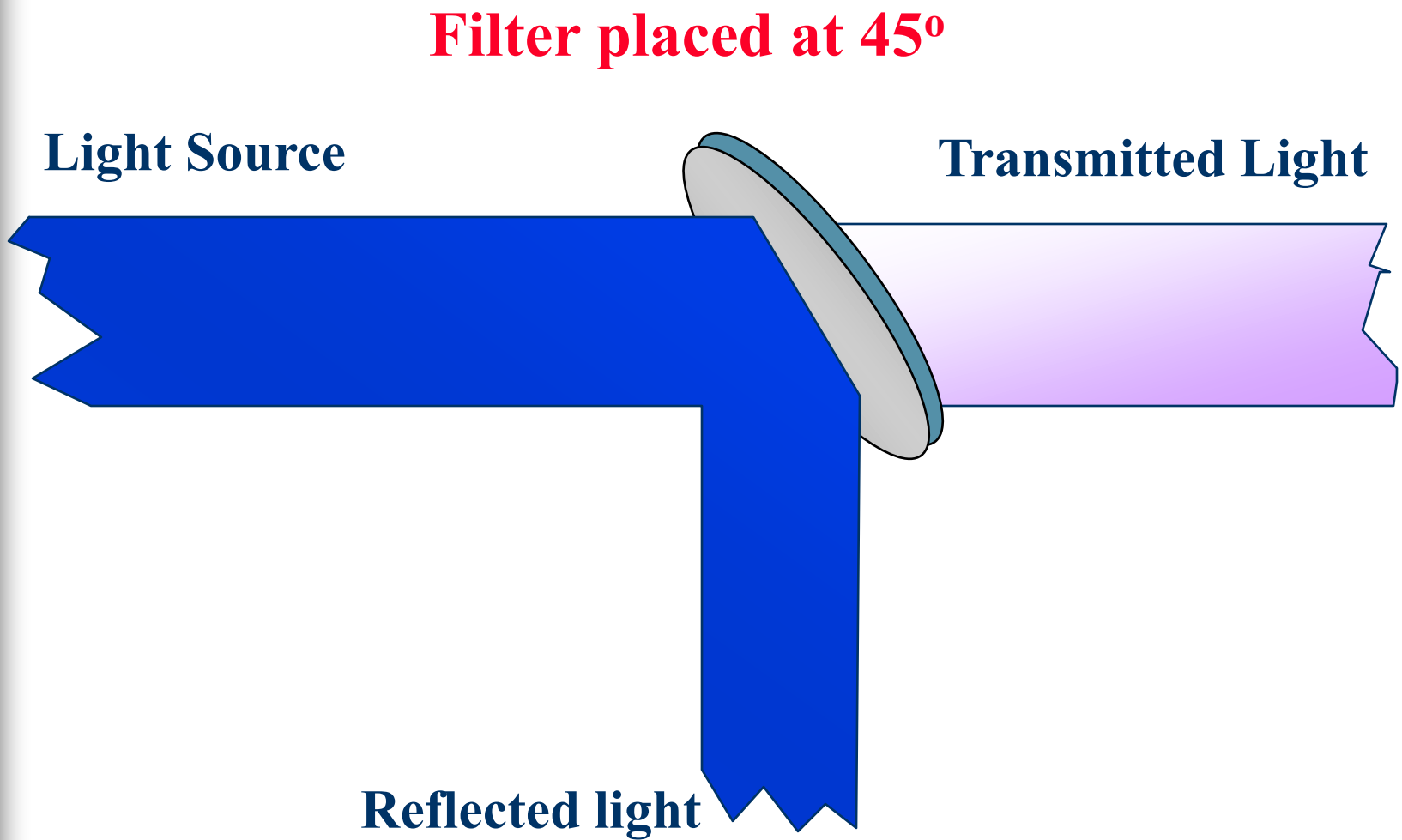

Optika - uspořádání filtrů

- k společnému měření více než jednoho „scatteru“ nebo fluorescence , používáme mnohonásobné kanály (a detektory)
- multikanálové uspořádání musí splňovat
  - spektrální vlastnosti použitého fluorochromu
  - správný řád uspořádání filtrů a zrcadel

Optika - detektory

- dva obecné typy detektorů
  - **fotodioda**
    - v minulosti zejména pro silný signál (forward scatter detector)
    - současnost – vysoce citlivé AVALANCHE“ fotodiody (APD)
  - **fotonásobič (photomultiplier tube - PMT)**
    - citlivější než běžná fotodioda, muže být poškozen přesvícením

Photomultiplier tubes (photomultipliers, PMTs)

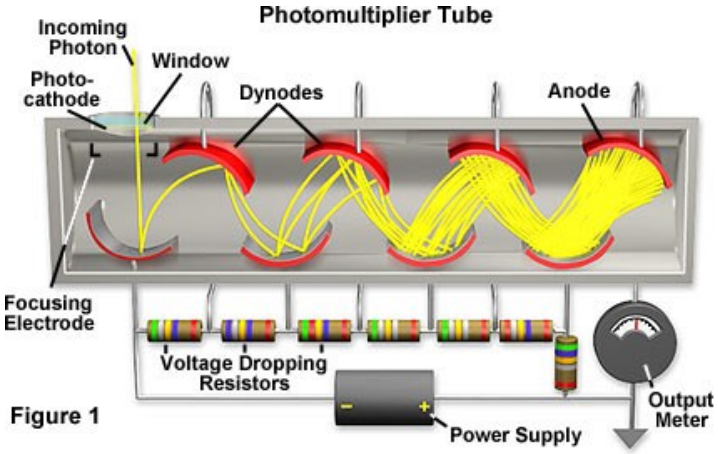

Figure 1

Základní charakteristika:

-vysoce citlivé detektory (jeden foton)

-velké zesílení signálu/nízký šum

-velká plocha detekce

-rychlá frekvence odpovědi

-velké pracovní napětí (1000 – 2000 V)

http://en.wikipedia.org/wiki/Photomultiplier

http://hamamatsu.magnet.fsu.edu/articles/photomultipliers.html

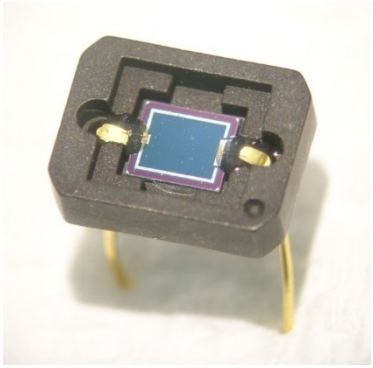

http://en.wikipedia.org/wiki/Photodiode

“bežná“ fotodioda

Porovnání s PMT

Výhody:

1. excelentní linearita signálu
2. rozsah spektrální detekce 190 nm to 1100 nm (silicon)
3. nízký šum
4. Odolnost vůči mechanickým vlivům
5. nízká cena
6. malá velikost a hmotnost
7. dlouhá životnost
8. Vysoká kvantová účinnost (~80%)
9. Nepotřebuje vysoká napětí

Nevýhody

1. Malá plocha
2. Nemožnost integrálního zesílení
3. Mnohem nižní citlivost
4. Počítání fotonů pouze u speciálních produktů
5. Kratší čas odpovědi

Současnost: „**AVALANCHE**“ fotodiody (APD)

- Vysoce citlivé polovodiče - srovnatelné s PMT

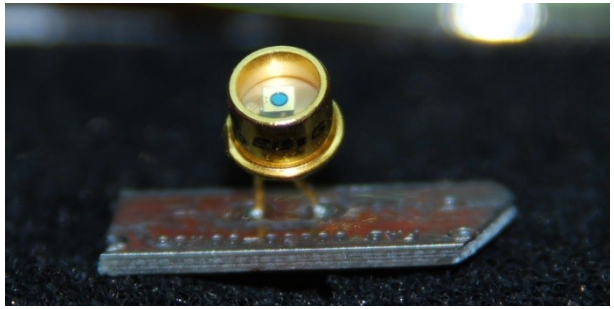

https://en.wikipedia.org/wiki/Avalanche_photodiode

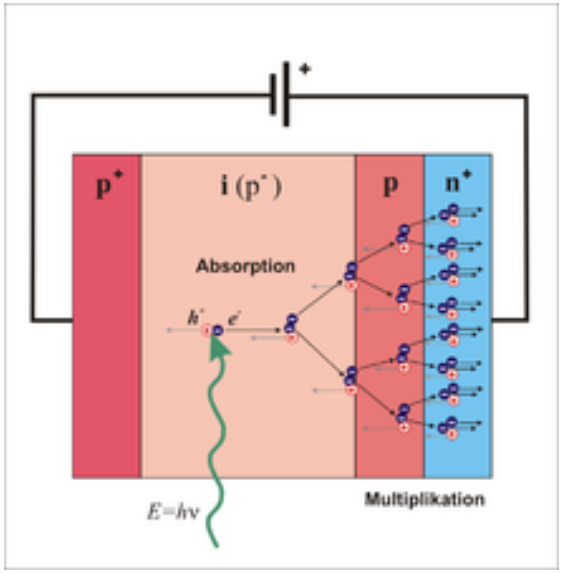

Example Channel Layout for Laser-based Flow Cytometry

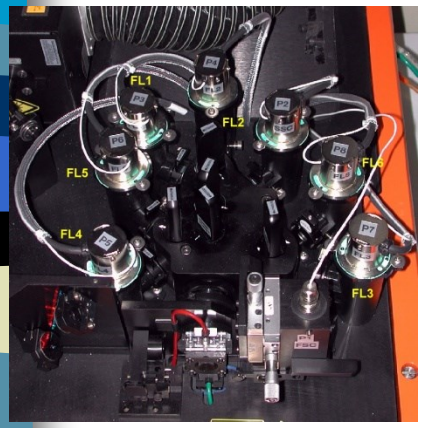

original from Purdue University Cytometry Laboratories; modified by R.F. Murphy

BD FACSCalibur system

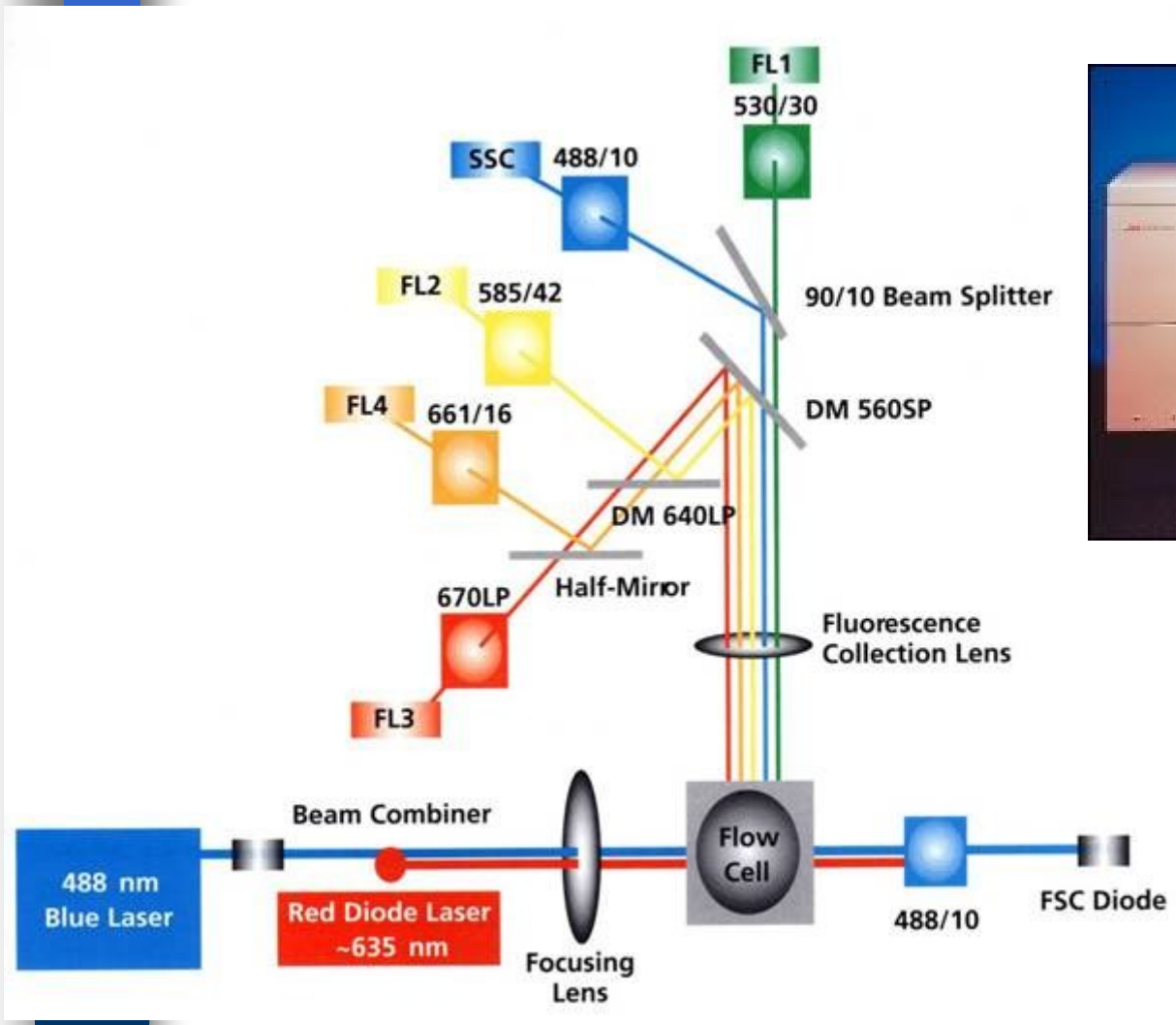

http://www.bdbiosciences.com/immunocytometry_systems/

BD LSR II system

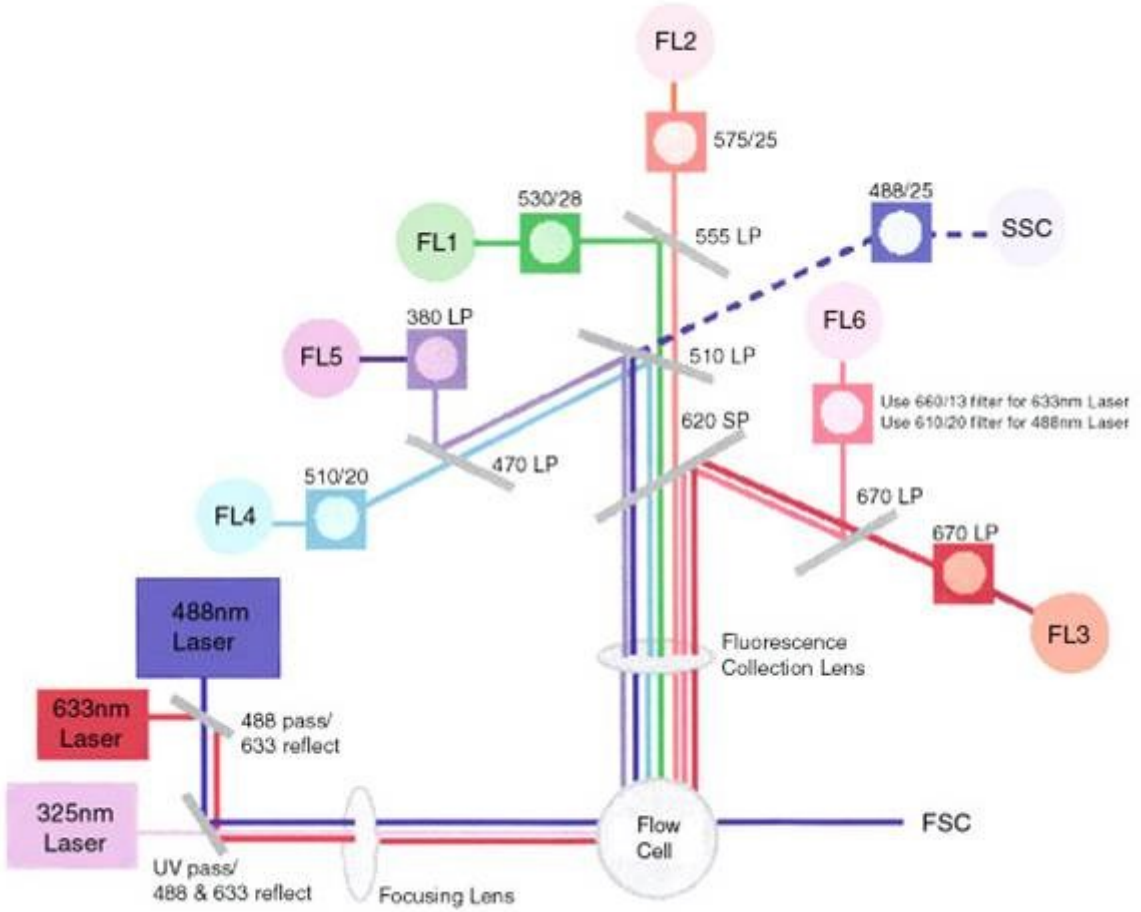

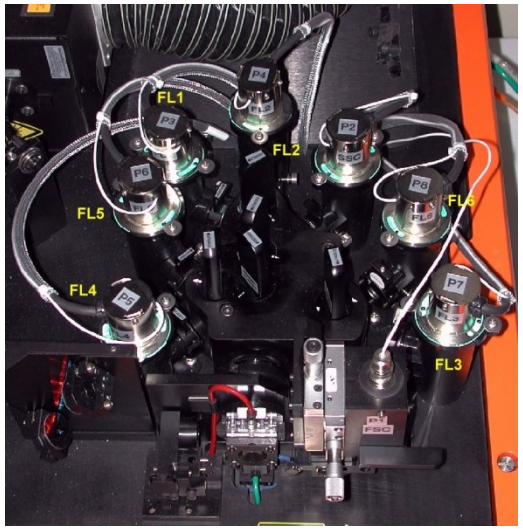

http://jcsmr.anu.edu.au/facslab/facs/LSR2.html

BD FACSVerse system

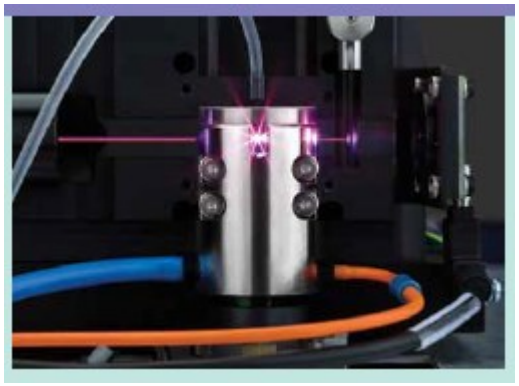

http://www.bdbiosciences.com/instruments/facsverse/features/index.jsp

Aria II

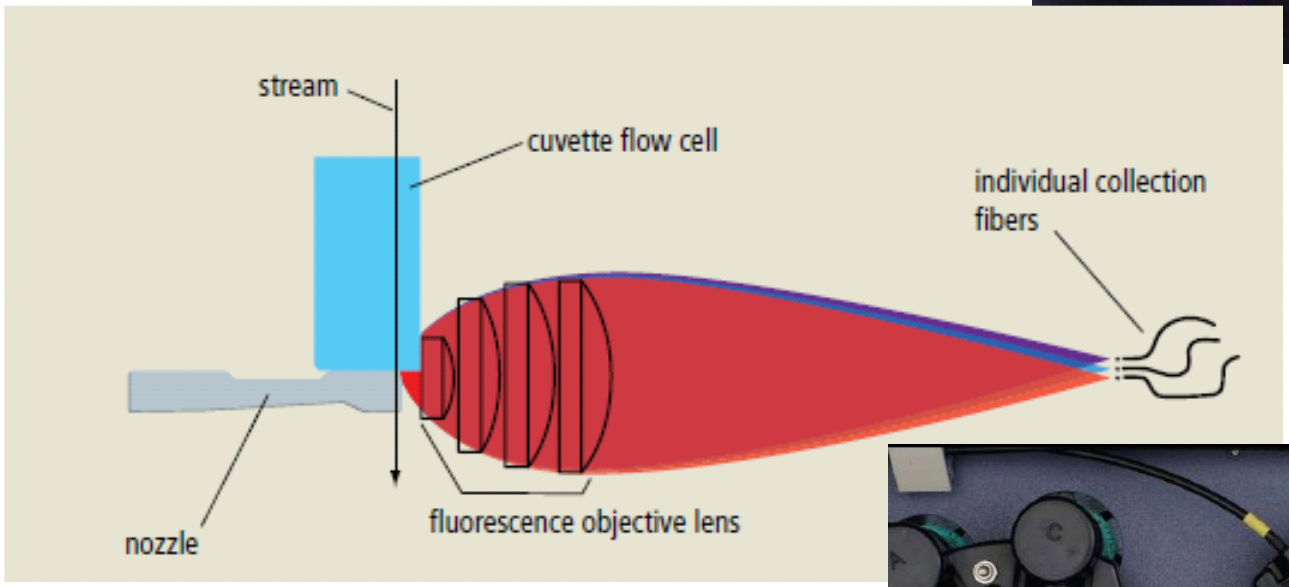
stream
cuvette flow cell
individual collection fibers
nozzle
fluorescence objective lens


780/60
735LP
660/20
695/40
655LP
585/42
556LP
488/10
730LP
610LP
616/23
530/30
502LP
780/60

BD

SP6800 spectral analyzer

The 405nm, 488nm and 638nm excitation lasers are positioned to reduce fluorescent noise. They enable the system to support 16 or more fluorescent parameters.

Microfluidics flow cell chip maximizes signal with auto positioning to guarantee high sensitivity. Made of durable plastic with an embedded quartz cuvette, the chip is easy to replace when needed.

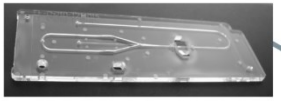

The Flowpoint detection system precisely tracks the core stream shape and position in the flow cell as well as the cross sectional position of each passing particle to provide highly reliable measurements. This patented technology visualizes core stability and enables the highest resolution.

Scatter analysis
Forward and Side Scatter parameters to allow relative size and complexity measurements.

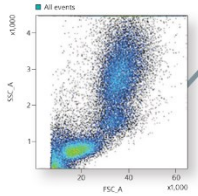

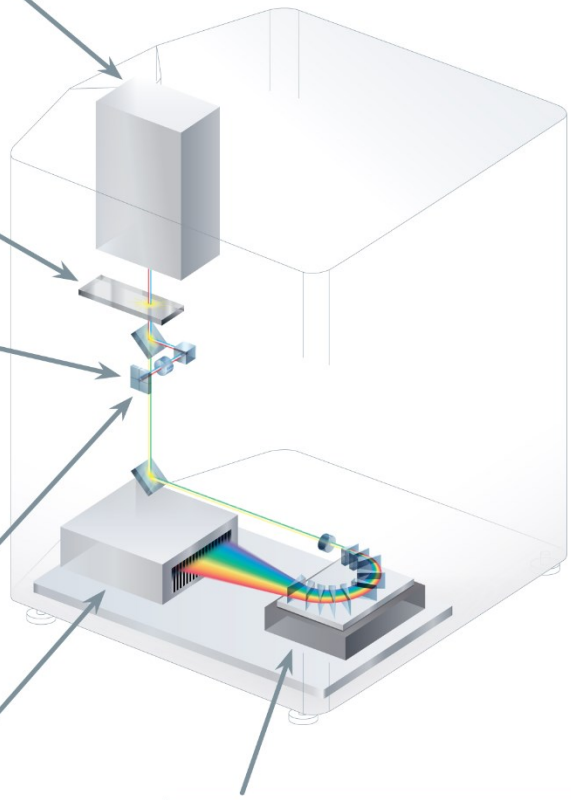

Emitted light is directed through through a 32 Channel PMT that produces 66 data points of signal detection to analyze emitted photons from 420nm to 800 nm to ensure accurate visualization.

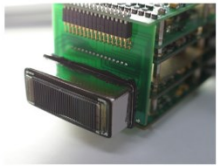

A unique prism collection system
Delivers light through 10 consecutive prisms allowing optimal signal separation while minimizing light loss.

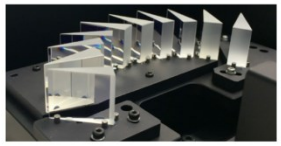

Image Stream & Flowsight **Amnis** – kombinace průtokové cytometrie a analýzy obrazu

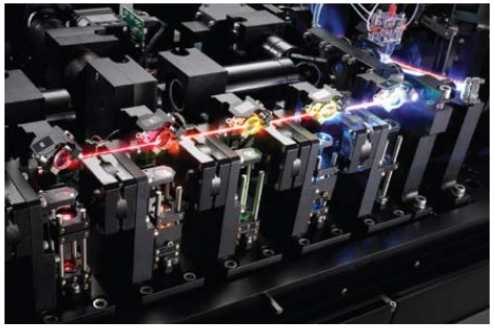

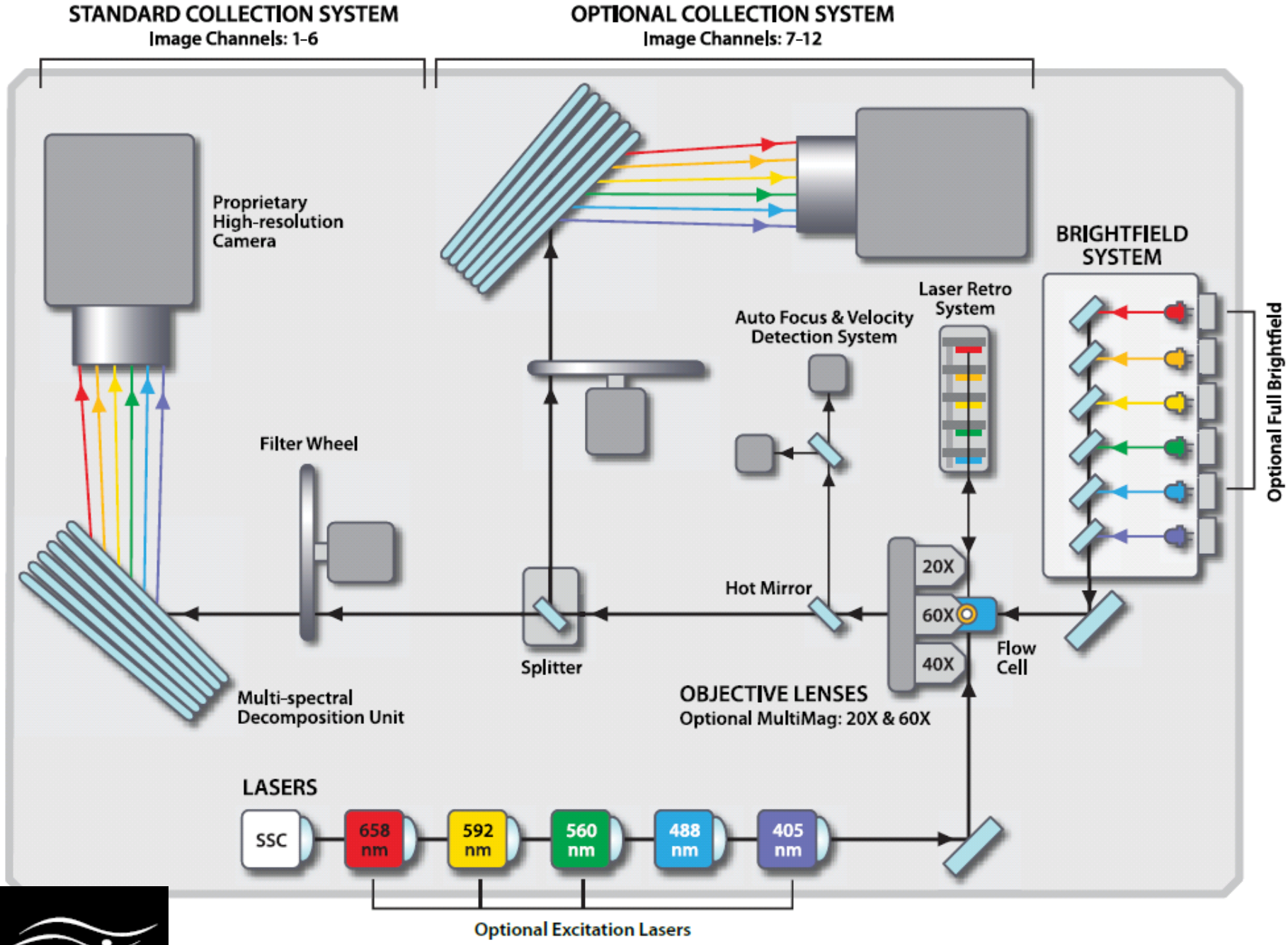
STANDARD COLLECTION SYSTEM
Image Channels: 1-6
OPTIONAL COLLECTION SYSTEM
Image Channels: 7-12
Proprietary
High-resolution
Camera
BRIGHTFIELD
SYSTEM
Laser Retro
System
Auto Focus & Velocity
Detection System
Optional Full Brightfield
Filter Wheel
Hot Mirror
20X
60X
40X
Flow
Cell
Splitter
Multi-spectral
Decomposition Unit
OBJECTIVE LENSES
Optional MultiMag: 20X & 60X
LASERS
SSC
658
nm
592
nm
560
nm
488
nm
405
nm
Optional Excitation Lasers

amnis

Amnis - aplikace

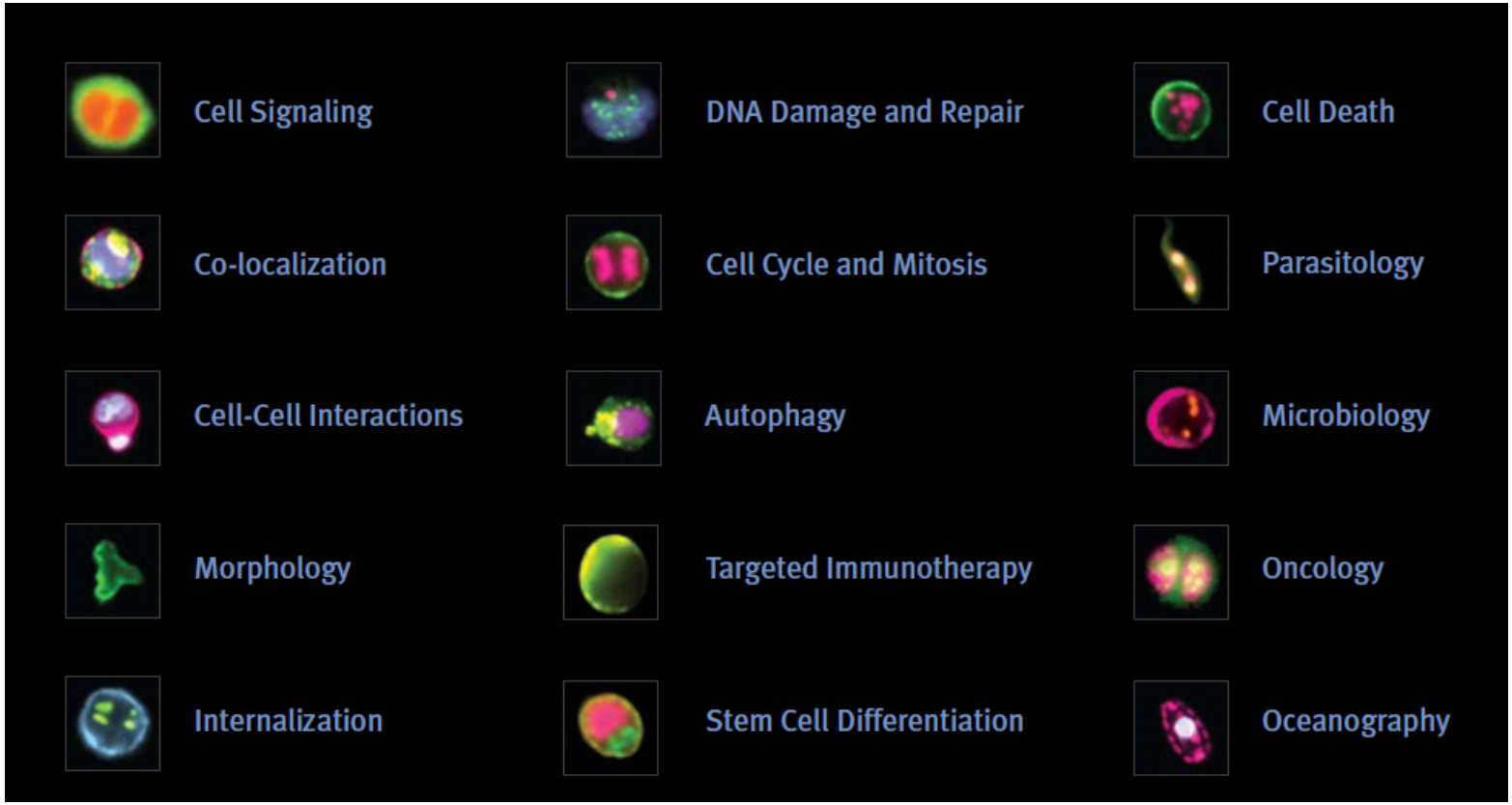

amnis

CellStream, Luminex

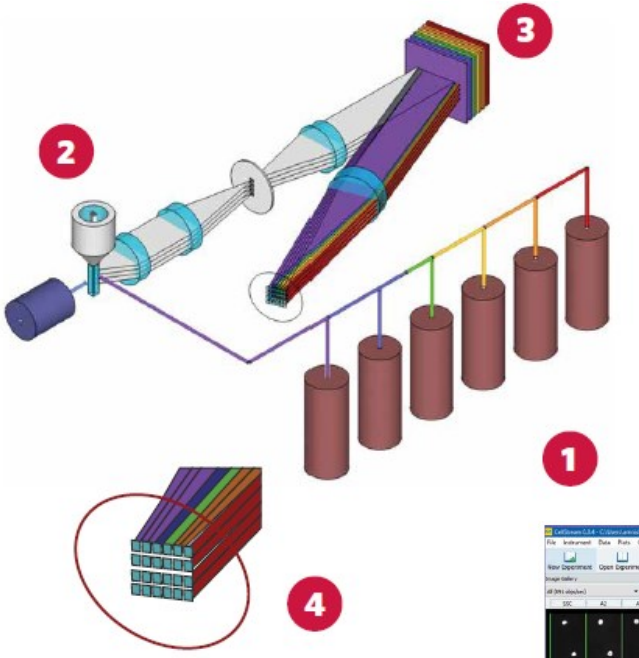

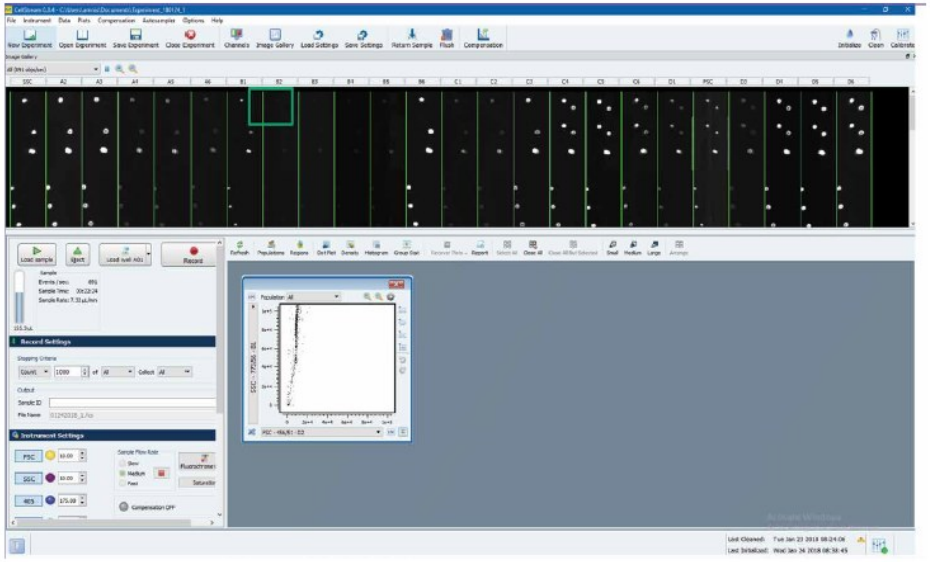

ThermoFisherScientific: Attune CytPix Flow Cytometer

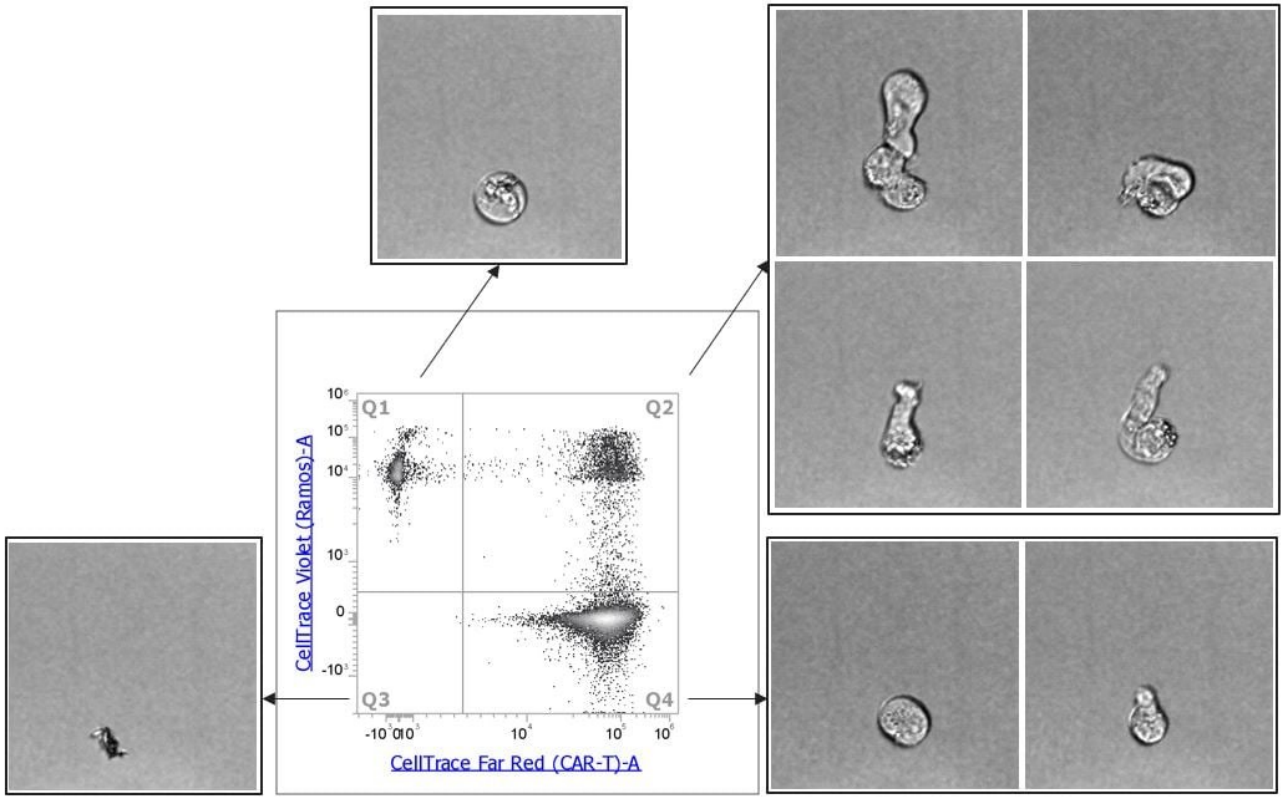

BD FACSDiscover S8

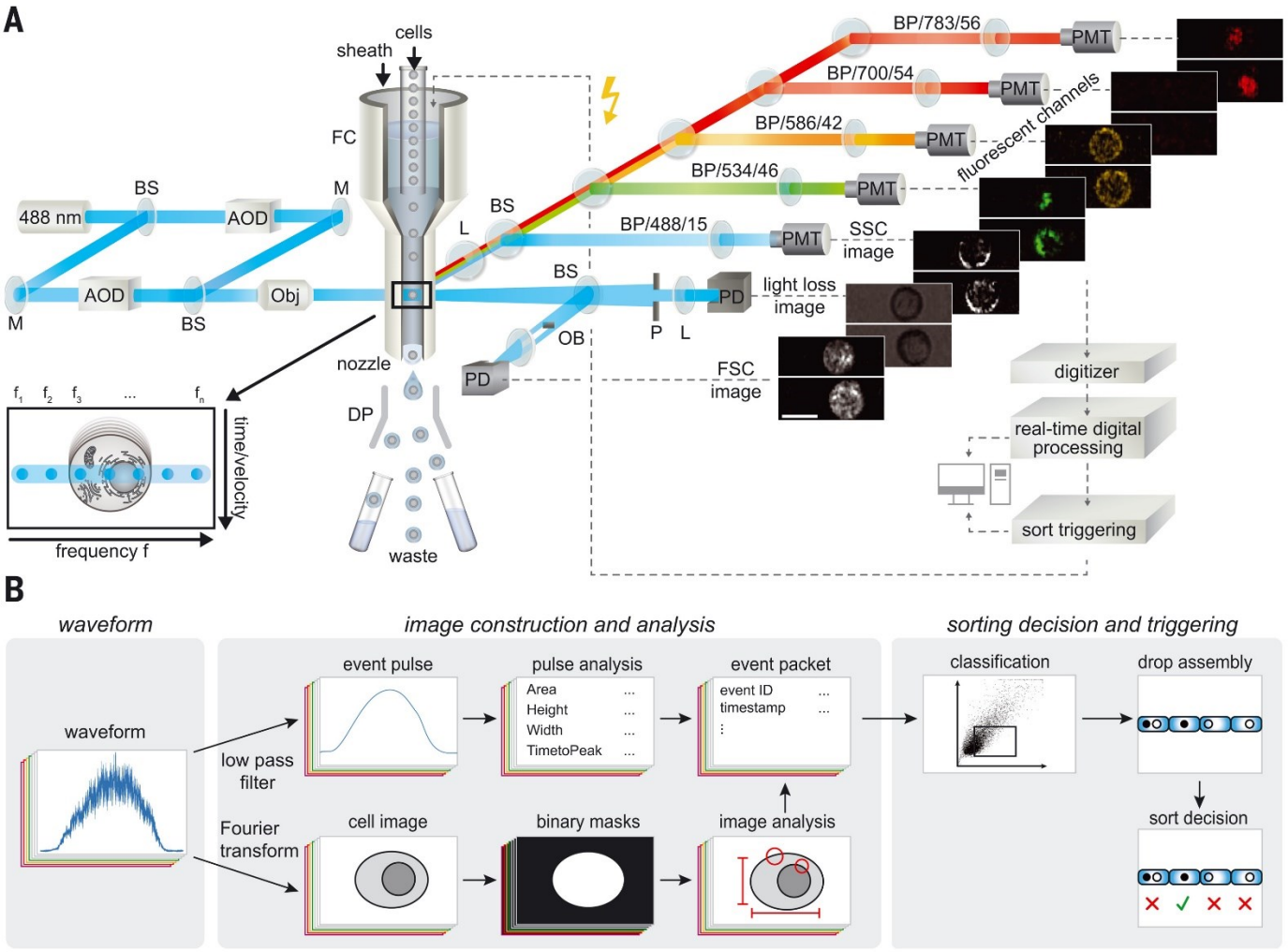

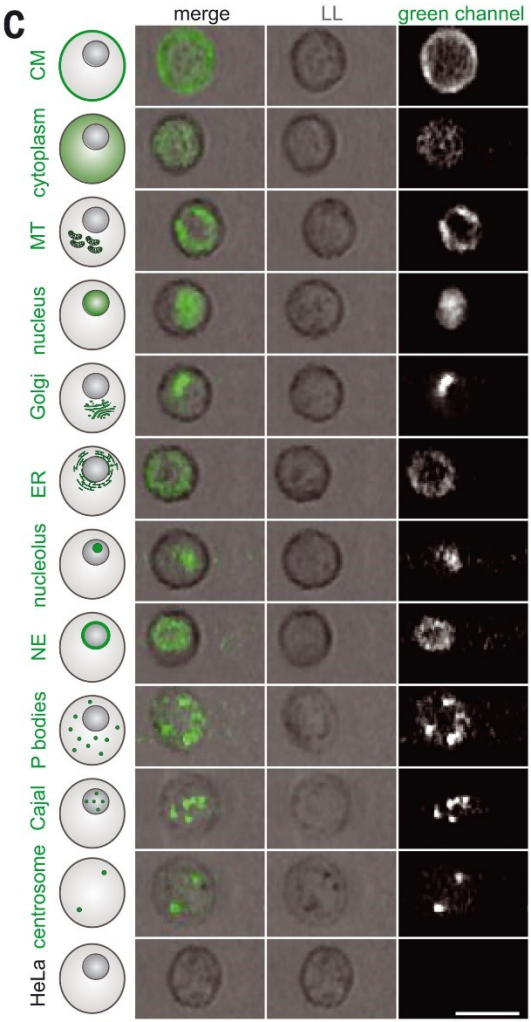

SCIENCE 20 Jan 2022 Vol 375, Issue 6578 pp. 315-320 DOI: 10.1126/science.abj3013

Common Laser Lines

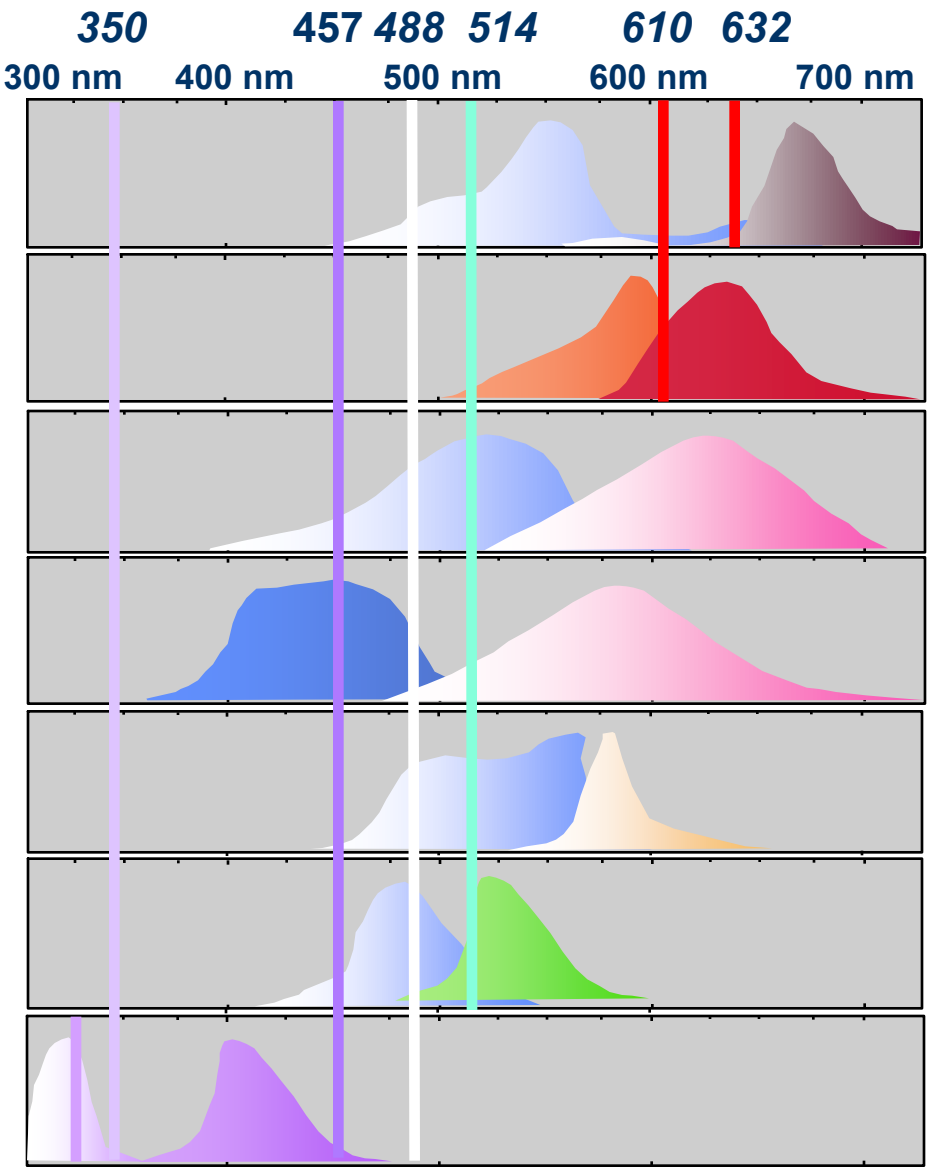

PE-TR Conj.

Texas Red

PI

Ethidium

PE

FITC

cis-Parinaric acid

Upraveno podle J.P. Robinson Purdue University BMS 631

Octagon Detection System

PerCP-Cy5.5

PE

FITC

SSC

PE-TxRed

PE-Cy7

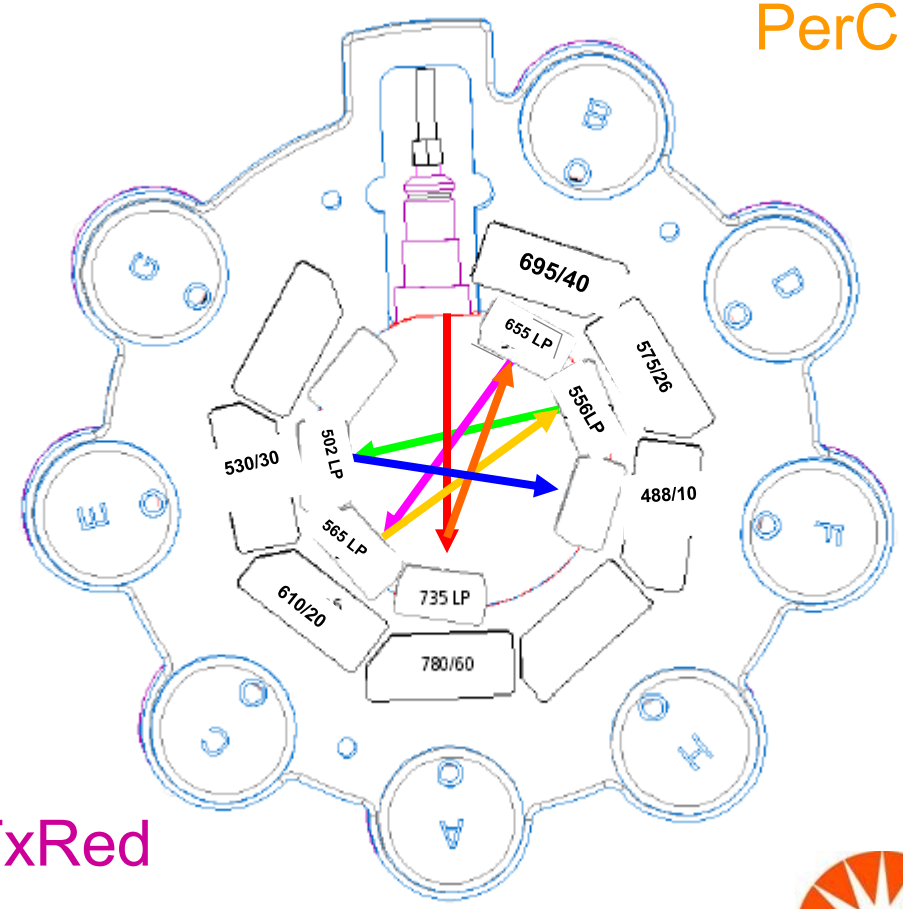

BD

“kostka” pro konvenční fluorescenční mikroskop

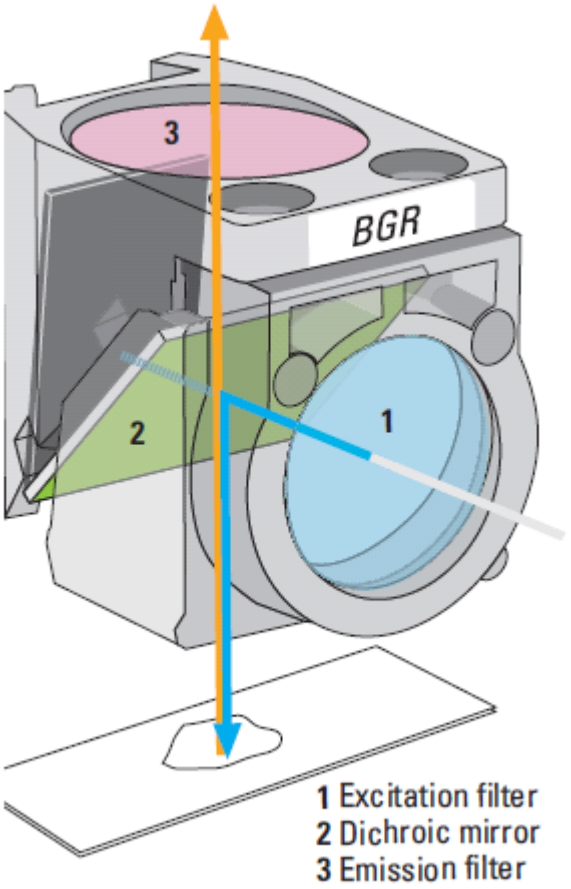

Acousto Optical Beam Splitter AOBS®

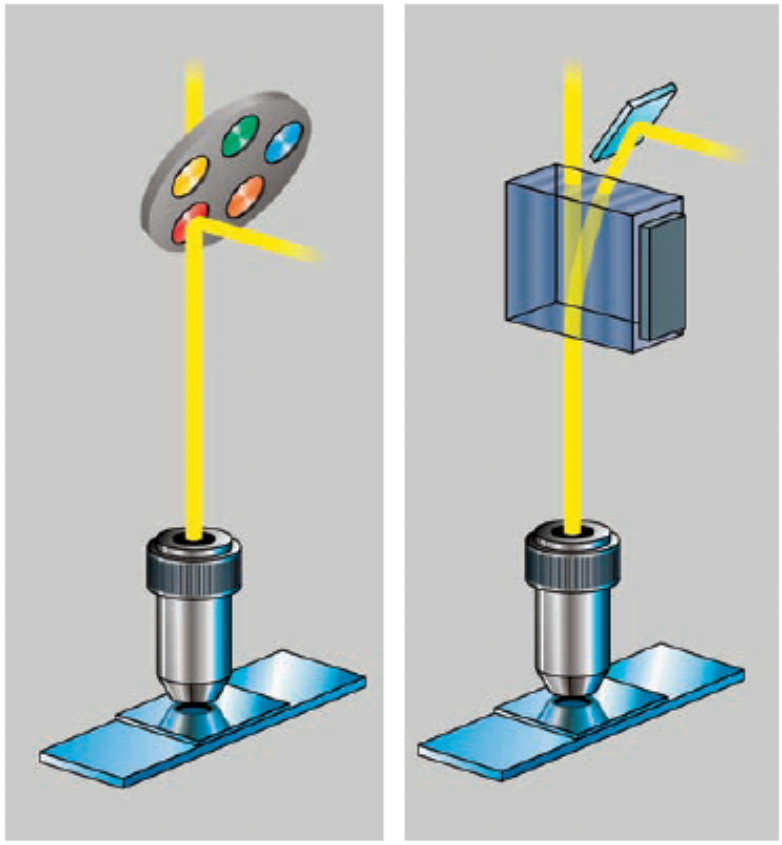

Left: conventional beam splitting by dichroic mirrors requires many optical elements with fixed properties.
Right: the AOBS® is electronically adaptable to all tasks.

Leica
MICROSYSTEMS

Acousto Optical Beam Splitter AOBS®

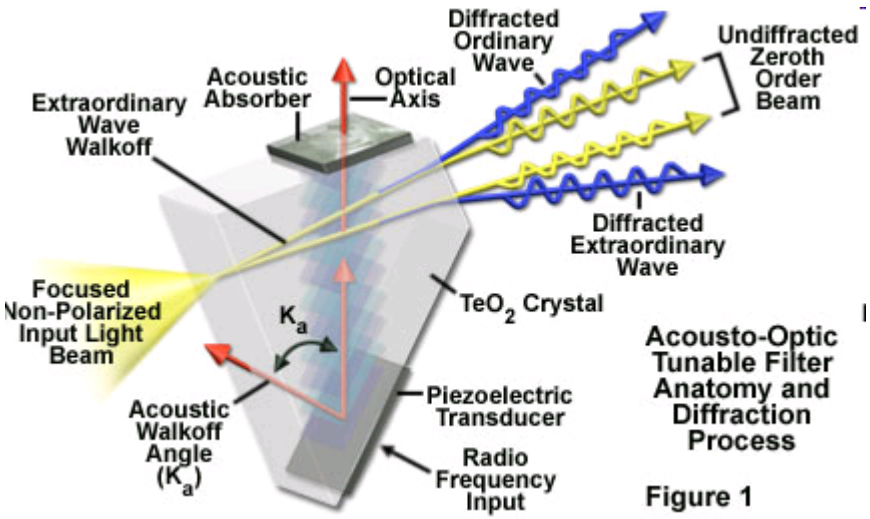

Acousto-Optic Tunable Filter Anatomy and Diffraction Process

Figure 1

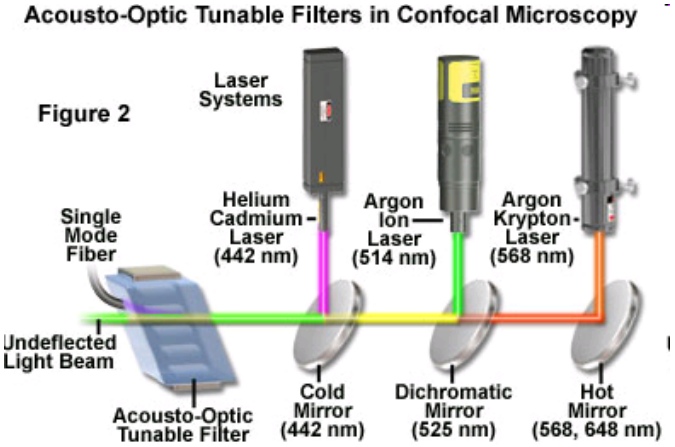

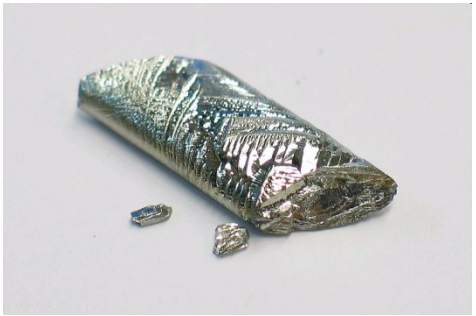

http://micro.magnet.fsu.edu/primer/java/filters/aotf/index.html

http://simple.wikipedia.org/wiki/Tellurium

Leica MICROSYSTEMS

Supercontinuum Generation

-a nonlinear process for strong spectral broadening of light

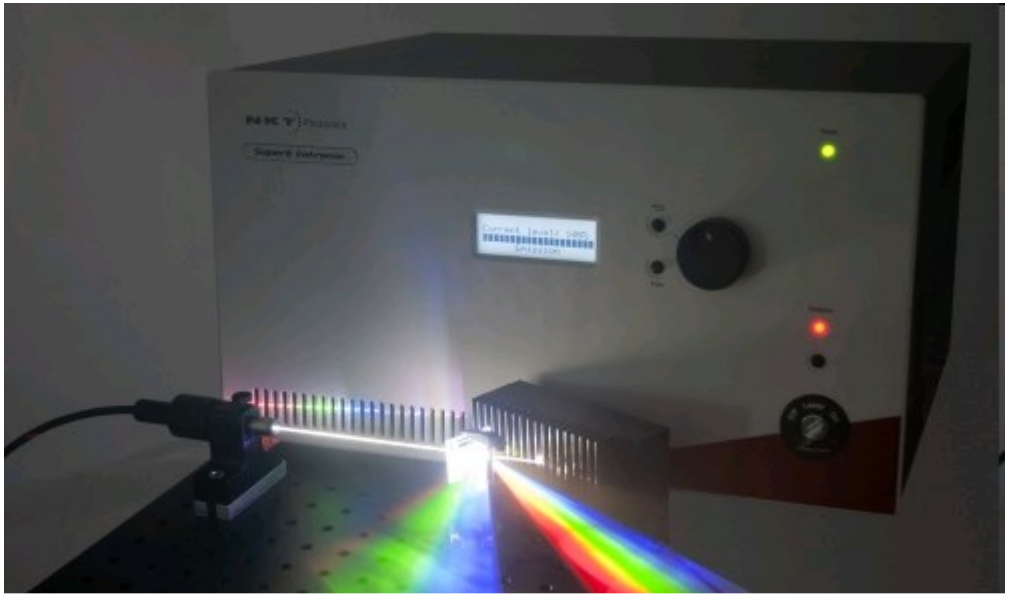

TECHNICAL NOTE

Cytometry
PART A
Journal of the International Society for Advancement of Cytometry

Supercontinuum White Light Lasers for Flow Cytometry

William G. Telford,[1*] Fedor V. Subach,[2] Vladislav V. Verkhusha[2]

Cytometry Part A • 75A: 450–459, 2009

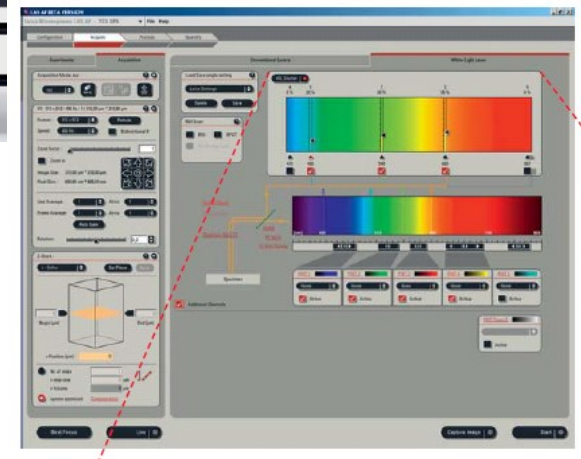

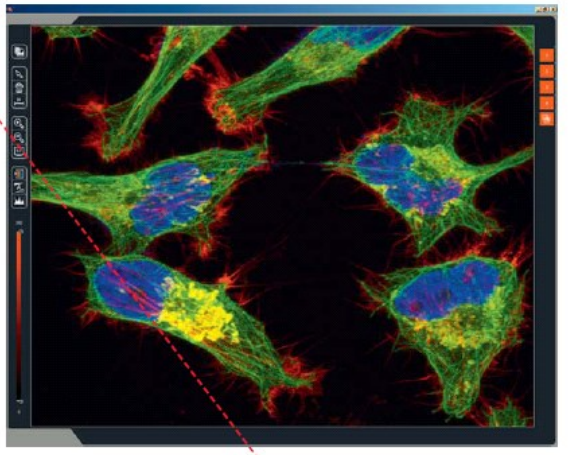

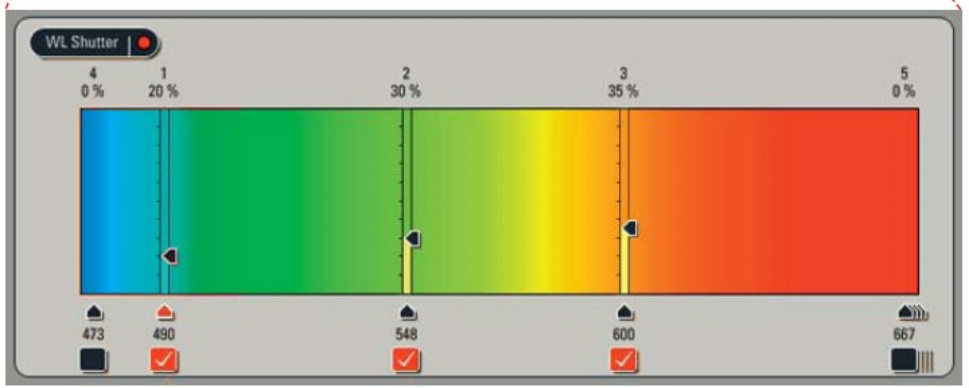
WL Shutter
4
0 %
1
20 %
2
30 %
3
35 %
5
0 %
473
490
548
600
667

The benefits of AOBS®

- Adaptable to any new dye
- 8 lines simultaneously
- Reflected light imaging
- High transmission
- Truly confocal – real optical sectioning
- Fast switching
- Freely tunable
- Fluorescence correlation spectroscopy with multi-line lasers

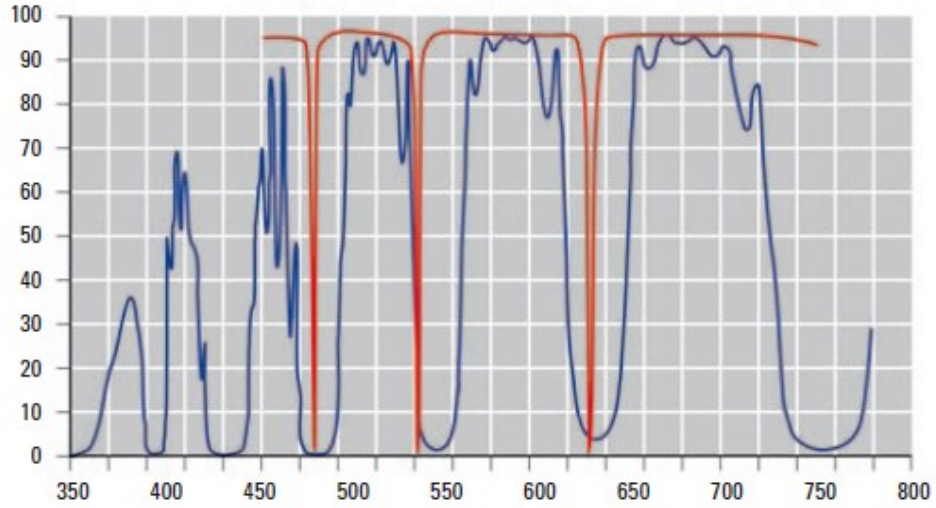

Transmission curves
Blue: triple dichroic, blue, green, red
Red: AOBS® tuned to 488, 543,594, 633 nm
Higher transmission, wider bands and steeper slopes with AOBS®

Fluorescence Spectrum Viewers

https://www.bdbiosciences.com/en-us/applications/research-applications/multicolor-flow-cytometry/product-selection-tools/spectrum-viewer

https://www.thermofisher.com/cz/en/home/life-science/cell-analysis/labeling-chemistry/fluorescence-spectraviewer.html

http://www.biolegend.com/panelselector

http://www.biolegend.com/spectraanalyzer

http://www.biolegend.com/webtoolstab

https://fluorofinder.com

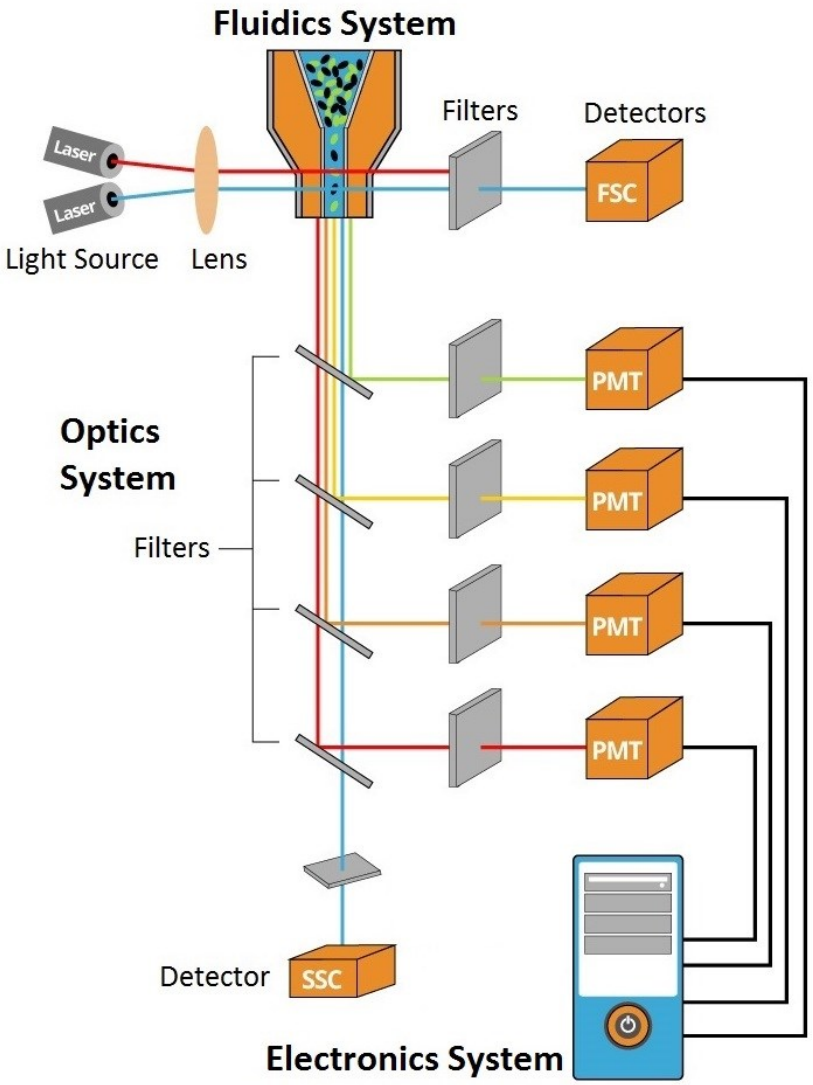

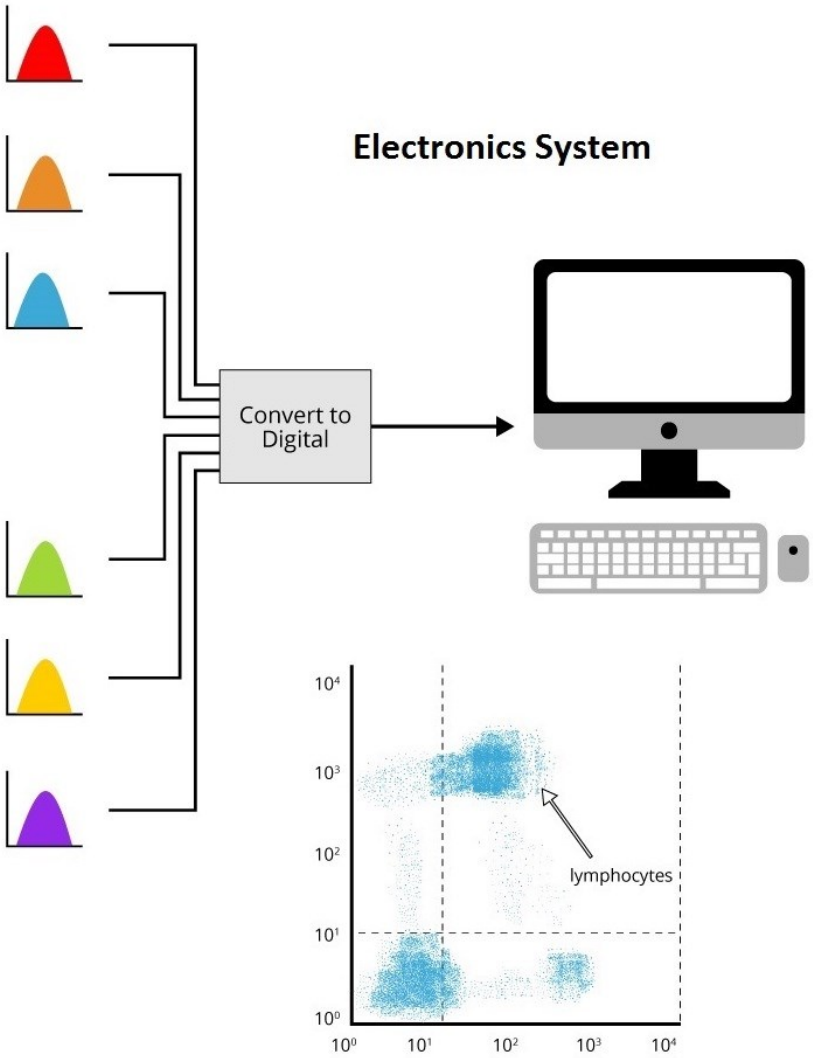

http[illegible]bosterbio.com/protocol-and-troubleshooting/flow-cytometry-principle

Průtokové systémy a hydrodynamika

Getting the cells in the right place (at the right time)! (Shapiro, pp 133-143 - 3rd ed)

Průtoková cytometr:

Pomocí hydrodynamicky zaostřeného fluidního systému analyzuje buňky v zaostřeném světelném paprsku (laseru).

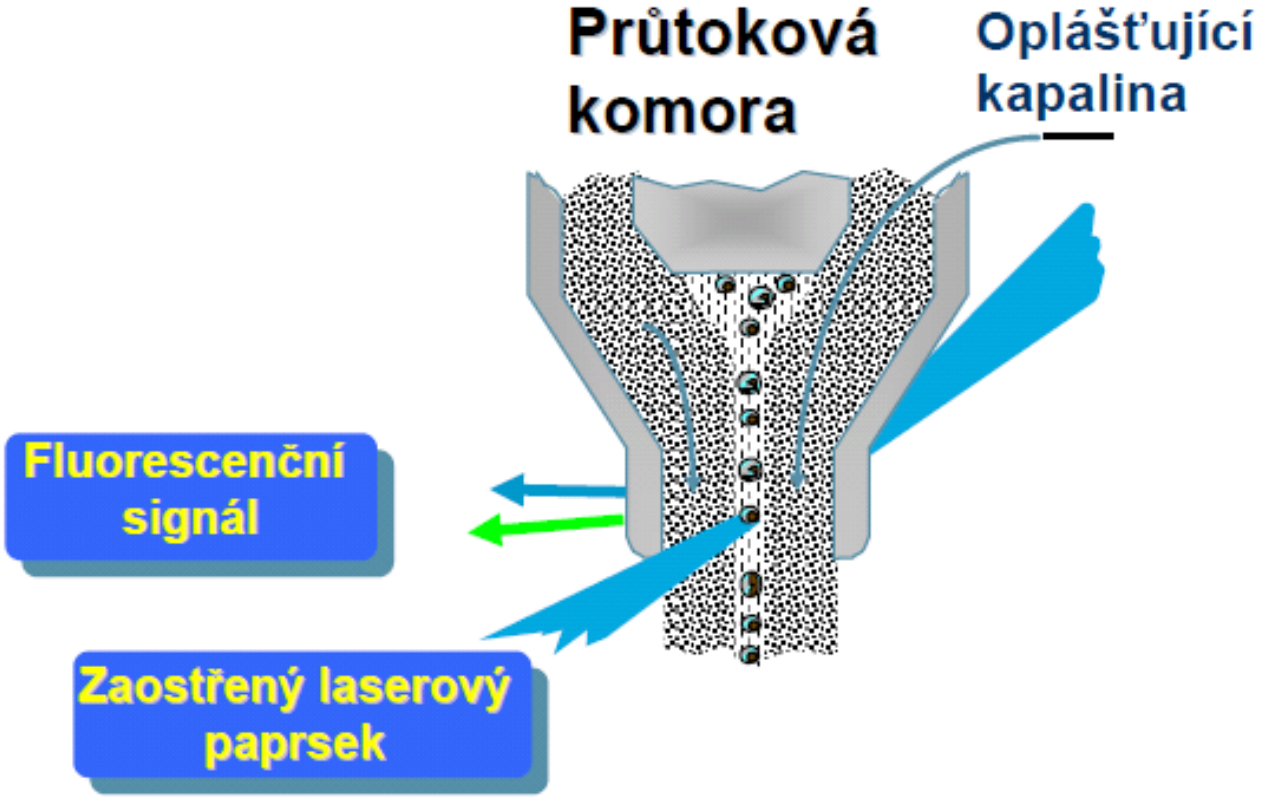

upraveno podle J.P.Robinson

Fluidní systém: BD FACSAria II

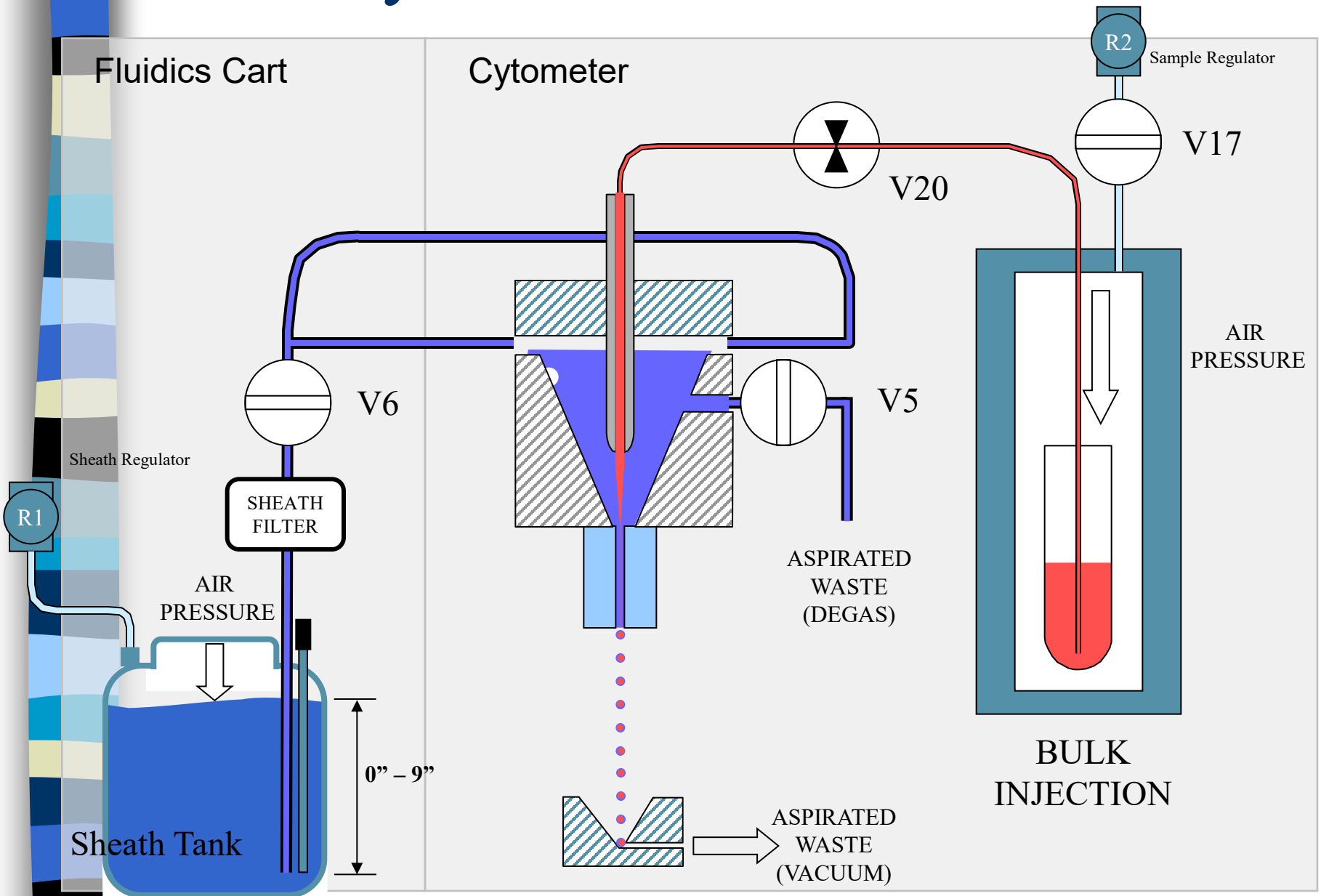

Hydrodynamic focussing in the cuvette

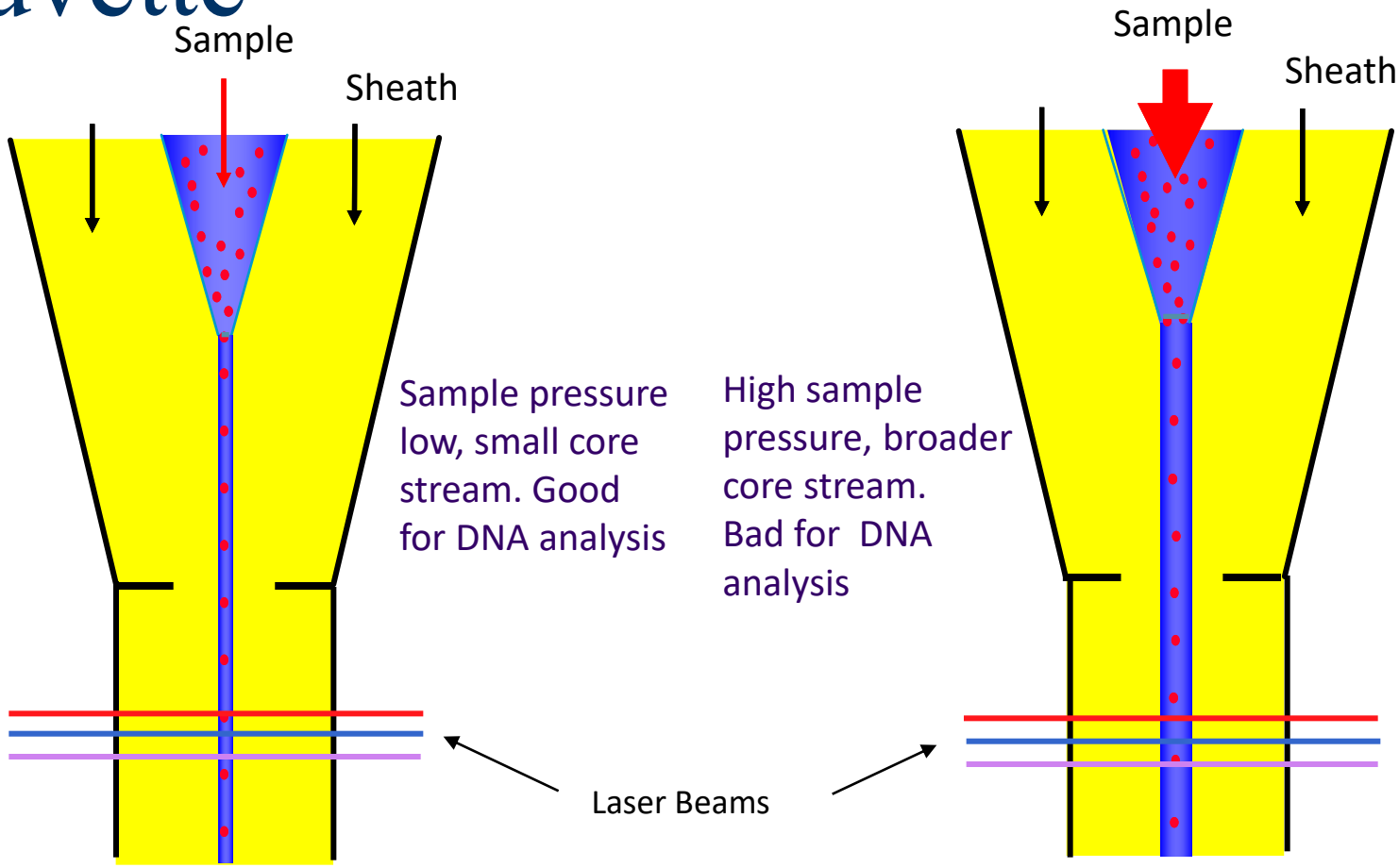

Fluidní systém

Pozitivní tlakový systém

- založen na rozdílném tlaku mezi nosnou kapalinou a vzorkem
- vyžaduje zdroj vyrovnaného tlaku (vzduch, dusík)
- rychlost průtoku mezi 6-10 m/s

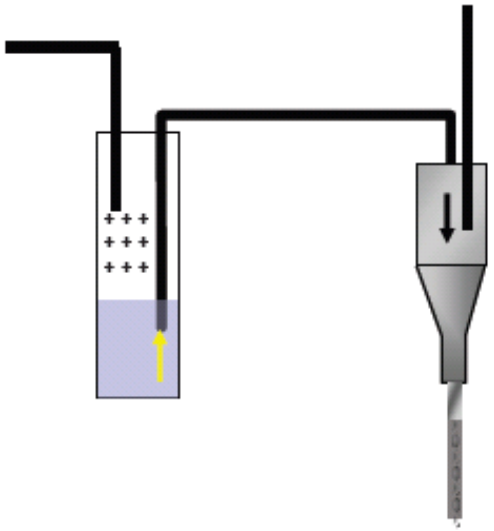

Pozitivní vytlačovaní injekční systém

- průtok 1-2 m/s
- fixní objem (50 µl, 100 µl)
- možnost určení absolutních počtů buněk

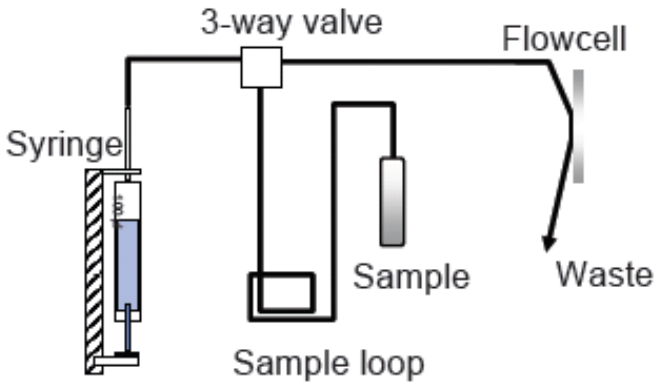

upraveno podle J.P.Robinson

Hydrodynamický a fluidní systém

- buňky jsou vždy v suspenzi
- vzorek je obvykle ve fyziologickém roztoku
- nosná kapalina je voda nebo fyziologický roztok
- nosná kapalina pro sortrování musí být fyziologický roztok
- vzorky jsou hnány tlakem nebo pomocí pístu

Fluidika

- potřebujeme buňky v suspenzi, protékající v jednom sloupci napříč osvíceným místem
- u většiny zařízení je toho dosaženo injekcí vzorku do proudu nosné kapaliny skrz malý otvor (50-300 μm)

Fluidika

- Pokud jsou podmínky optimální pak vzorek proudí středem bez směšování s nosnou kapalinou
- takový stav nazýváme laminární proudění **(laminar flow)**

Fluidika - Laminární vs. turbulentní proudění

- **Turbulentní** proudění je charakteristické chaotickými (stochastickými) změnami
- **Laminární** proudění – kapalina proudí v paralelních vrstvách které se vzájemně nemísí

Fluidika - Laminární vs. turbulentní proudění

- Osborne Reynolds (1842 -1912) definoval podmínky laminárního proudění (1883)

"http://en.wikipedia.org/wiki/Osborne_Reynolds"

Fluidika - Laminární proudění

- Zda bude průtok laminarní je možné určit pomocí **Reynoldova čísla**

$$R_e = \frac{d\rho\bar{v}}{\eta}$$

where

d = tube diameter

ρ = density of fluid

$\bar{v}$ = mean velocity of fluid

η = viscosity of fluid

- když $R_e < 2300$, průtok je vždy laminární (v trubici)
- $R_e > 2300$, průtok může být turbulentní

Fluidika

- Zavedení malého objemu kapaliny do velkého způsobem, kdy se stává „zaostřeným“ ve směru toku, nazýváme hydrodynamické zaostřování.

APPLIED MICROBIOLOGY, Sept. 1972, p. 384-388

Vol. 24, No. 3
Printed in U.S.A.

Hydrodynamic Focusing and Electronic Cell-Sizing Techniques

M. L. SHULER, R. ARIS, AND H. M. TSUCHIYA

Department of Microbiology, Department of Chemical Engineering and Materials Science, University of Minnesota, Minneapolis, Minnesota 55455

Received for publication 24 May 1972

The technique of hydrodynamic focusing, used to improve the resolution of the Coulter counter for the sizing of bacteria, was examined. Latex particles of 0.26 μm^3 to 6.7 μm^3 volume were used to examine the characteristics of the system with and without hydrodynamic focusing. The system then was evaluated for sizing mixed bacterial populations as well as single populations. Possible applications are also discussed.

Fluidika

- Jak vstřikovat vzorek a regulovat rychlost proudění?
  - **Rozdílným tlakem**
  - **Volumetrickou injekcí**

Fluidika – systém s rozdílným tlakem

- Pomocí vzduchu se natlakuje vzorek a zásobník s nosnou kapalinou
- Pomocí tlakových regulátorů se tlak kontroluje odděleně

Fluidika – systém s rozdílným tlakem

- Tlak nosné kapaliny určuje objem v jakém proudí
- Rozdíl v tlaku mezi nosnou kapalinou a vzorkem určuje objem proudícího vzorku
- Kontrola není úplná – změny tření mohou způsobit změny v rychlosti proudění vzorku

Fluidika – průtokové komory

- Průtokové komory
  - Určují osu a velikost průtoku nosné kapaliny a vzorku
  - Vymezují místo pro hydrodynamické zaostření
  - Slouží také jako místo kde dochází k ozáření buněk zdrojem světla

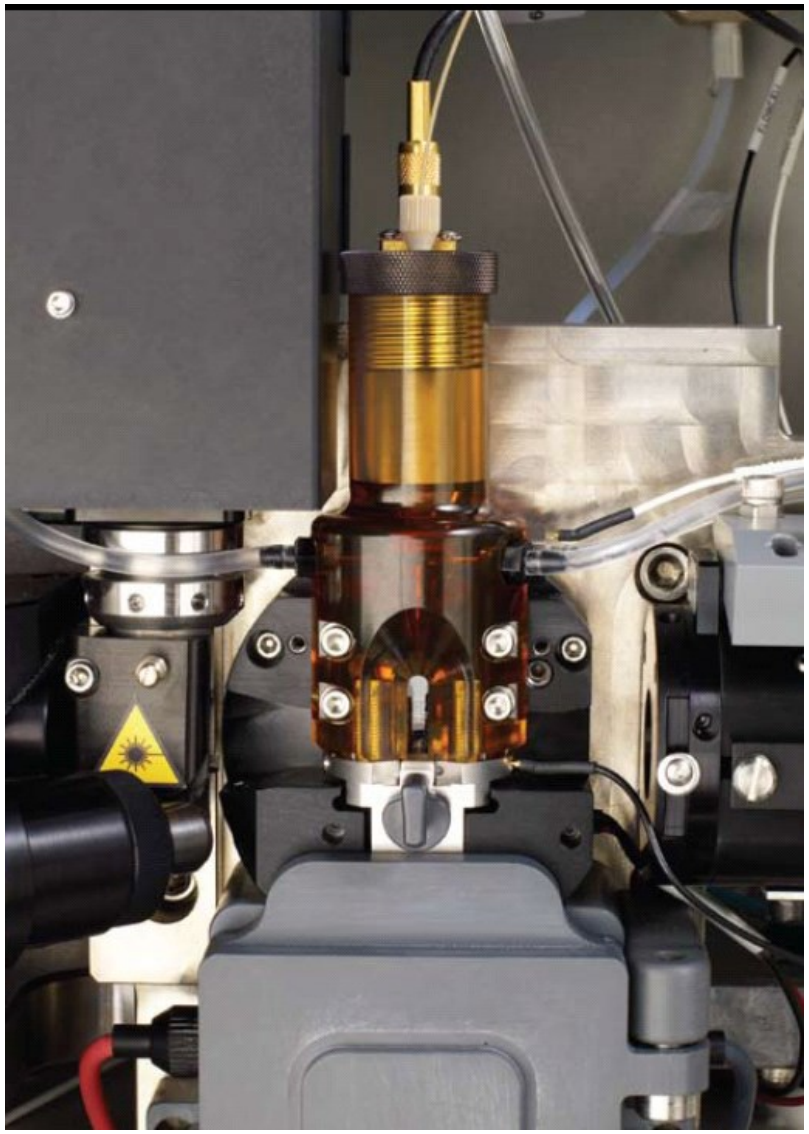

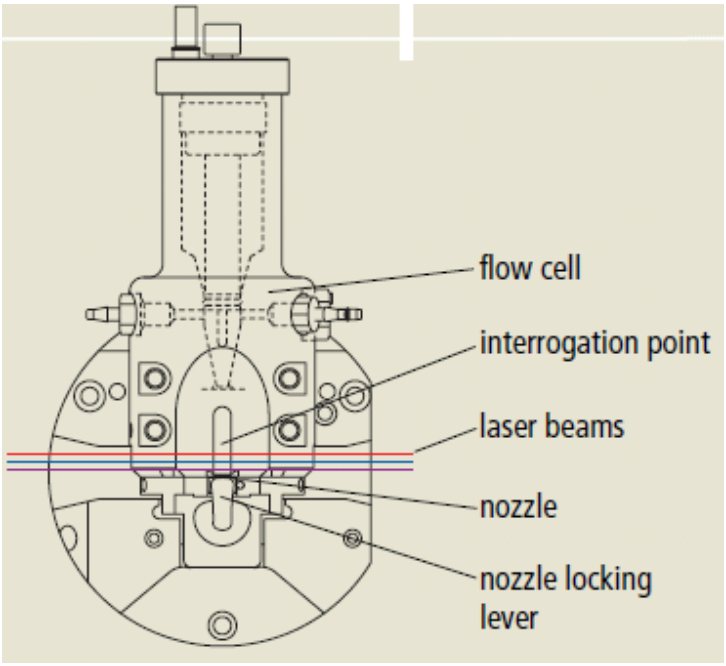
flow cell
interrogation point
laser beams
nozzle
nozzle locking lever


BD FACSAria II

Fluidika – průtokové komory

Základní typy průtokových komor

- **Jet-in-air**
  - Nejlepší pro sortrování, horší optické vlastnosti
- **Flow-through cuvette**
  - Výborné optické vlastnosti, může být použita pro sortrování
- **Closed cross flow**
  - Nejlepší optické charakteristiky, nelze sortrovat
- **Open flow across surface**
  - Nejlepší optické charakteristiky, nelze sortrovat

Upraveno podle J.P. Robinson Purdue University BMS 631

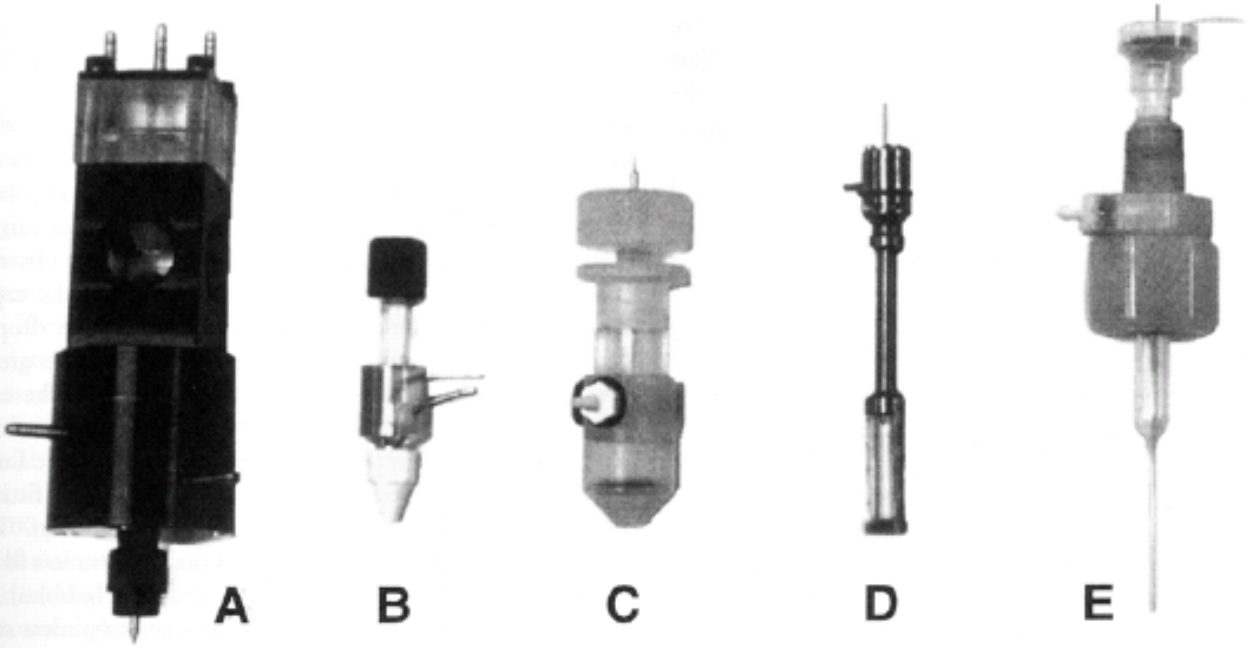

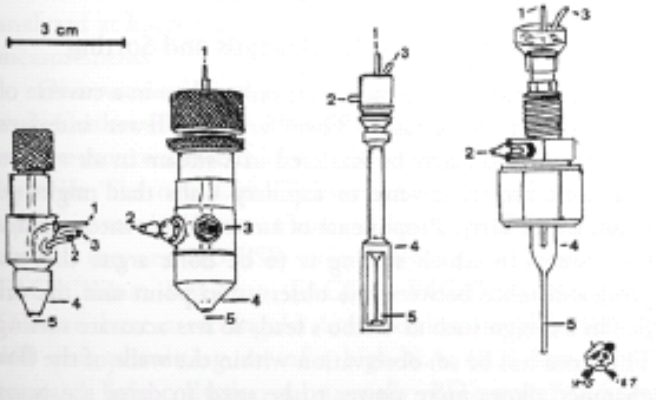

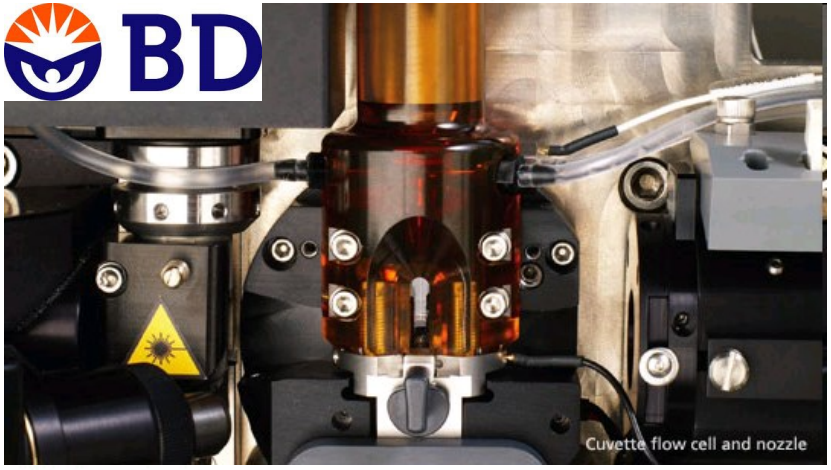

Shapiro 4.ed.p 169

Particle Delivery: Hydrodynamic Focusing

Conventional Instrumentation: **Low Flow Rates (12µL/min)**

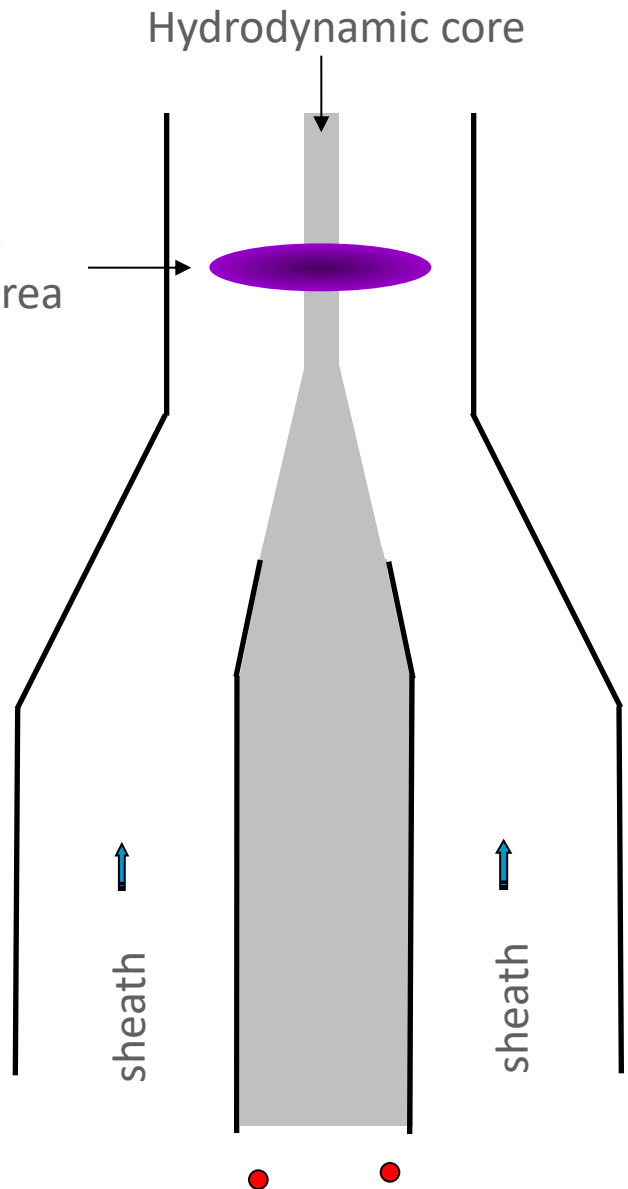

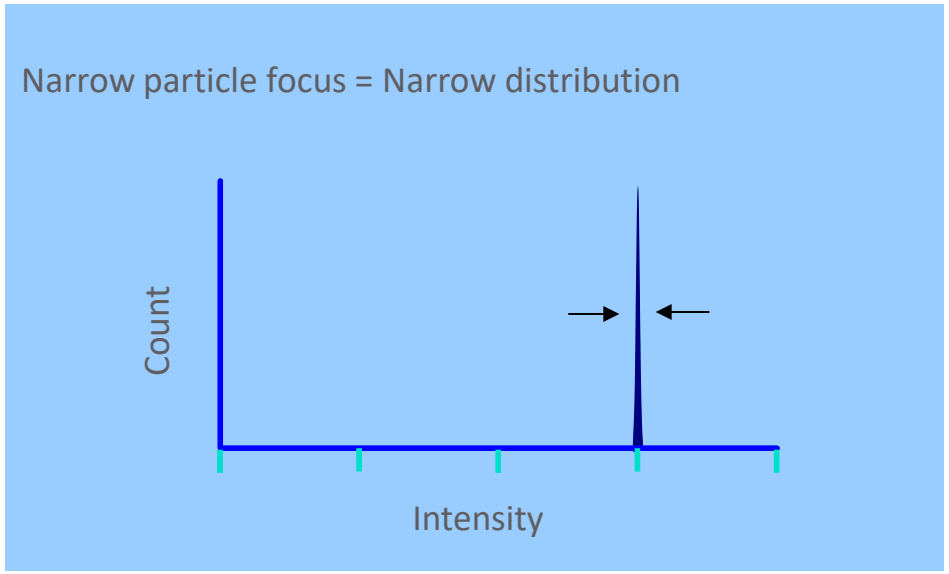

- Sample core is 'pinched' by fast flowing sheath
- Sample volume ratios of 100 – 1000
- Large ratios => low sample inputs
- Resolution of particle populations

molecular probes® by life technologies™

Particle Delivery: Hydrodynamic Focusing

Conventional Instrumentation: **High Flow Rate (60µL/min)**

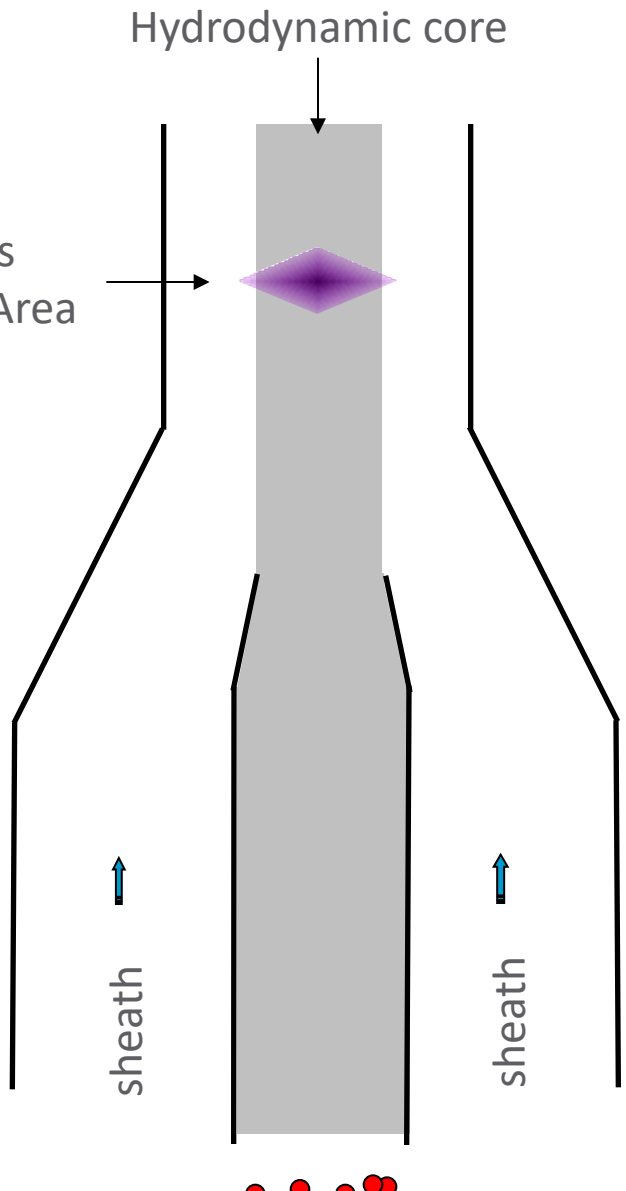

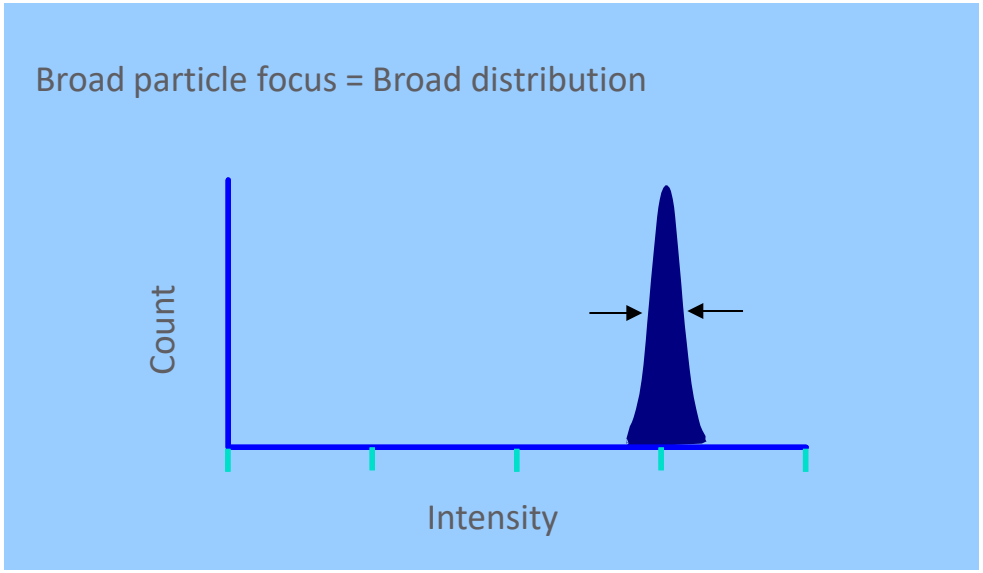

- Increased sample input = increase core size
- Particle distributions broadened, CVs increase
- Instrument resolution decreased
- Historically, low volumetric sample rates used (25 µl/min – 150 µl/min)

molecular probes® by life technologies™

Attune® Acoustic Focusing Cytometer

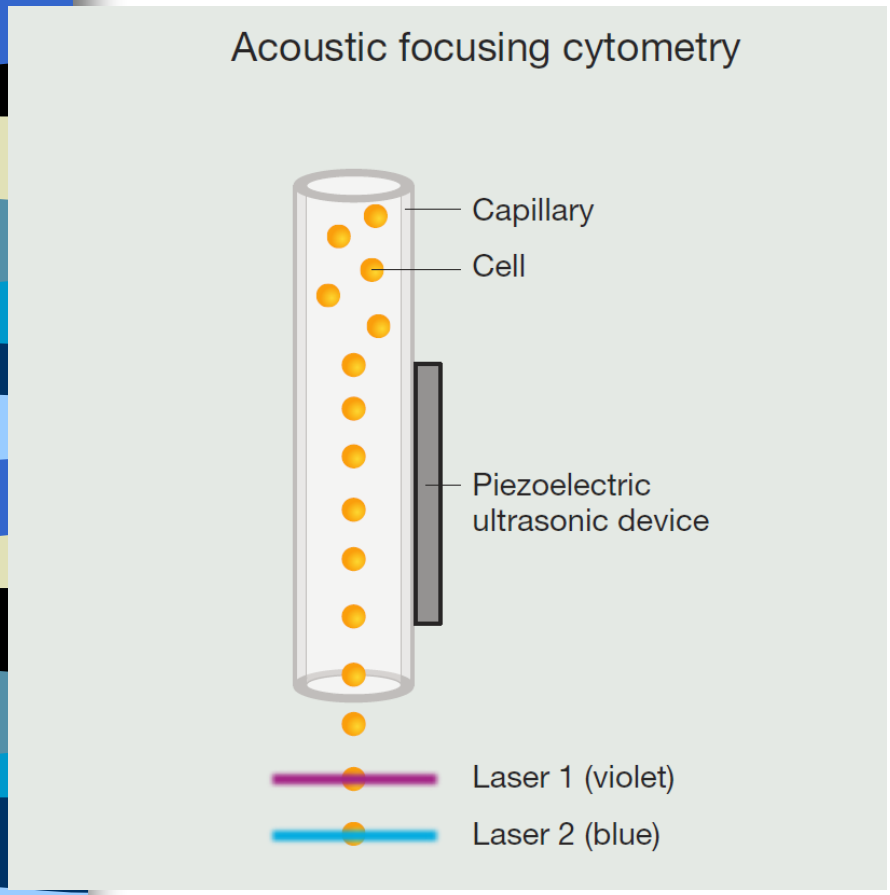

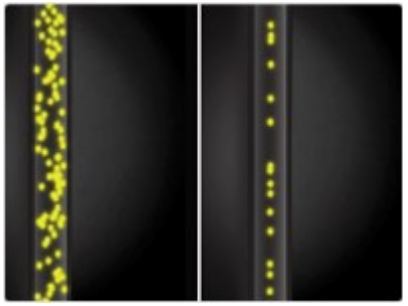

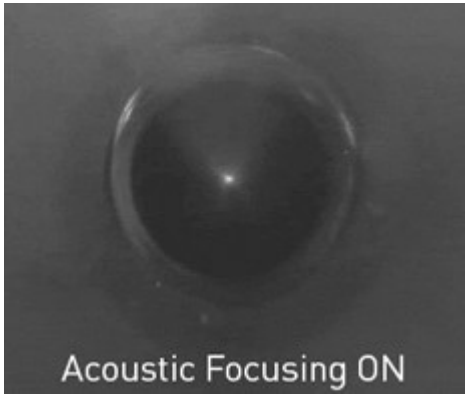

ThermoFisher
SCIENTIFIC

Acoustic Focusing = Better Precision

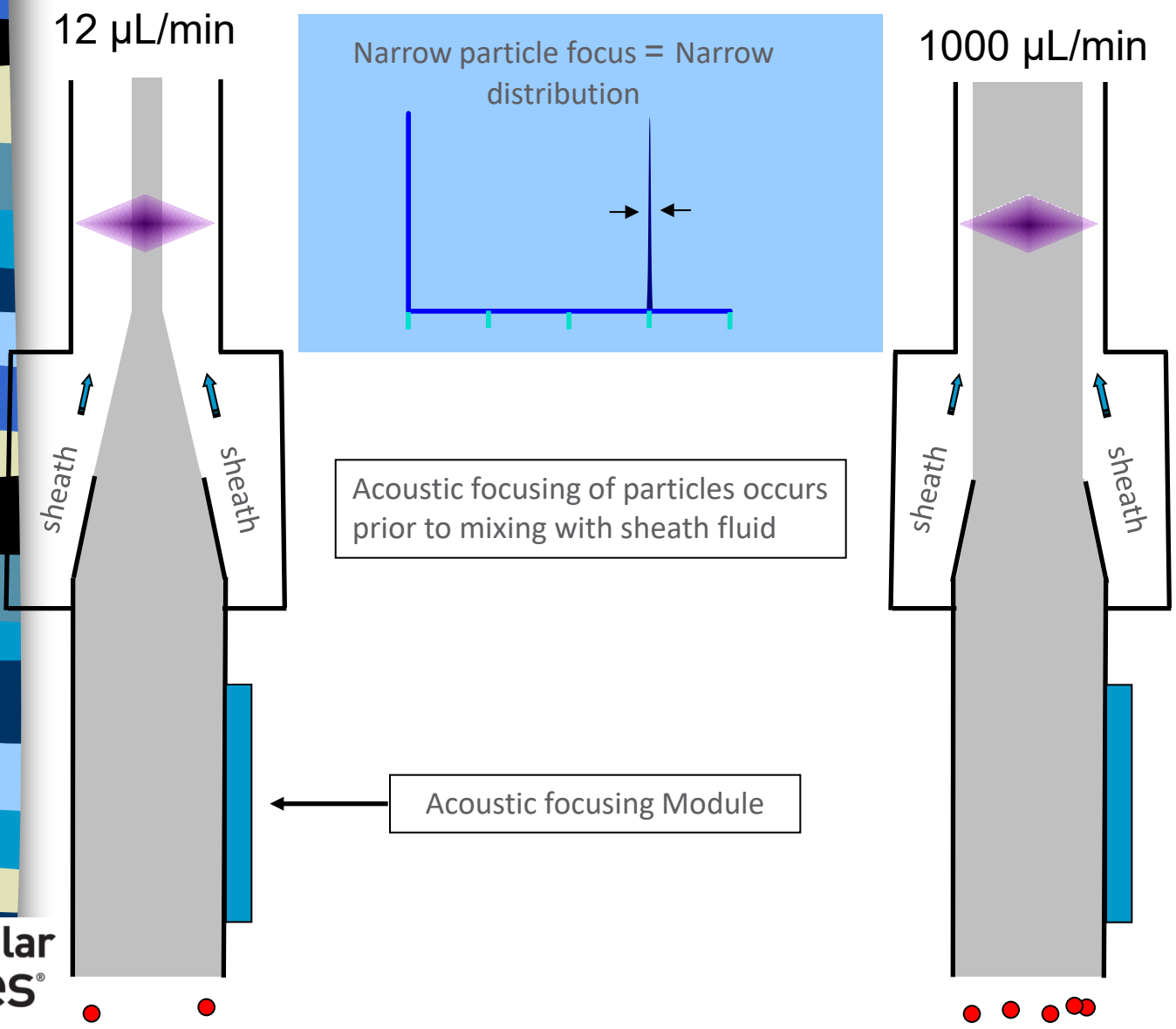

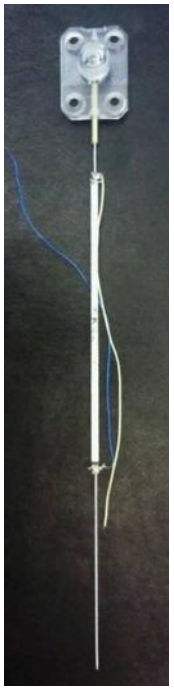

molecular probes® by life technologies™

1. Kundt A, Lehmann O (1874) *Annalen der Physik und Chemie (Poggendorff's Annalen)* 153:1–11.
2. Curtis HW, Stephans EJ (1982) *IBM Technical Disclosure Bulletin* 25(1).
3. Yasuda K, Haupt SS, Unemura S (1997) *J Acoust Soc Am* 102:642–645.
4. Jonsson H, Nilsson A, Petersson F et al. (2005) *Perfusion* 20:39–43.
5. Kaduchak G, Goddard G, Salzman G et al. (2008) US Patent 7,340,957.

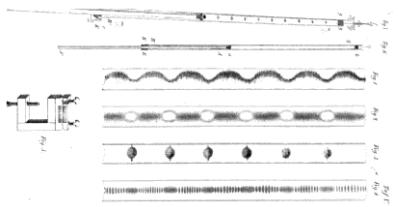

Using acoustic radiation force as a concentration method for erythrocytes

Kenji Yasuda,[a] Stephan Shuichi Haupt, and Shin-ichiro Umemura
Advanced Research Laboratory, Hitachi, Ltd., 2520 Akanuma, Hatoyama, Saitama 350-03, Japan

Toshiki Yagi
Zoological Institute, Faculty of Science, University of Tokyo, Hongo, Tokyo 113, Japan

Masaharu Nishida and Yasuhisa Shibata
Instrument Division, Hitachi, Ltd., 882 Ichige, Hitachinaka, Ibaraki 312, Japan

(Received 20 May 1996; accepted for publication 7 March 1997)

We investigated the potential damage in icted on erythrocytes by acoustic radiation force when the cells are concentrated by a 500-kHz ultrasonic standing wave at the pressure node. The extent of the damage was estimated from the concentrations of potassium ions, iron complexes, and lactate dehydrogenase released from the cells. After 2 min of ultrasound irradiation at 12.8 mJ/m^3, the cells concentrated on the pressure node, with a cell distribution half-width of 138 μm; no significant release of intracellular components was detected, even after 15 min of irradiation. The results indicate that even small ions like potassium are not released as a result of ultrasound irradiation on cell membranes without cavitation, and they demonstrate the potential use of acoustic radiation force for concentrating living cells in biomedical applications. © *1997 Acoustical Society of America.* [S0001-4966(97)01407-0]

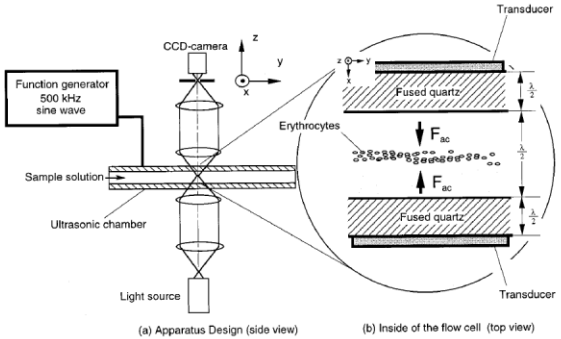

FIG. 1. Schematic diagram of the apparatus for concentration of erythrocytes.

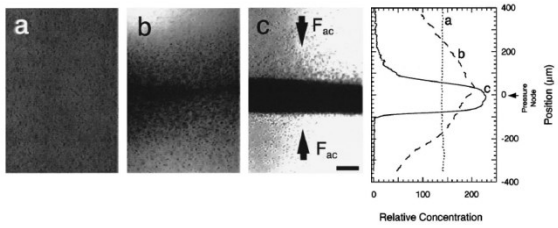

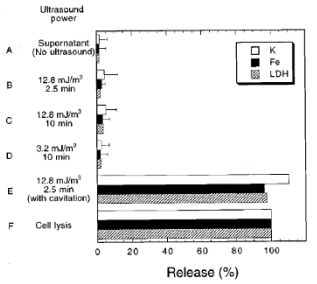

US007340957B2

(12) **United States Patent**
Kaduchak et al.

(10) **Patent No.: US 7,340,957 B2**
(45) **Date of Patent: Mar. 11, 2008**

(54) **ULTRASONIC ANALYTE CONCENTRATION AND APPLICATION IN FLOW CYTOMETRY**

(75) Inventors: **Gregory Kaduchak**, Los Alamos, NM (US); **Greg Goddard**, Los Alamos, NM (US); **Gary Salzman**, White Rock, NM (US); **Dipen Sinha**, Los Alamos, NM (US); **John C. Martin**, Los Alamos, NM (US); **Christopher Kwiatkowski**, Los Alamos, NM (US); **Steven Graves**, San Juan Pueblo, NM (US)

(73) Assignee: **Los Alamos National Security, LLC**, Los Alamos, NM (US)

(*) Notice: Subject to any disclaimer, the term of this patent is extended or adjusted under 35 U.S.C. 154(b) by 143 days.

(21) Appl. No.: **10/979,065**

(22) Filed: **Nov. 2, 2004**

4,523,982	A *	6/1985	Lee	522/21
5,831,166	A *	11/1998	Kozuka et al.	73/570
6,003,388	A *	12/1999	Oeftering	73/864.01
6,216,538	B1 *	4/2001	Yasuda et al.	73/570.5
6,449,563	B1 *	9/2002	Dukhin et al.	702/22
2004/0139792	A1 *	7/2004	Cobb	73/61.75

FOREIGN PATENT DOCUMENTS

JP	63139231	A *	6/1988
JP	06241977	A *	9/1994
JP	08266891	A *	10/1996

OTHER PUBLICATIONS

King, L. V., "On the acoustic radiation on spheres," *Proc. R. Soc. A.*, 147, 212-240, (1933).

(Continued)

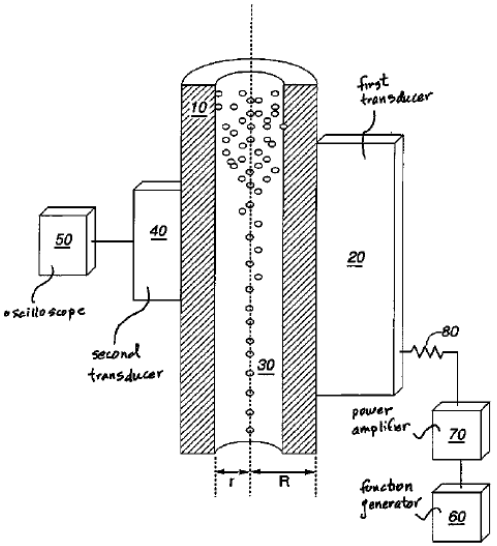

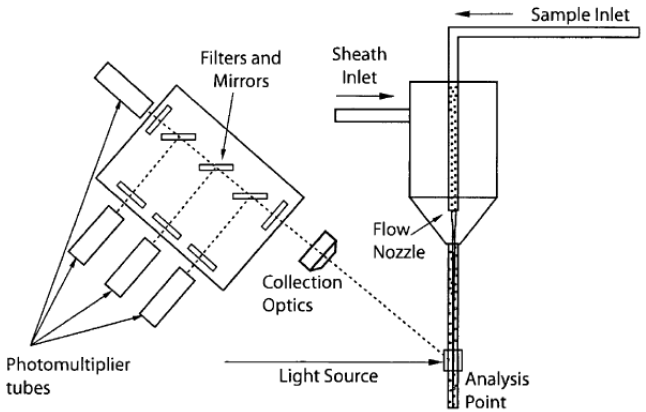

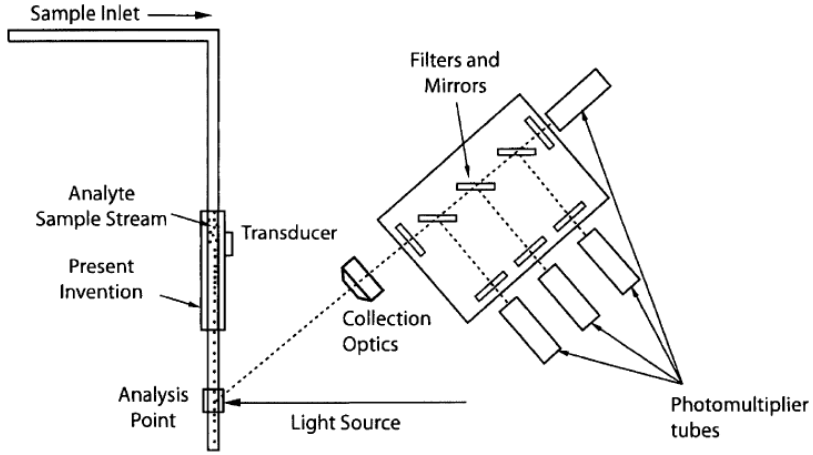

life technologies™

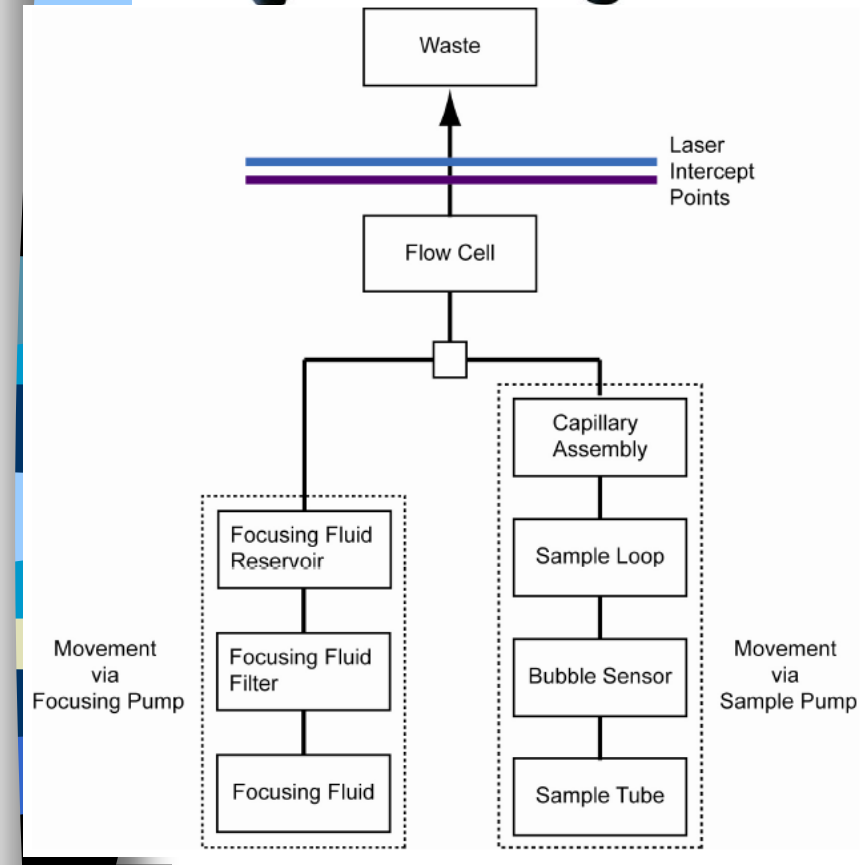

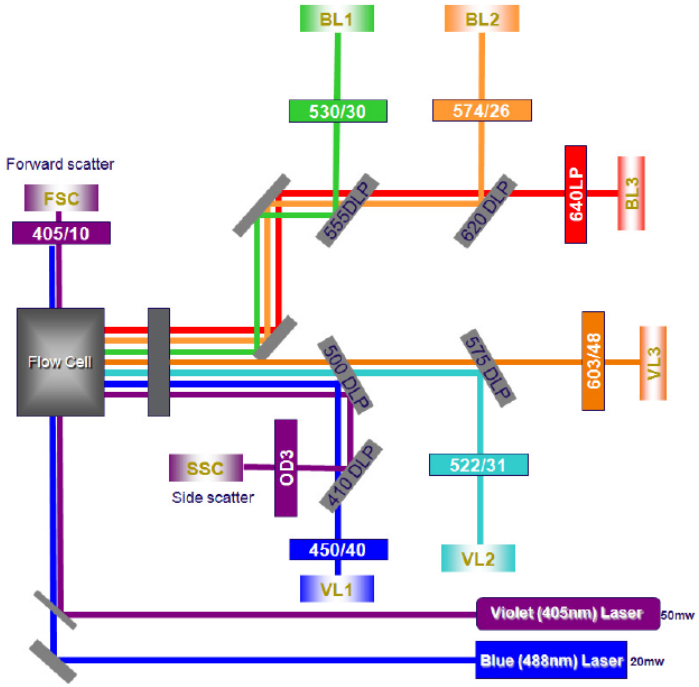

Attune NxT (2nd generation)

ThermoFisher SCIENTIFIC

Lasers	Laser configuration (Cat. No.)	Violet 405 nm	Blue 488 nm	Yellow 561 nm	Green 532 nm	Red 637 nm	Total detection channels*
1	Blue (A24864)	Available as upgrade	4	Available as upgrade	Available as upgrade	Available as upgrade	6
2	Blue/green (A28995)	Available as upgrade	3	–	4	Available as upgrade	9
	Blue/yellow (A24861)	Available as upgrade	3	4	–	Available as upgrade	9
	Blue/violet (A24862)	4	4	Available as upgrade	Available as upgrade	Available as upgrade	10
	Blue/red (A24863)	Available as upgrade	4	Available as upgrade	Available as upgrade	3	9
3	Blue/green/red (A28997)	Available as upgrade	3	–	4	3	12
	Blue/green/violet (A28999)	4	3	–	4	Available as upgrade	13
	Blue/red/yellow (A28993)	Available as upgrade	3	4	–	3	12
	Blue/violet/yellow (A24859)	4	3	4	–	Available as upgrade	13
	Blue/red/violet (A24860)	4	4	Available as upgrade	Available as upgrade	3	13
4	Blue/red/violet/ green (A29001)	4	3	–	4	3	16
	Blue/red/yellow/ violet (A24858)	4	3	4	–	3	16

* Includes forward scatter (FSC) and side scatter (SSC).

Attune® Throughput Compared to Hydrodynamic Focused Instruments

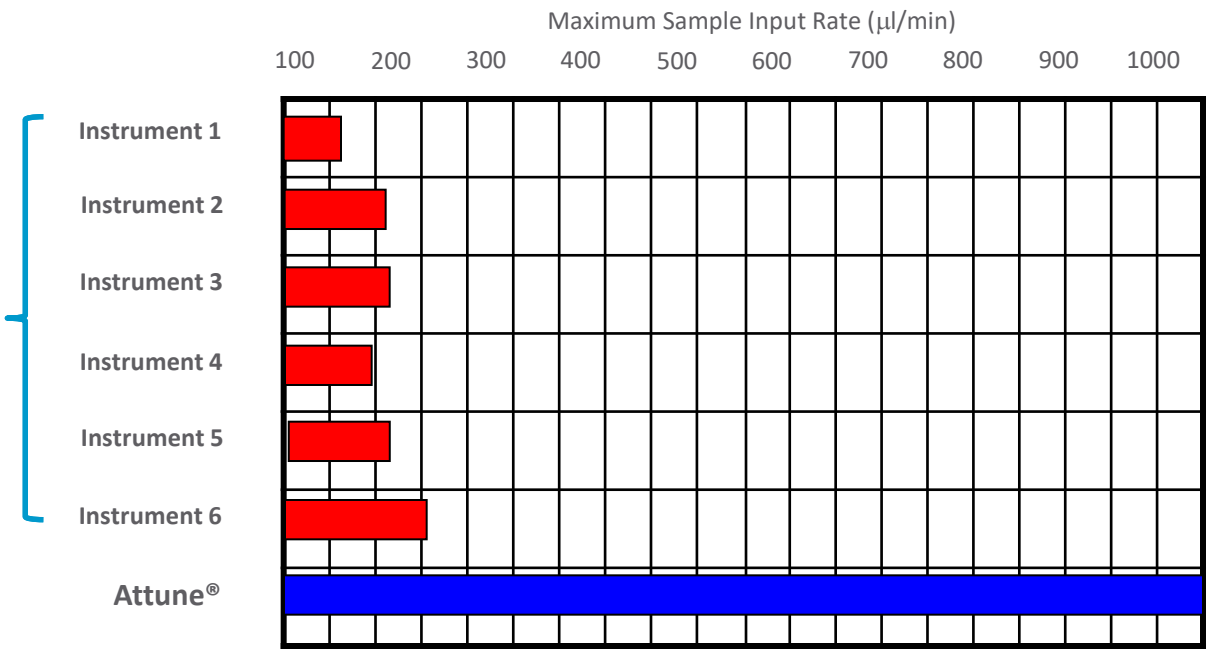

- Attune® can analyze at sample rates from 25µL/min to 1000µL/min without losing accuracy
- Traditional Flow Cytometers can only run at most 150µL/min and will sacrifice data quality
- Higher sample rates enable dilution of limited samples and analysis of Rare Events Faster

molecular probes® by life technologies™

Fluidika - shrnutí

- Průtok musí být laminární (Reynoldovo #)
  - R_e < 2300, flow je vždy laminarní
- Vzorky mohou být injikovány a nebo proudit na základě rozdílných tlaků
- Existuje mnoho typů průtokových komor
- Pro přesnost měření je nutné odstranit a zabránit ucpání komory

Fluidika – shrnutí 2

• tlak nosné (oplašťující) kapaliny vede pufr kyvetou a vyšší tlak ve zkumavce se vzorkem zavádí vzorek do kyvety.

• Princip hydrodynamického zaostření zarovná buňky v kyvetě „jako perly na šňůrce“ předtím než dojdou do bodu kde protnout paprsek laseru.

•Hydrodynamické zaostření nemůže oddělit buněčné agregáty. Průtoková cytometrie vyžaduje suspenzi jednotlivých buněk!

Principy průtokové cytometrie a sortrování

- sorting

Doležel (1999)

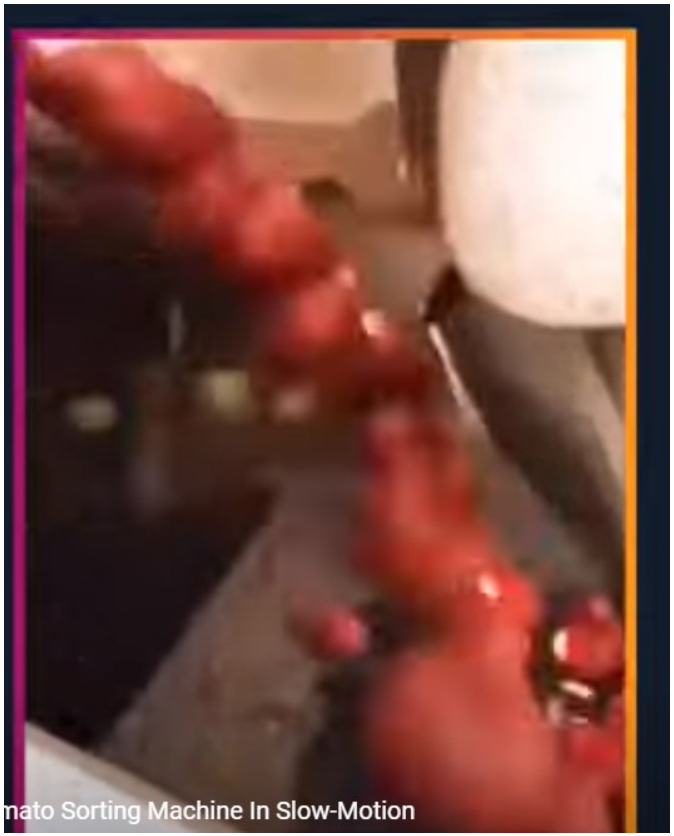
mato Sorting Machine In Slow-Motion

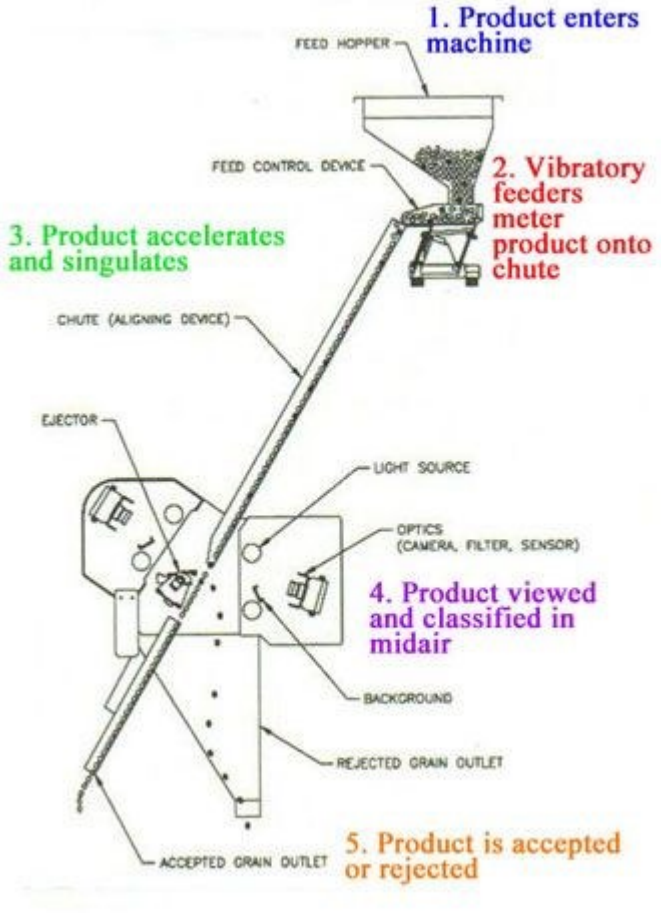
1. Product enters machine
FEED HOPPER
FEED CONTROL DEVICE
2. Vibratory feeders meter product onto chute
3. Product accelerates and singulates
CHUTE (ALIGNING DEVICE)
EJECTOR
LIGHT SOURCE
OPTICS (CAMERA, FILTER, SENSOR)
4. Product viewed and classified in midair
BACKGROUND
REJECTED GRAIN OUTLET
ACCEPTED GRAIN OUTLET
5. Product is accepted or rejected

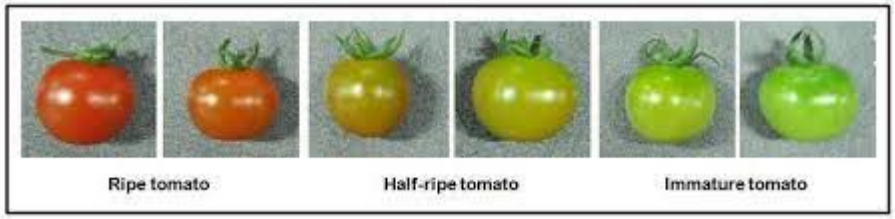
Ripe tomato
Half-ripe tomato
Immature tomato

ELECTROSTATIC DROPLET SORTER

- High speed (~10^4/sec)
- Concentrated sorted fraction

- Biosafefy hazard
- Mechanical shearing
- Problems to sort large particles

Used by:
Becton Dickinson
Beckman Coulter
Cytomation

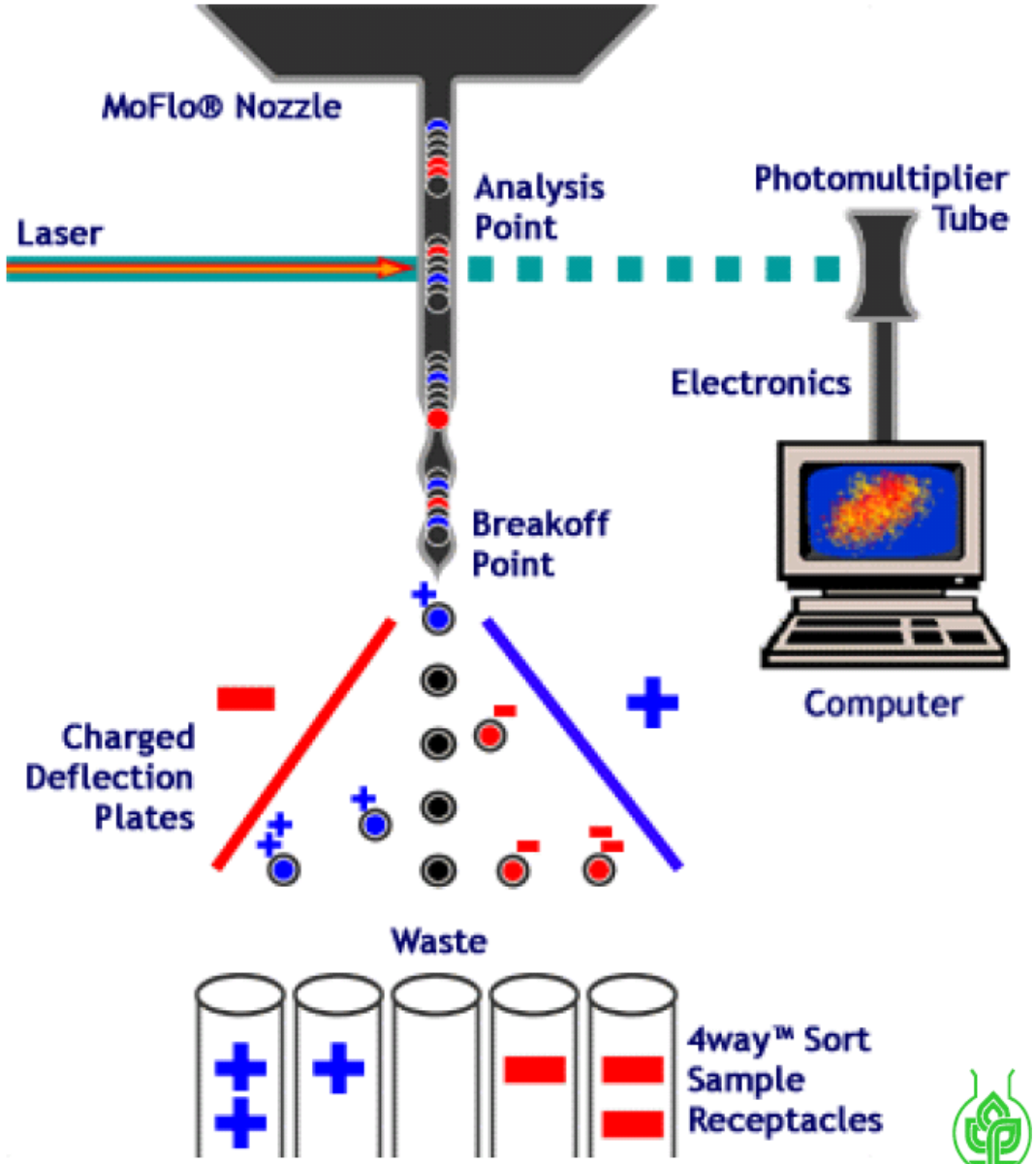

Doležel (1999)

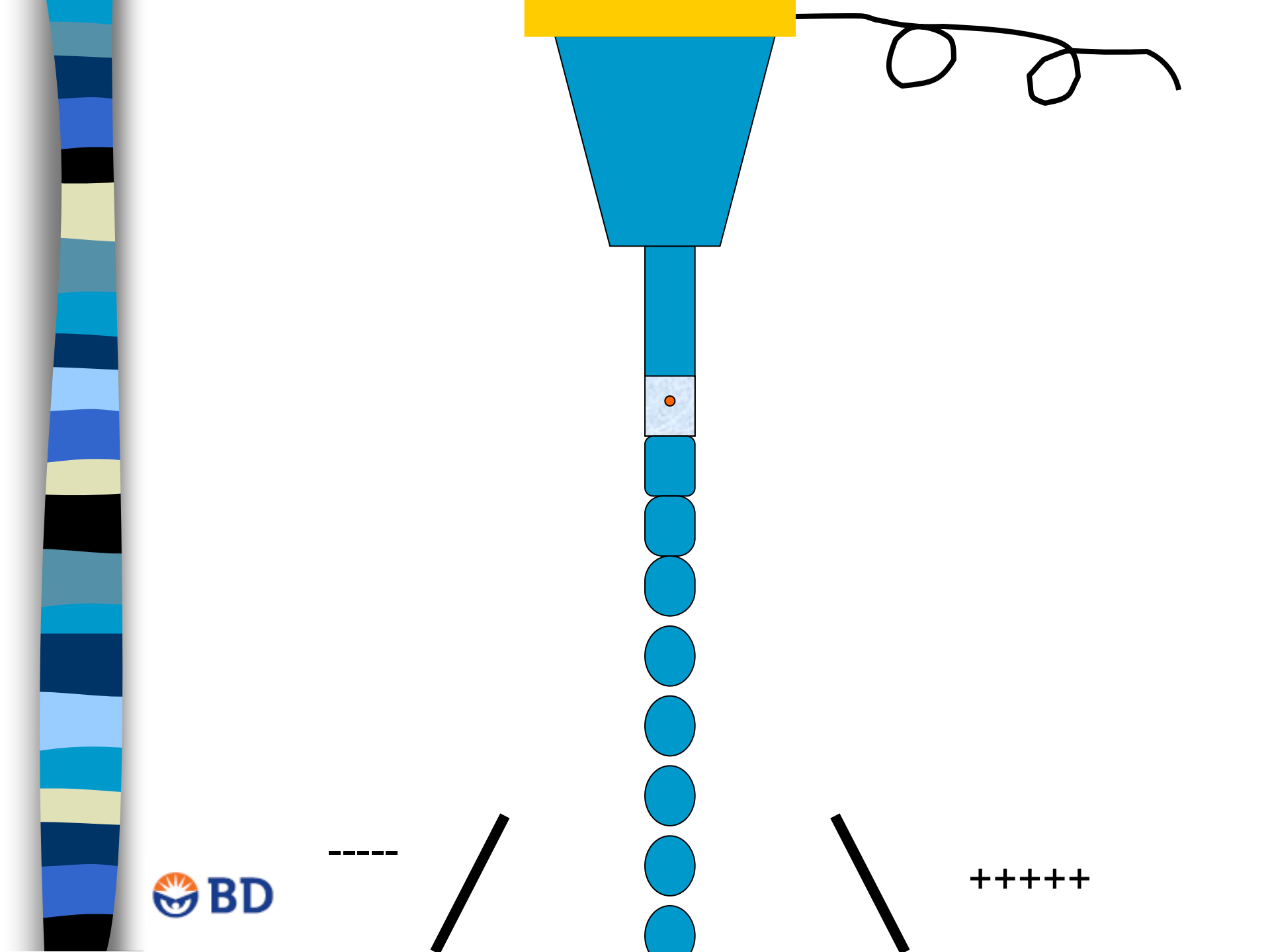

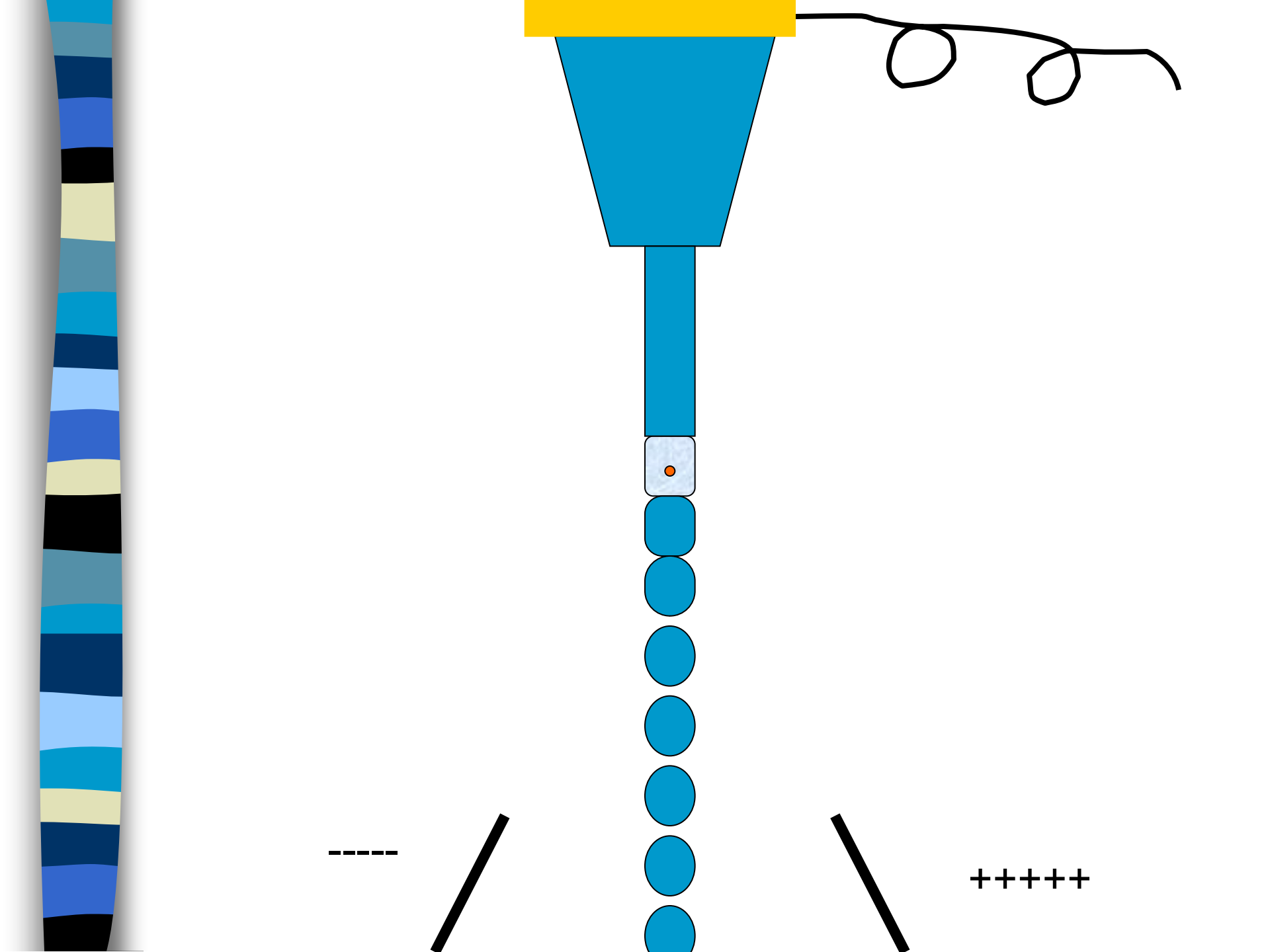

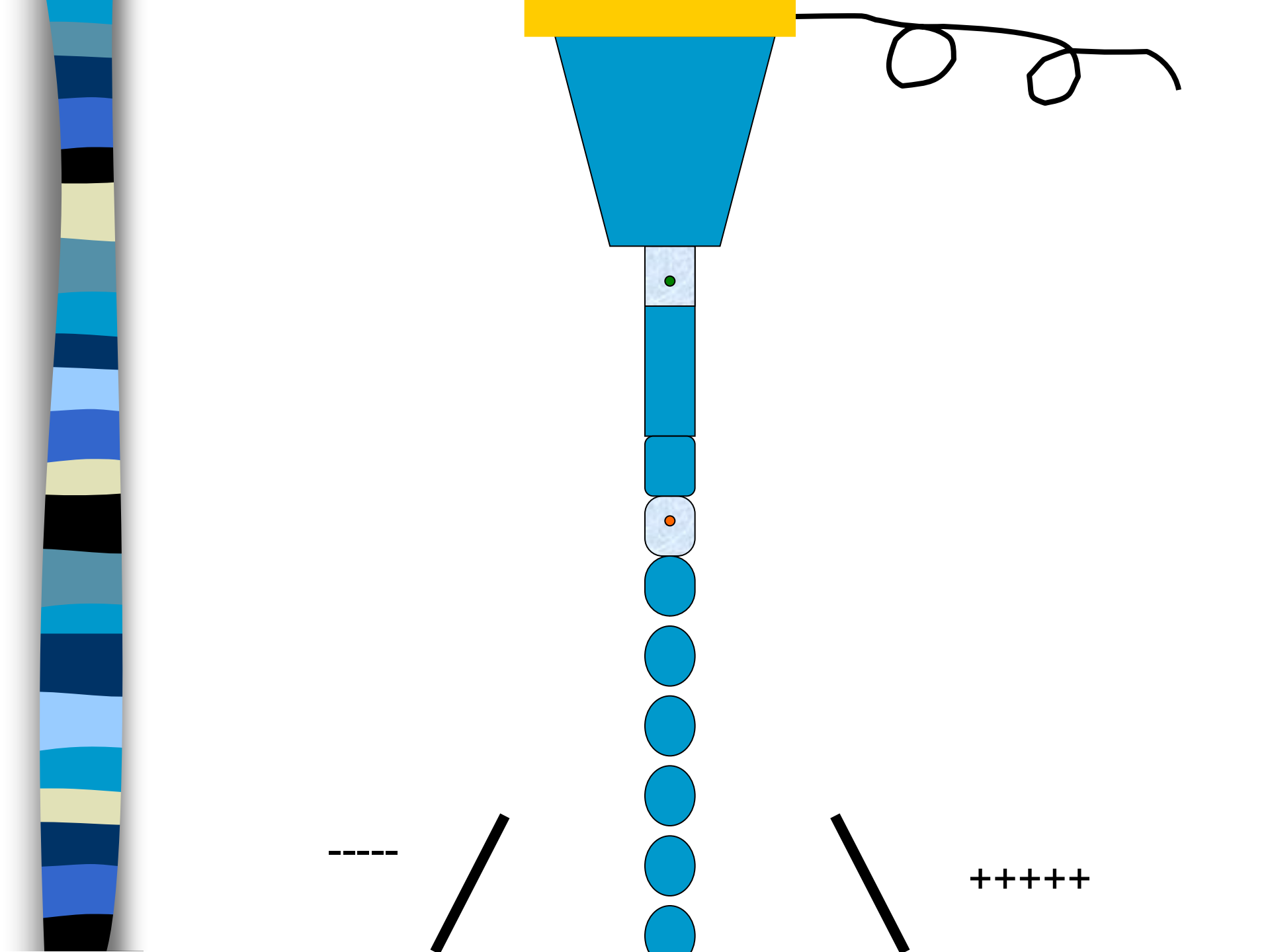

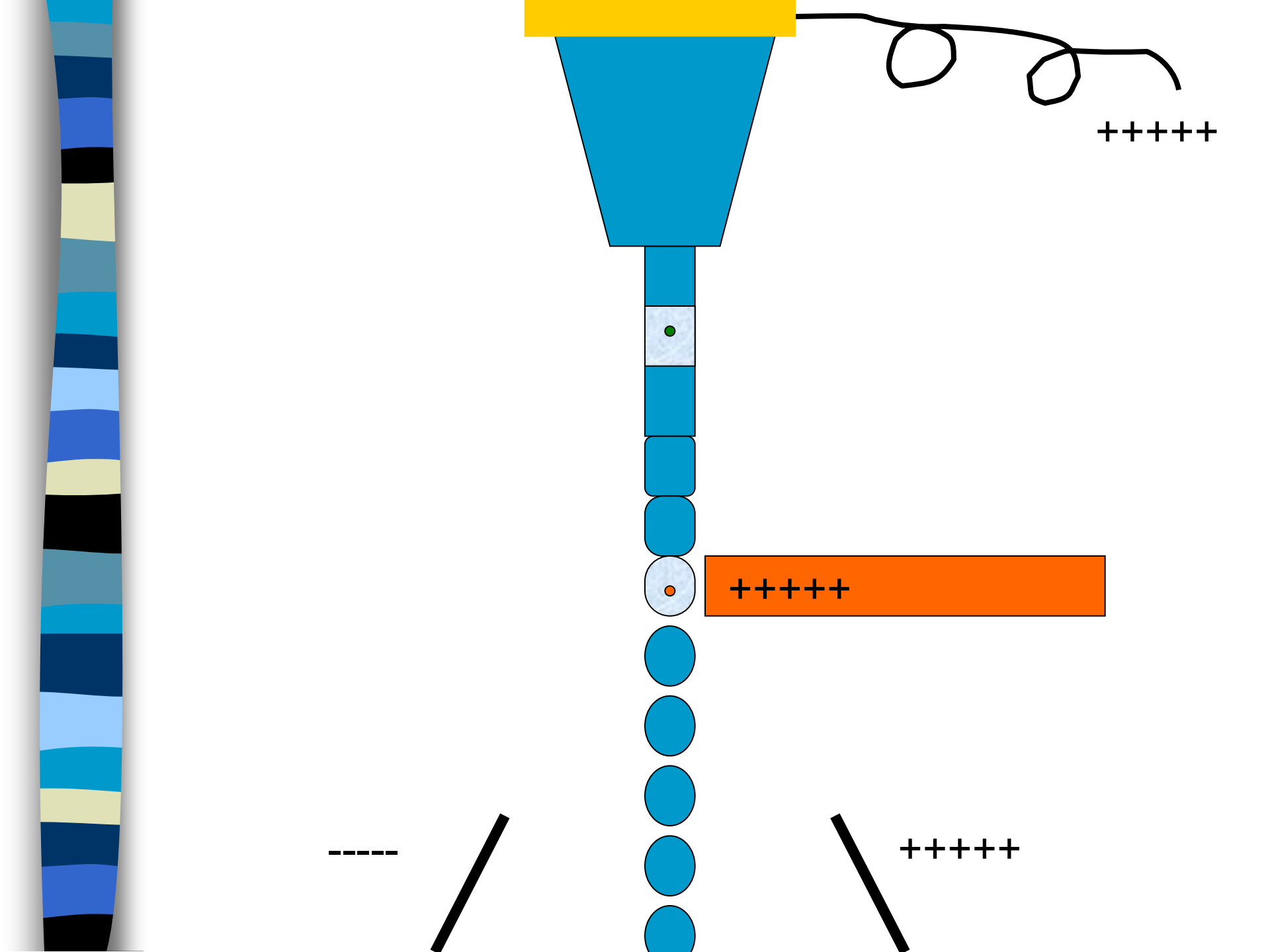

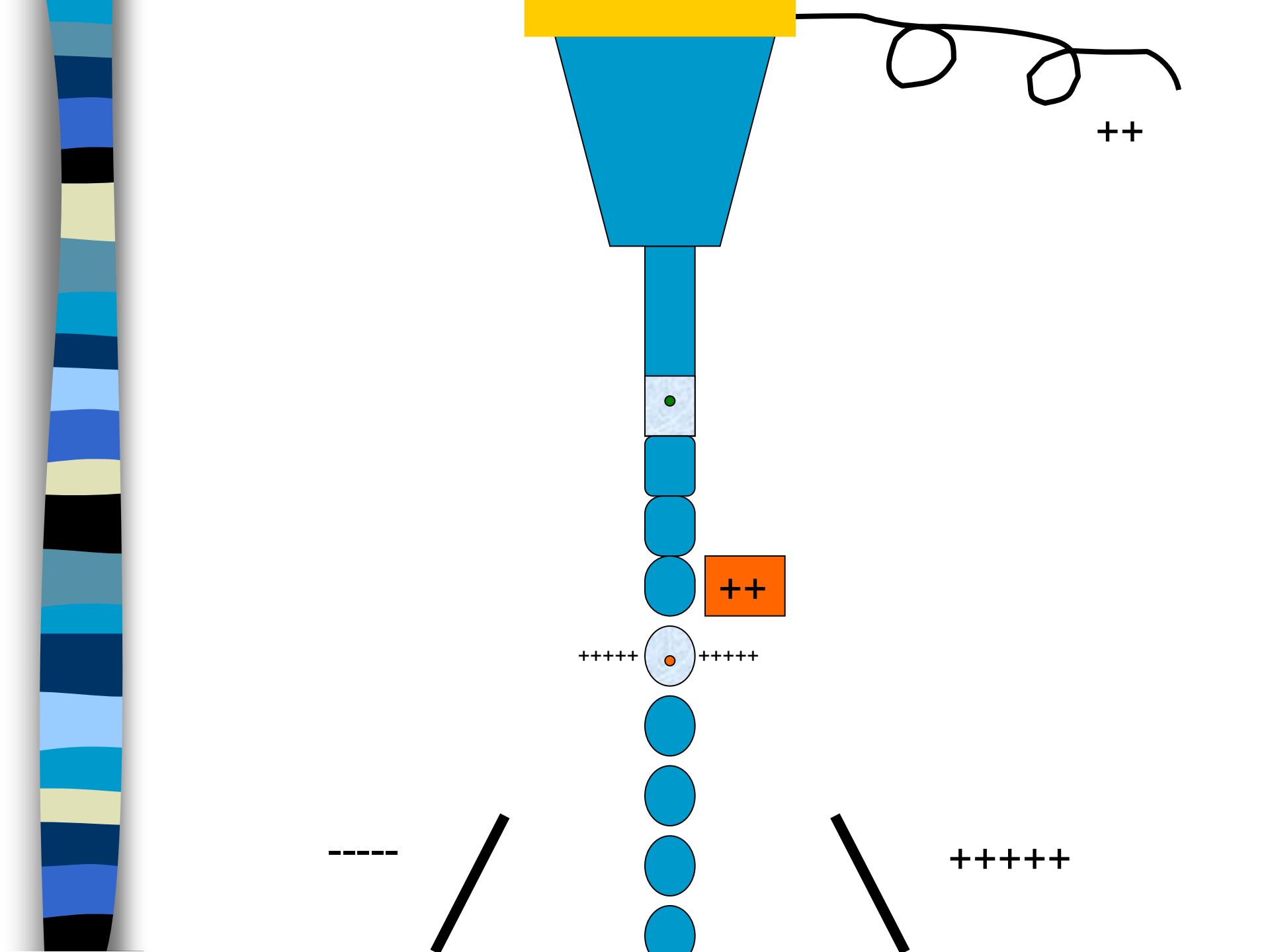

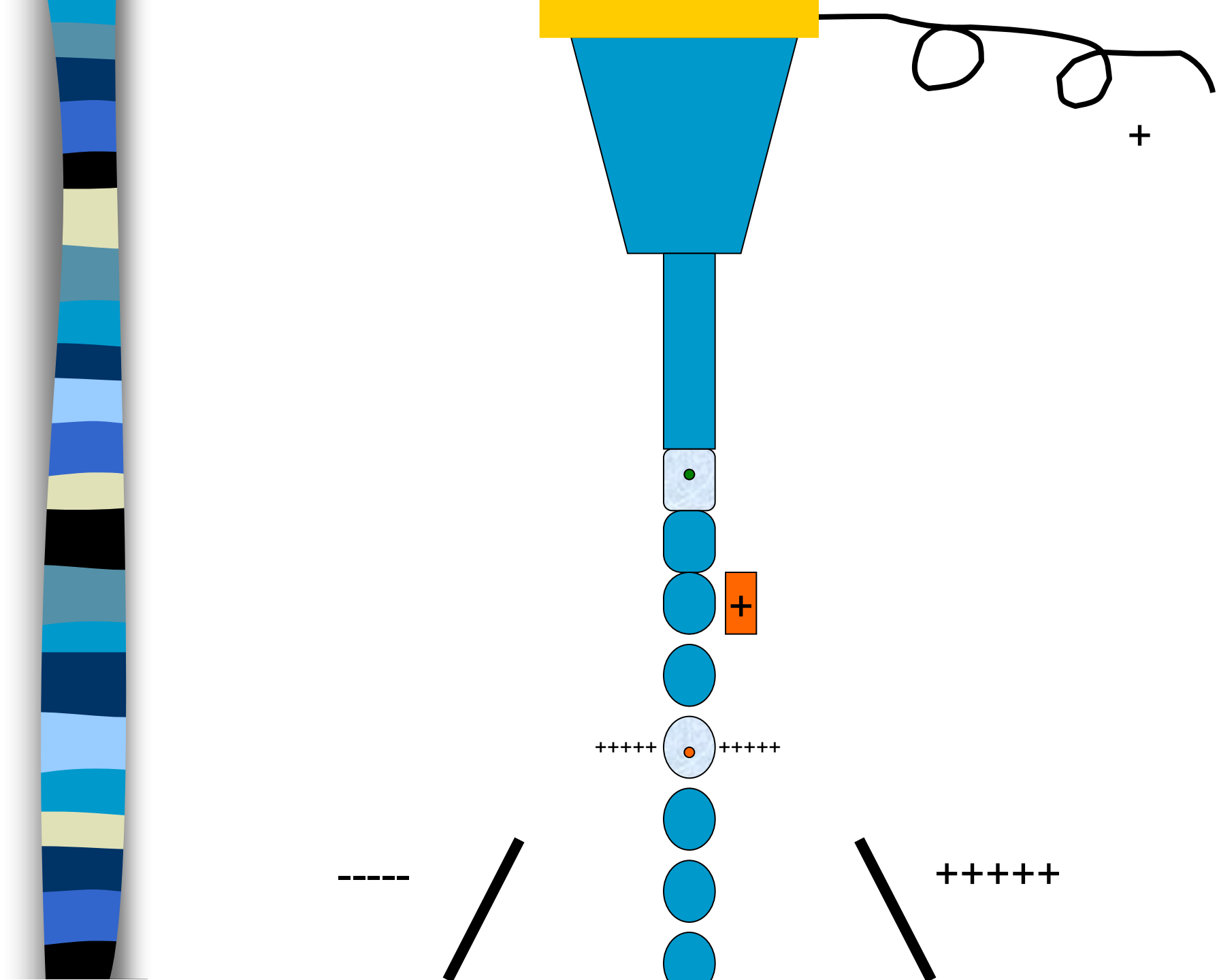

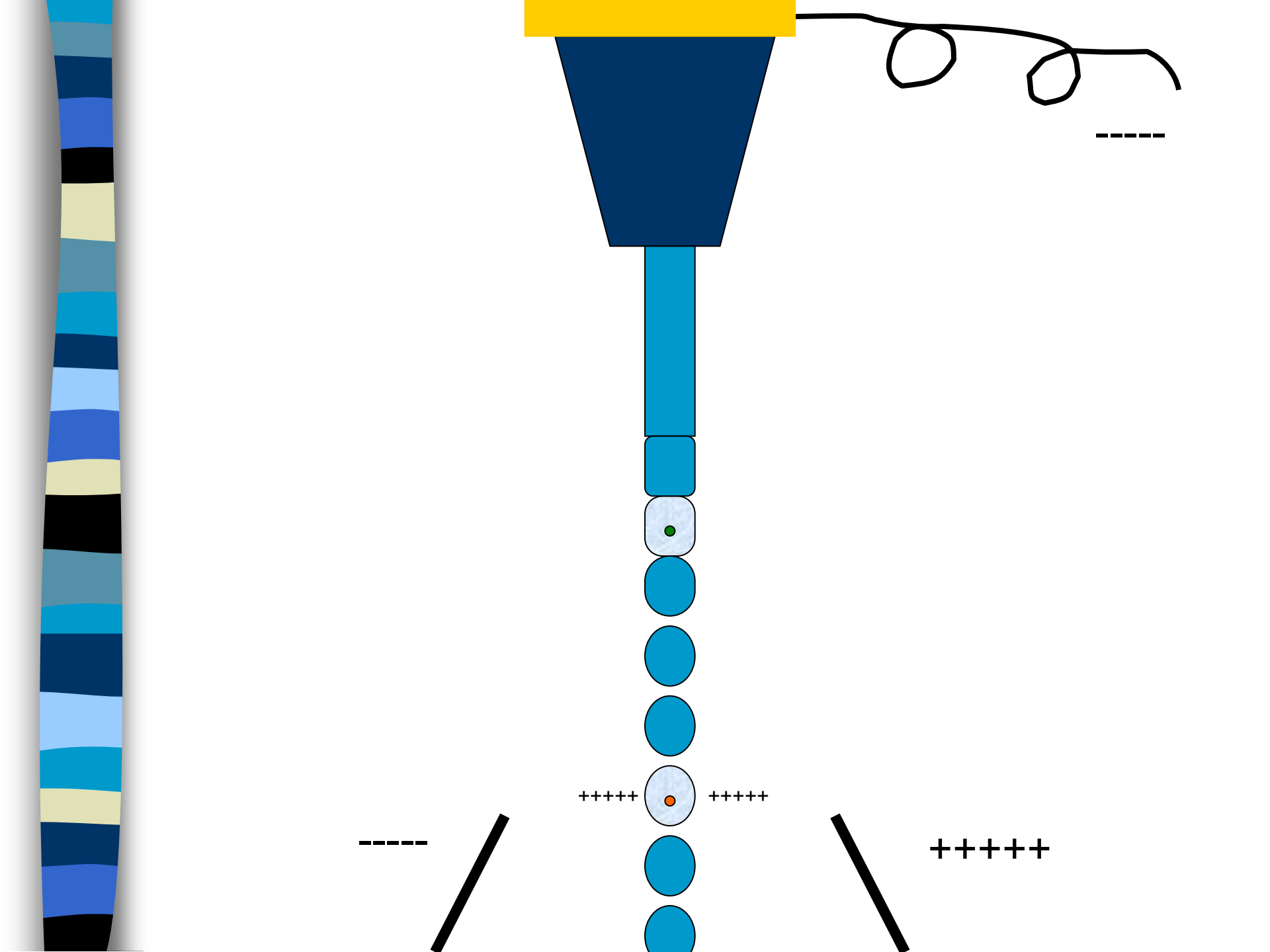

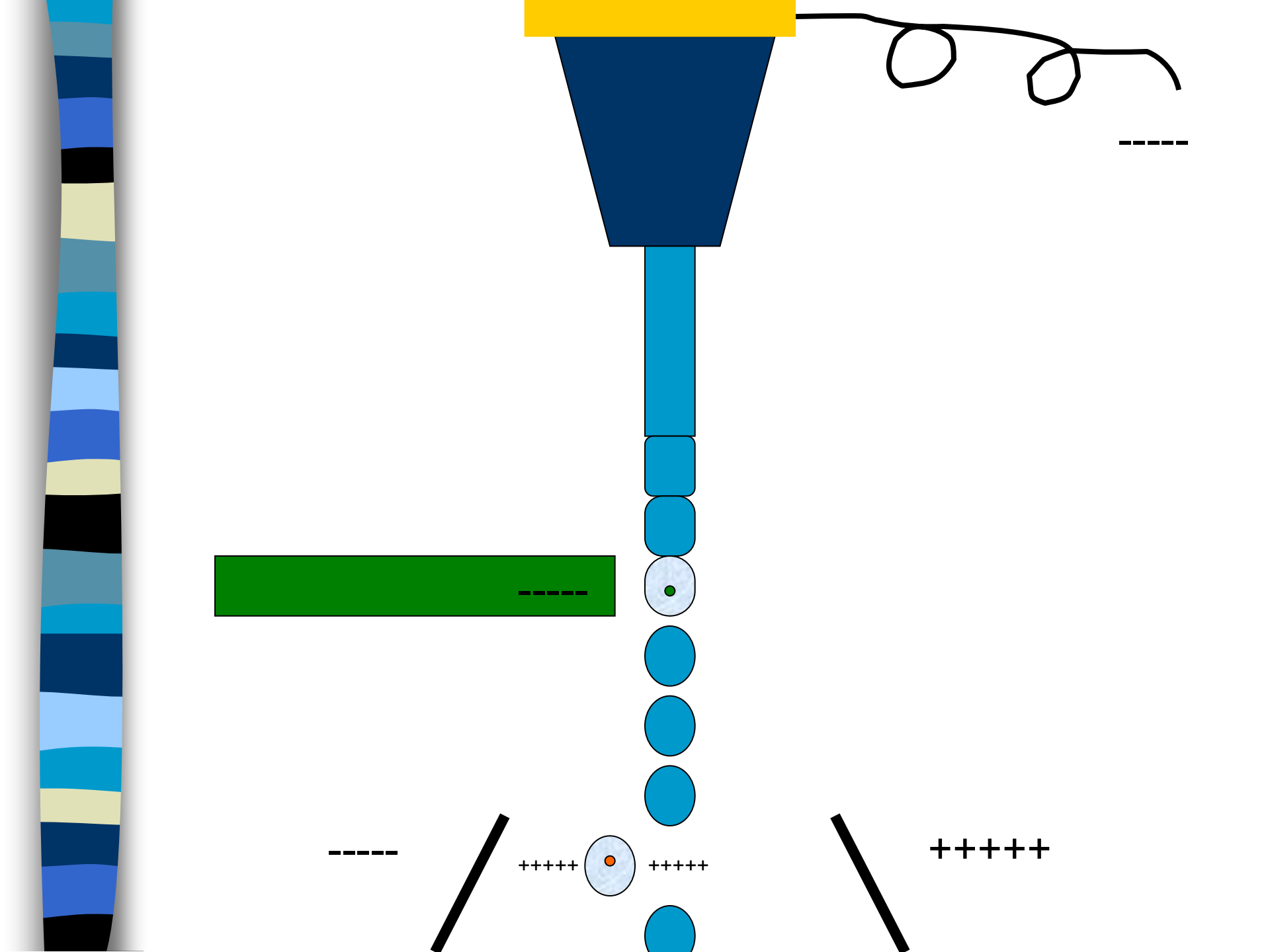

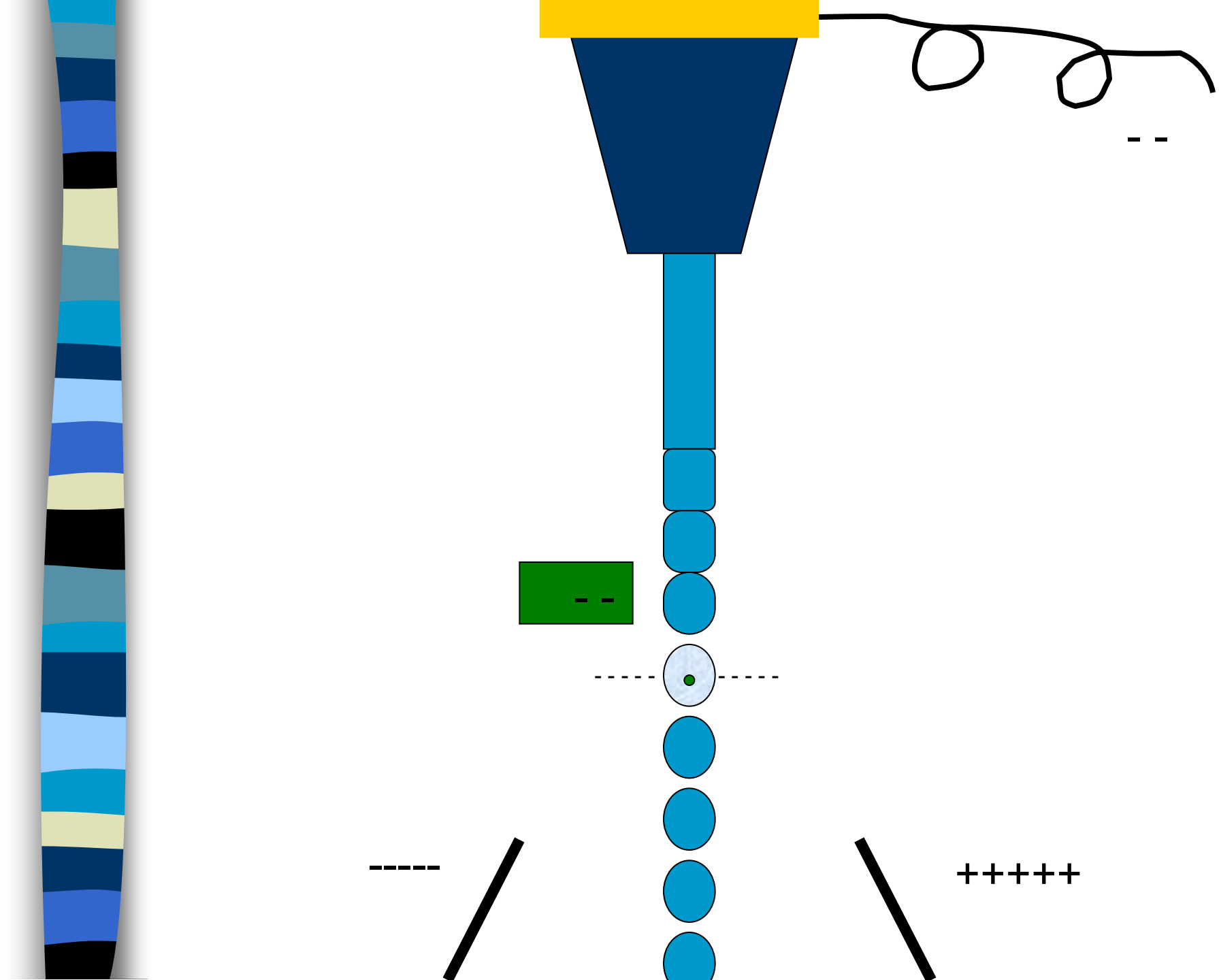

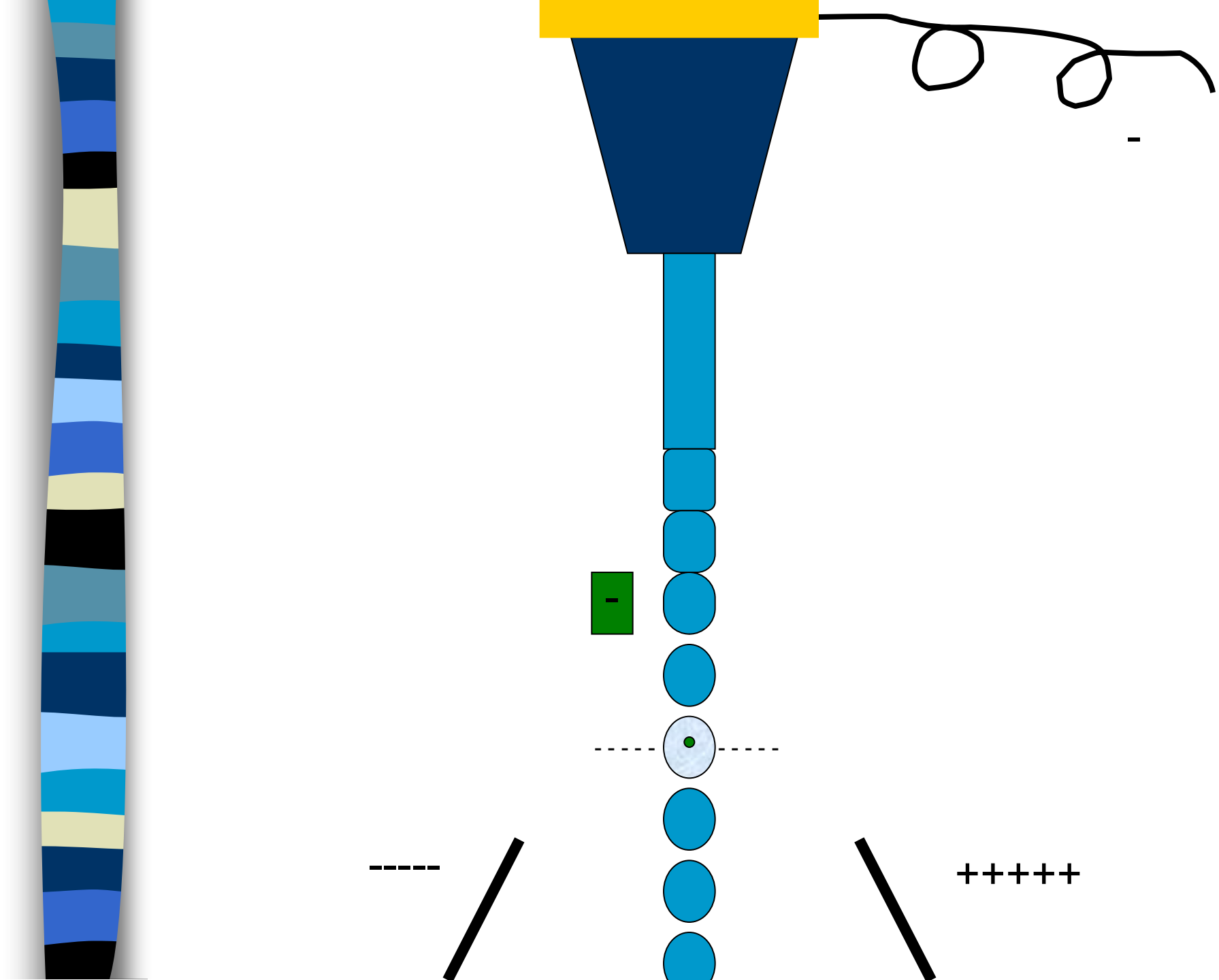

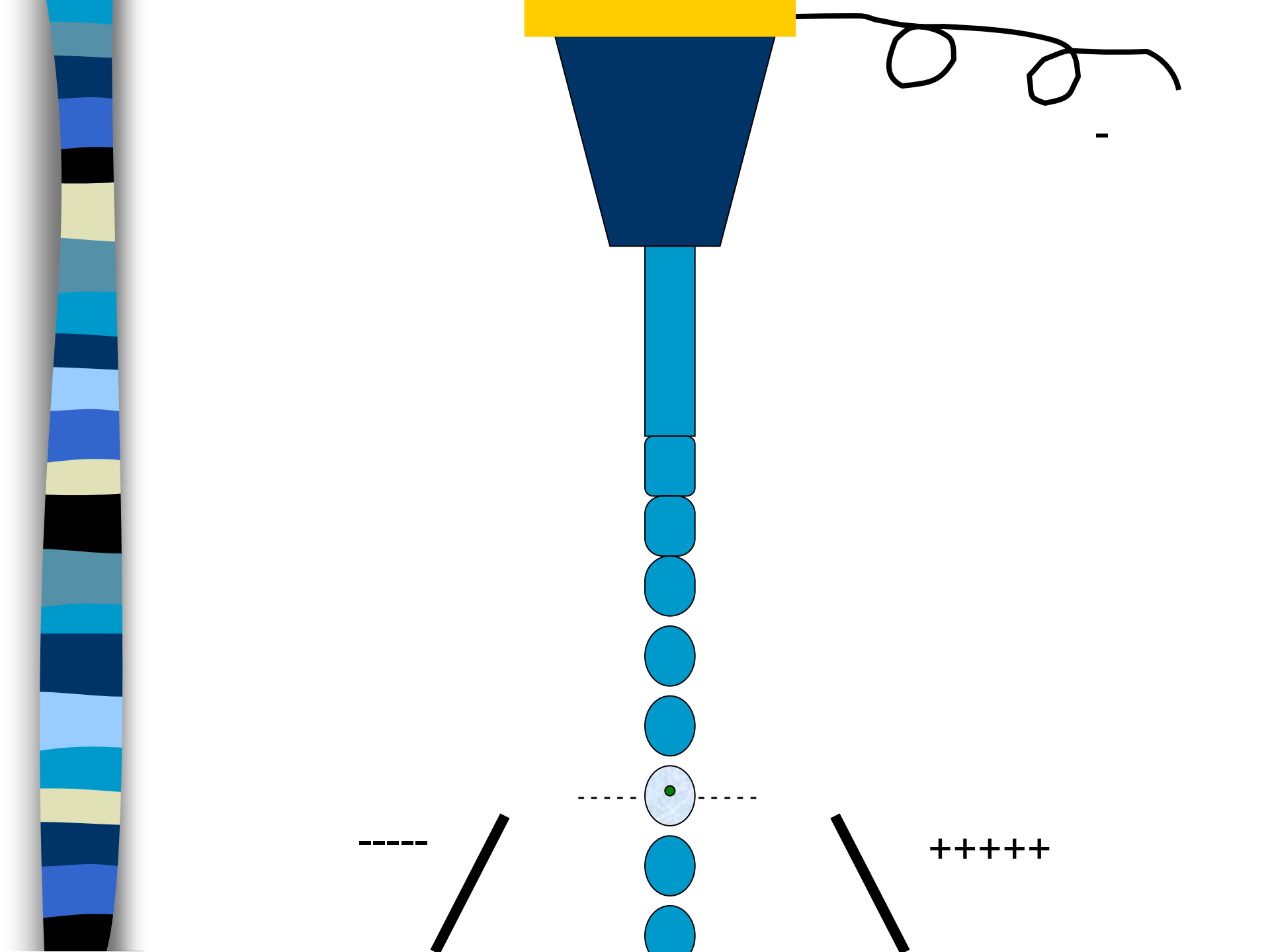

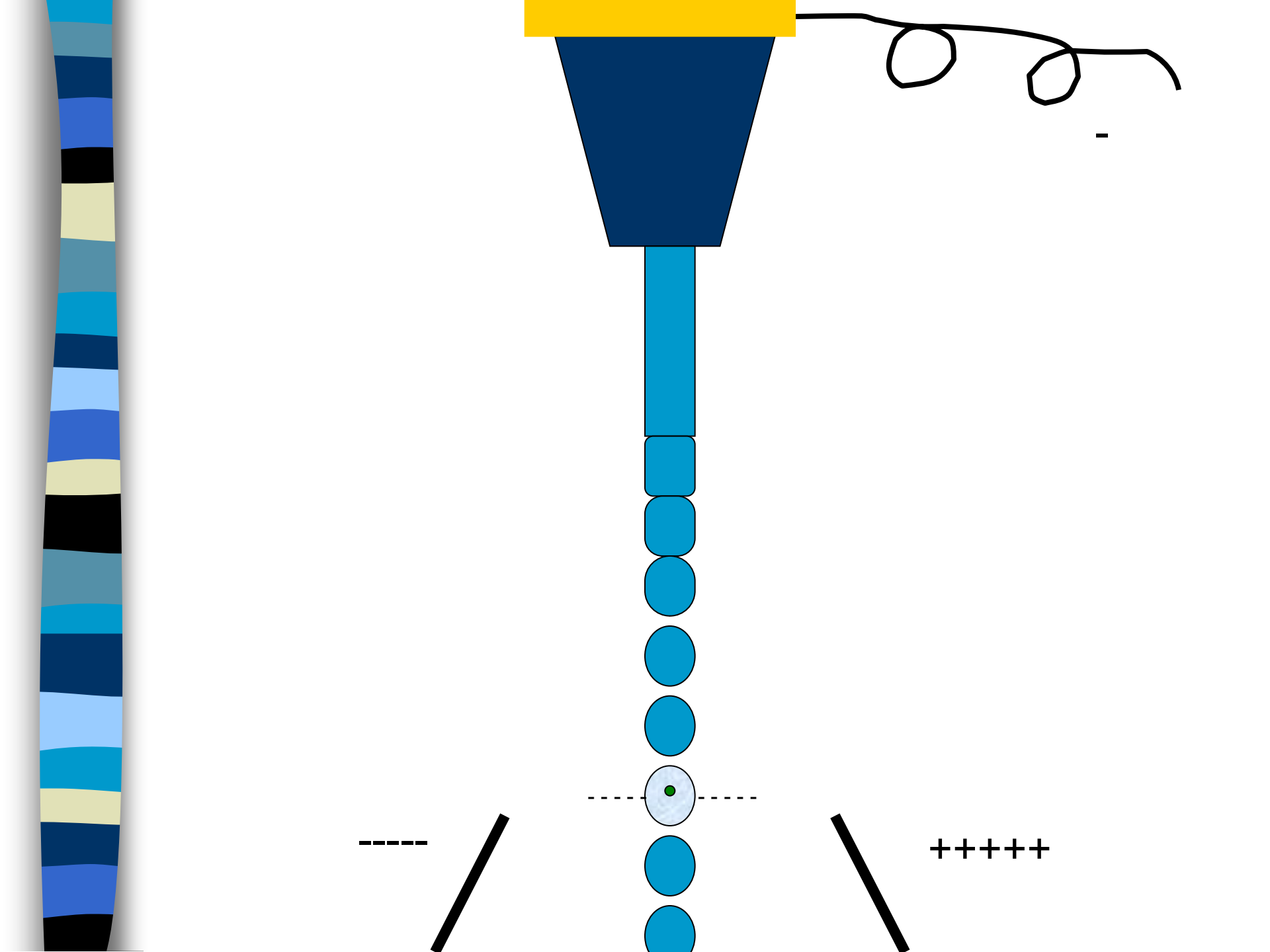

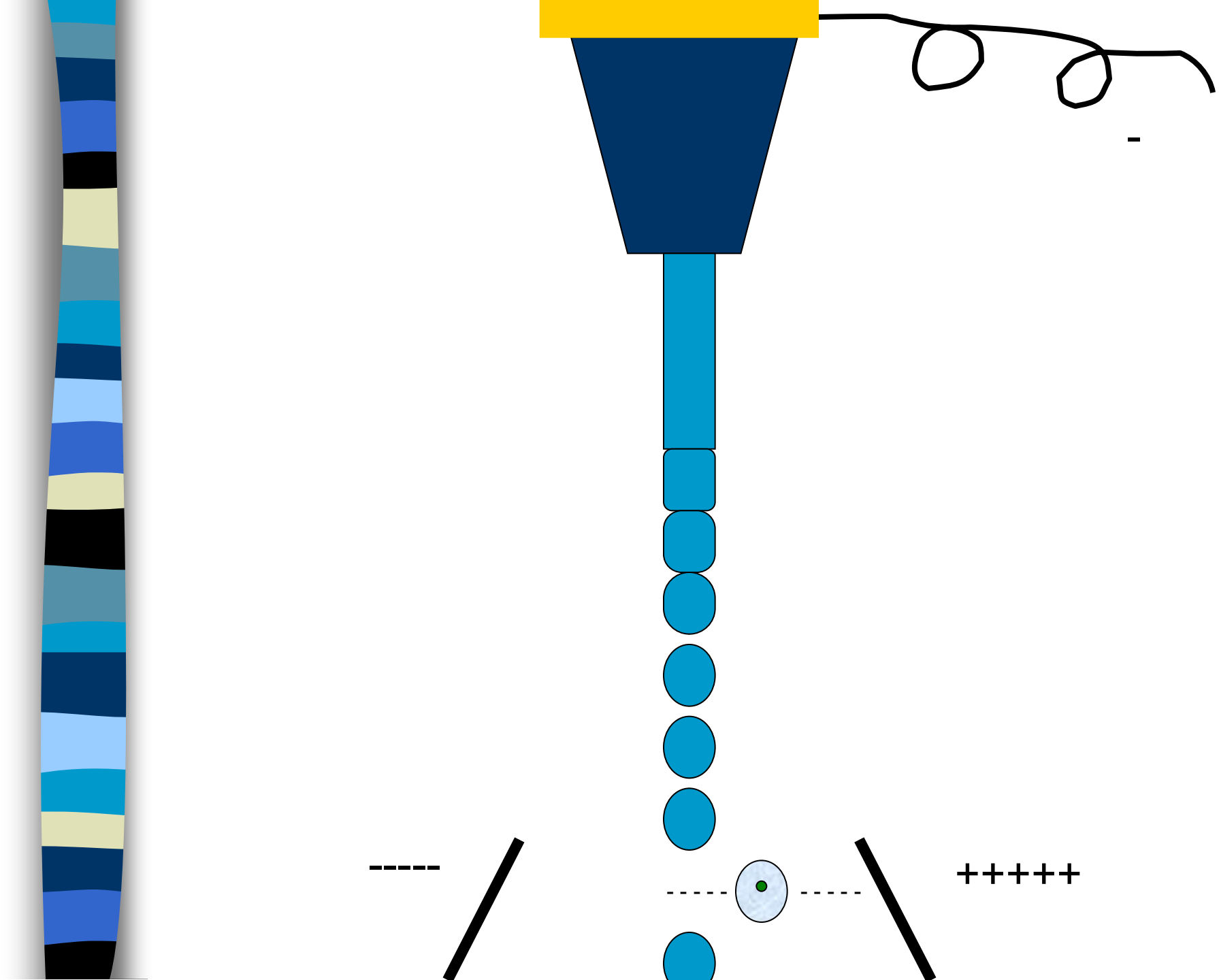

ISAC presents: Mack Fulwyler - Innovator, Inventor & Pioneer

http://www.cyto.purdue.edu/cdroms/cyto10a/seminalcontributions/fulwyler.html

FLUIDIC SWITCH SORTER

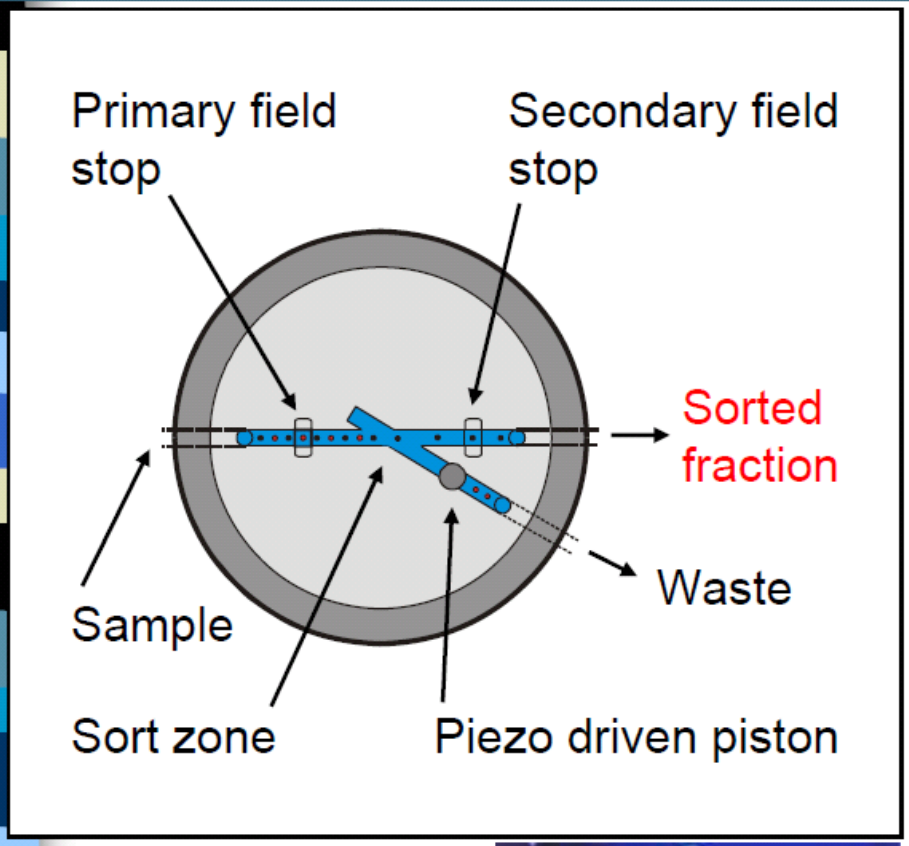

- **Safety (enclosed stream)**
- **Gentle to cells**
- **Sorting of large particles (>100 µm)**

Low speed (~100/sec)

- **Dilute sorted fraction**
- **Noisy**

Used by: Partec

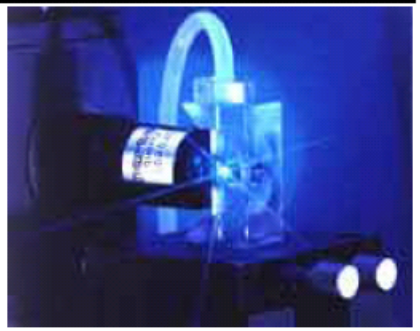

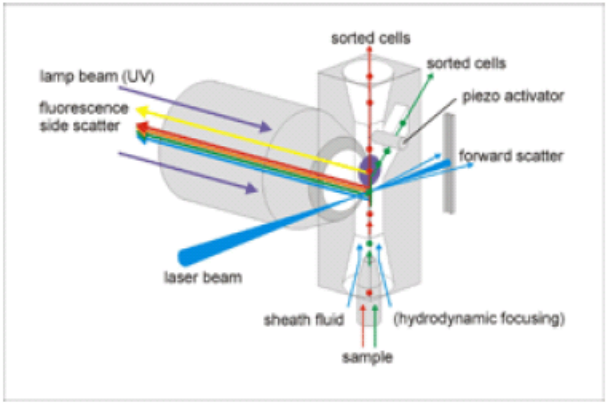

Doležel (1999)

FLUIDIC SWITCH SORTER

- Safety (enclosed stream)
- Gentle to cells

- Low speed (~ 100 / sec)
- Dilute sorted fraction
- Noisy

Used by: Becton Dickinson

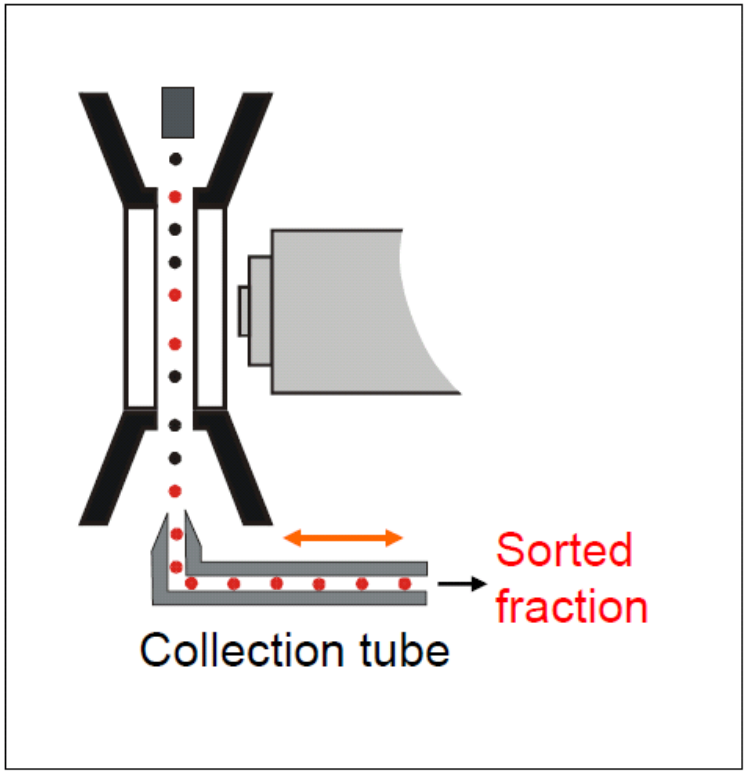

Doležel (1999)

SORTING

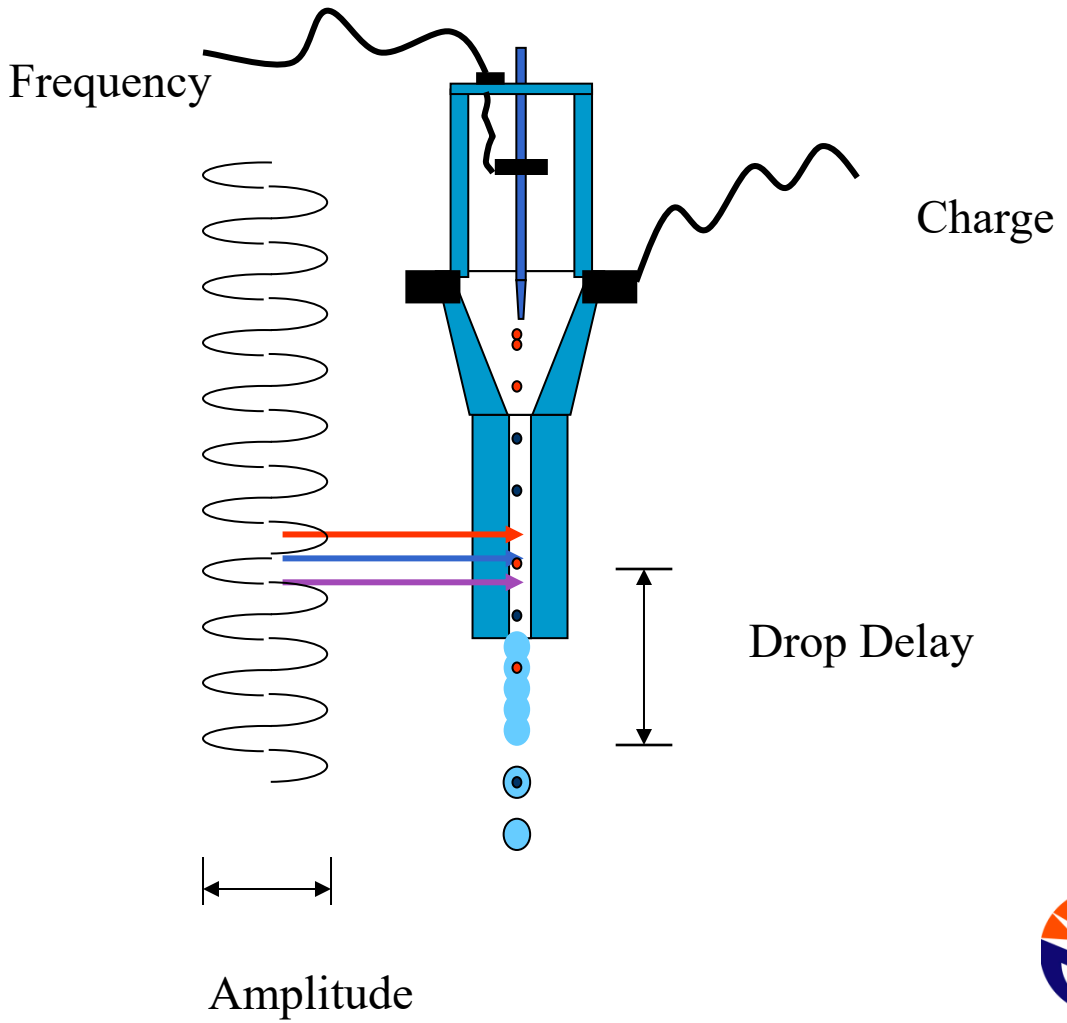

SORTING

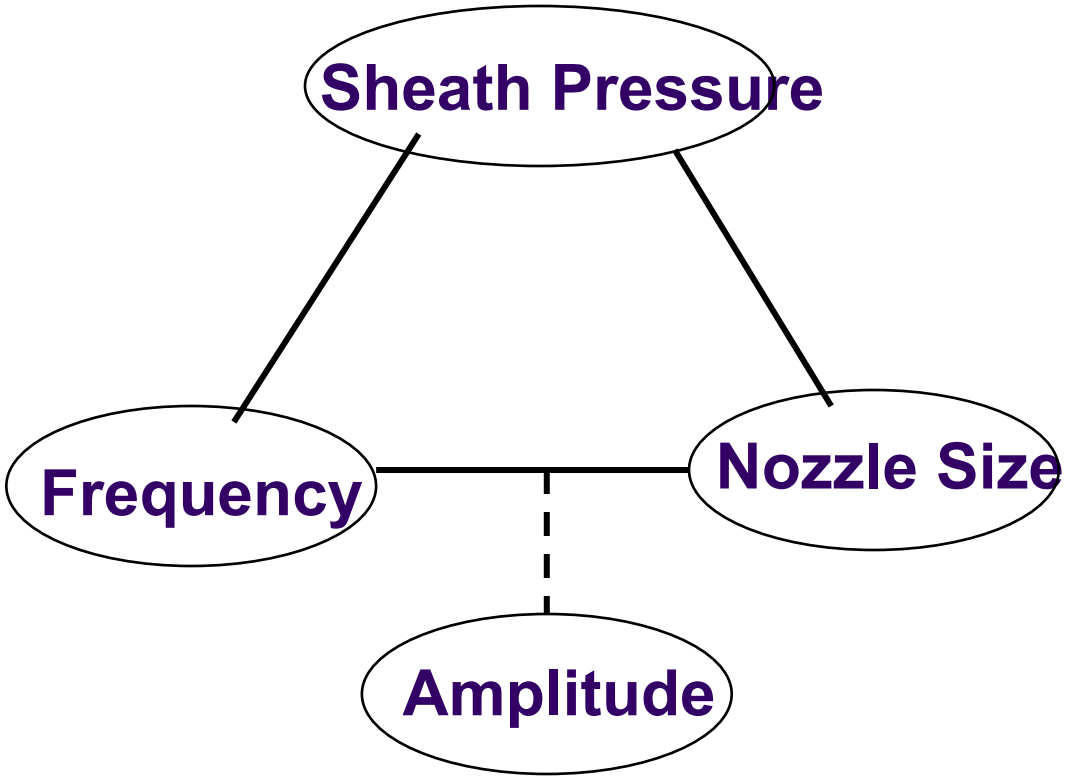

SORTING

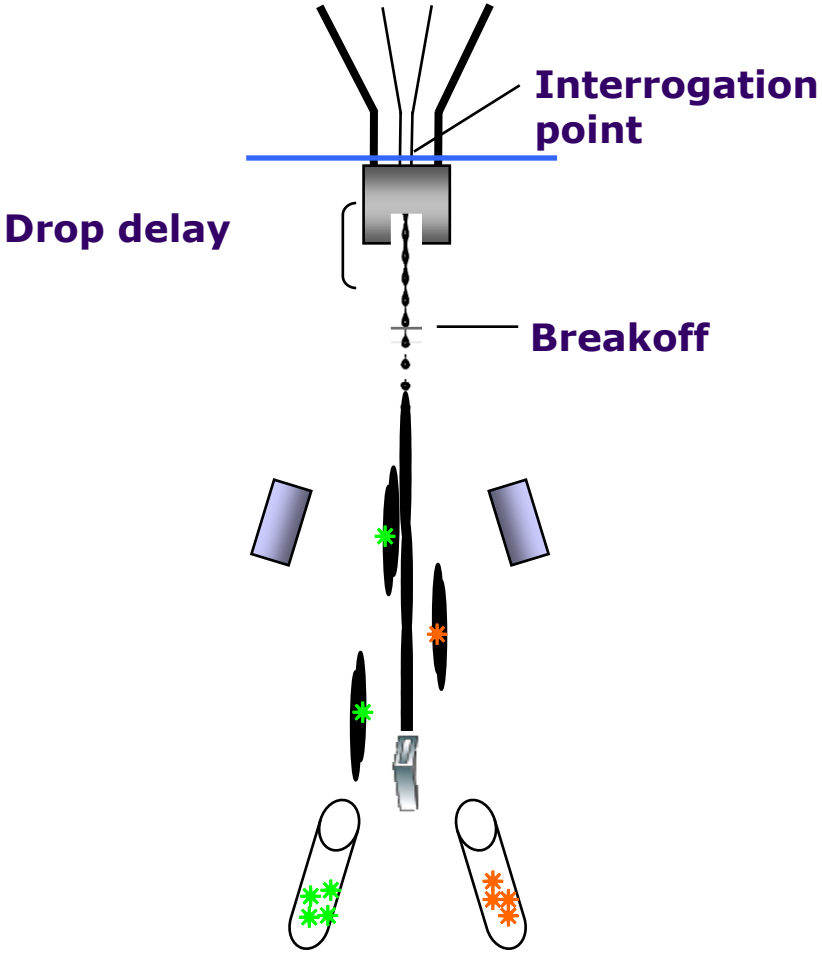

SORTING

Each sort setup includes:

- Sheath pressure
- Breakoff window values
- Side Stream window values

Table 3-2 Default Sort Setup values

Setting	70 micron	85 micron	100 micron	130 micron
Sheath Pressure	70	45	20	10
Amplitude	60	32	12	24
Frequency	87	47	30	12
Drop 1	150	150	150	150
Gap (upper limit)	6 (14)	7 (17)	10 (21)	12 (21)
Attenuation	Off	Off	Off	Off
Drop Delay	47.00	30.00	27.00	16.00
Far left voltage	100	100	80	60

BD

SORTING - Streams

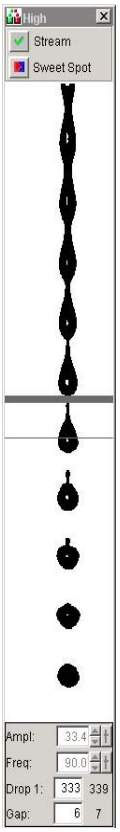

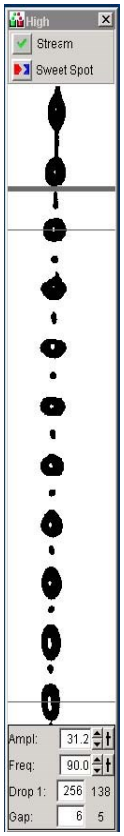

Good

Bad

BD

SORTING – Setup Side Streams

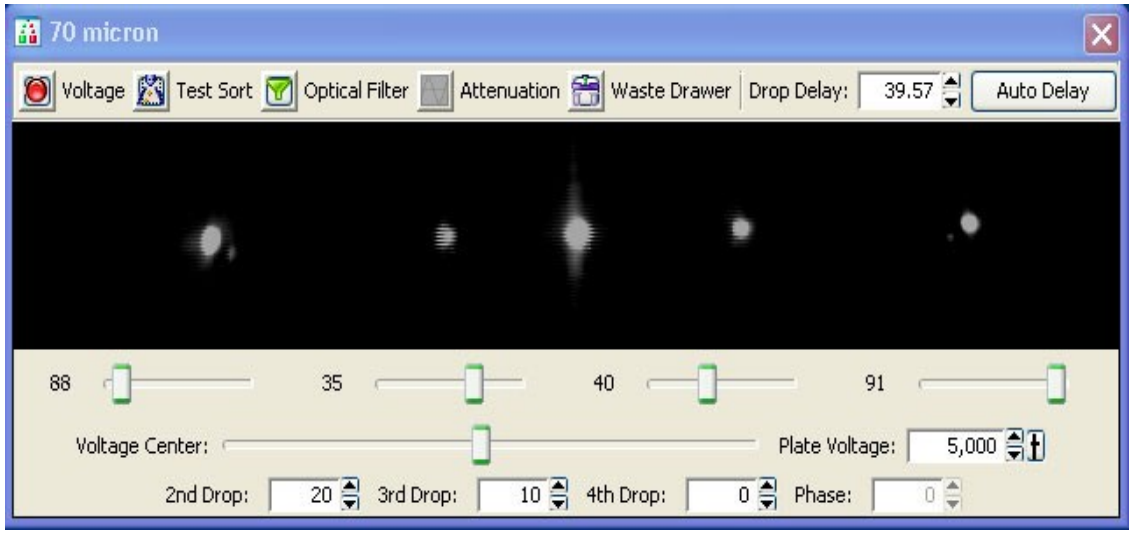

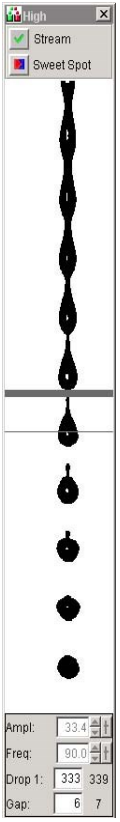

BD

Drop Delay

BD FACS™ Accudrop technology

- Accudrop beads
- Diode laser
- Camera
- Optical filter

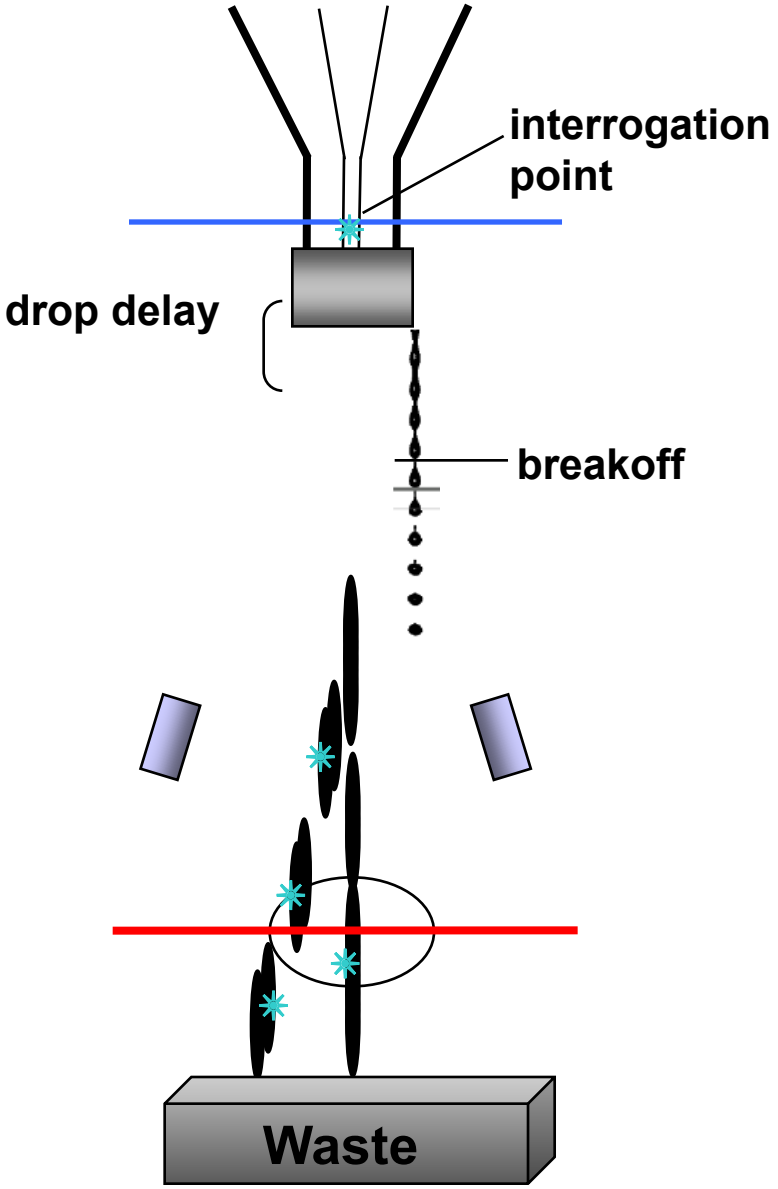

BD

Sorting - Sort Masks

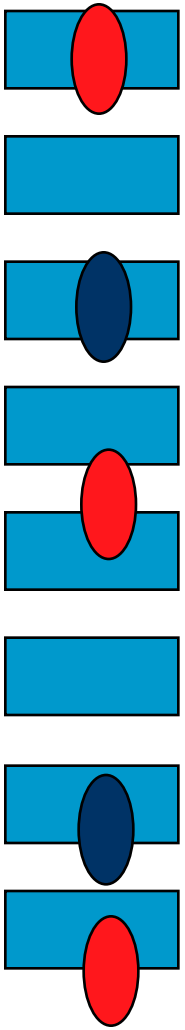

Cells are randomized distributed over the stream

BD

Sorting - Sort Masks

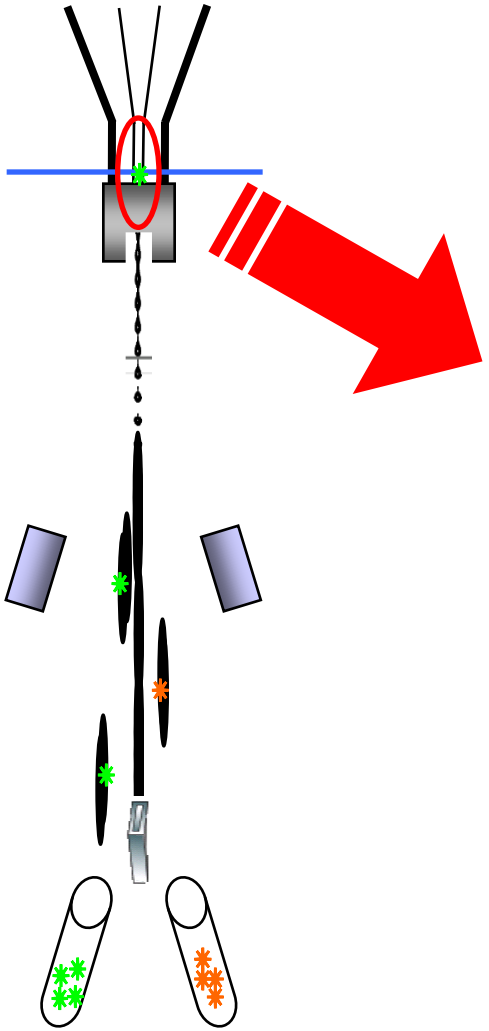

Trailing

Interrogated

Leading

Mask

- A region of the stream monitored for the presence of cells
- Determines how drops will be deflected if a sorting conflict occurs
- Measured in 1/32 drop increments

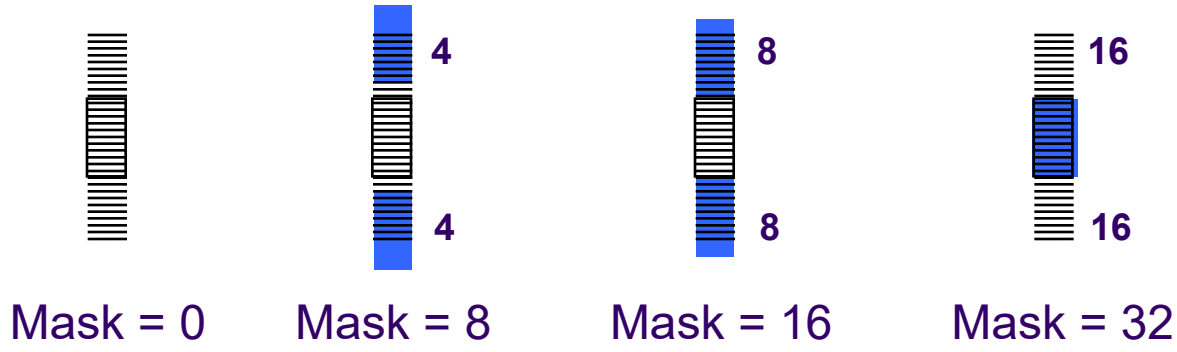

Conflict Resolution

- Precision modes include three types of masks
  - Yield
  - Purity
  - Phase

	Precision Mode				
	Purity	Yield	Single Cell	Initial	Fine Tune
Yield Mask:	32	32	0	32	0
Purity Mask:	32	0	32	0	0
Phase Mask:	0	0	16	0	0
Single Cell:	☐	☐	☒	☐	☐

Sorting - Sort Masks

Sort decisions are determined by sort masks

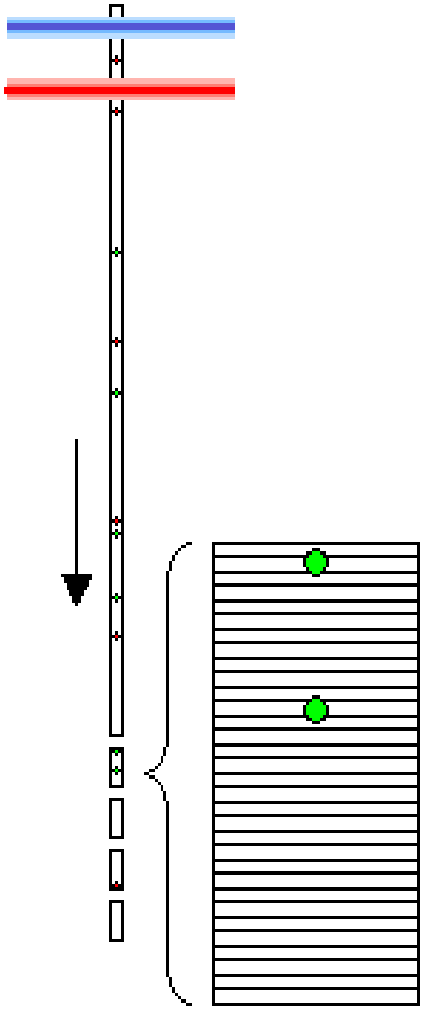

Target particles in a drop with
1/32-drop resolution

Sorting - Yield Mask

The yield mask defines how many drops will be sorted Yield mask of 8/32 indicated in blue; target particle shown in green

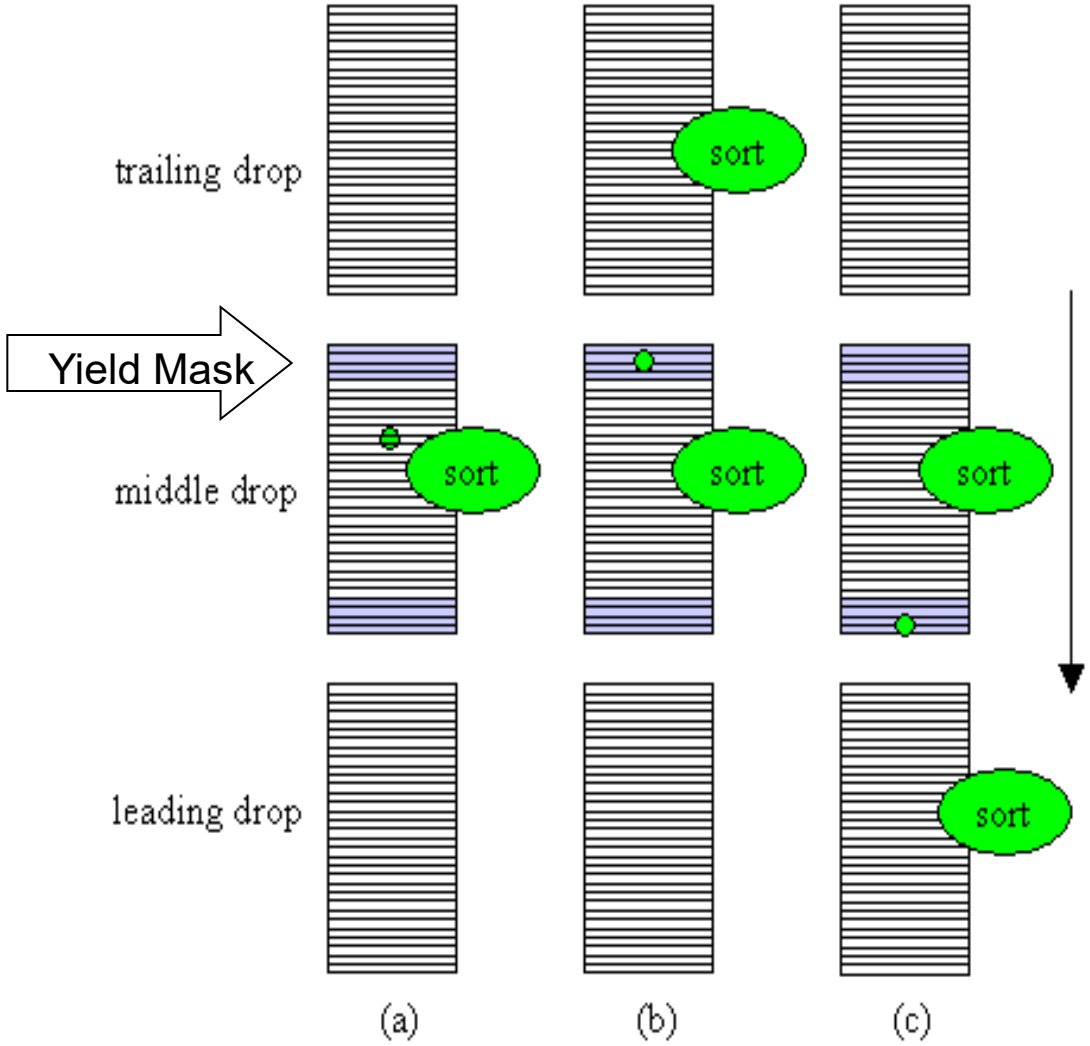

Sorting - Purity Mask

Purity mask of 8/32 in blue, 4/32 in each adjacent drop; target particles in green, non-target particles in red

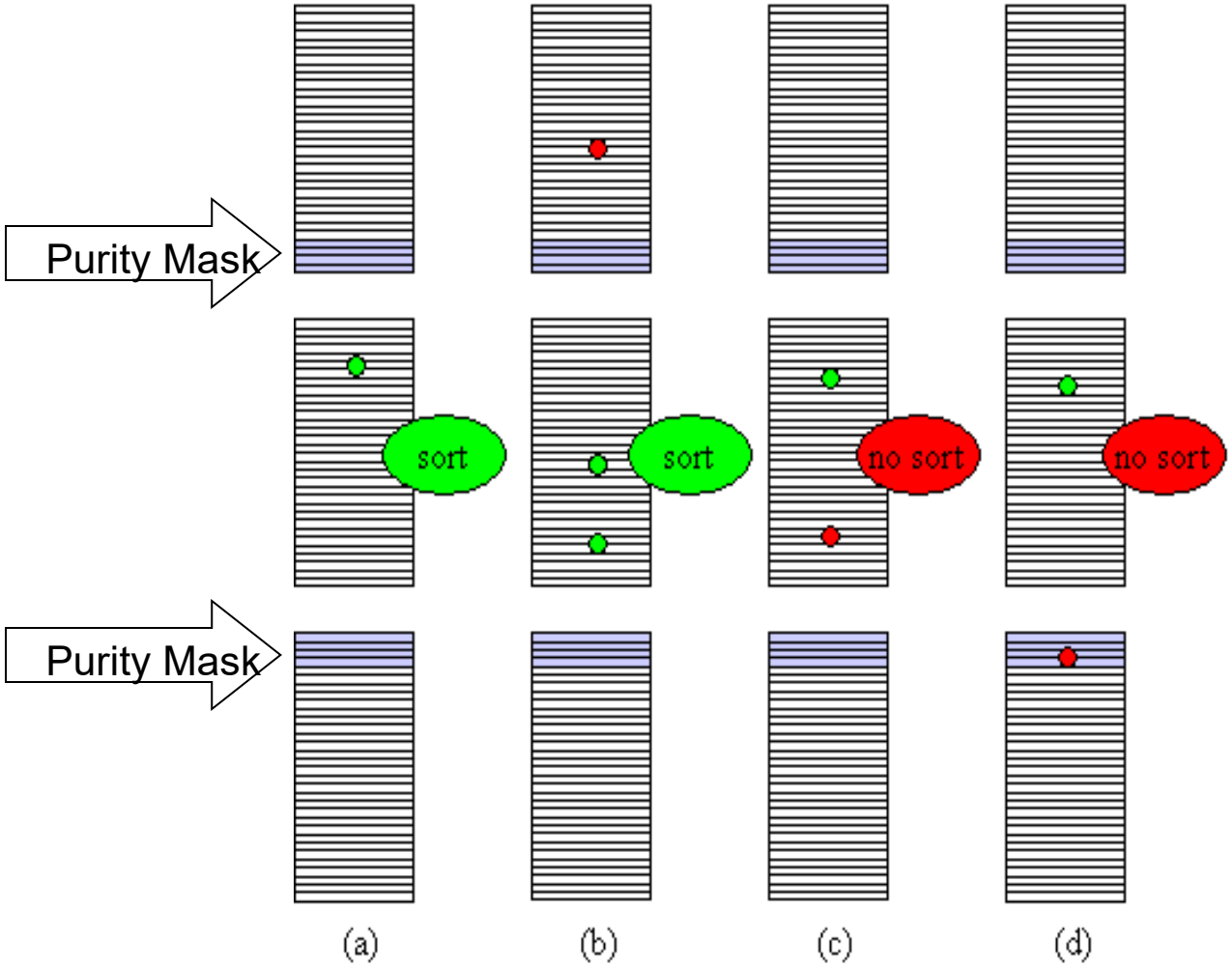

Why Choose the Cytek® Aurora CS?

So Many Colors

40 colors demonstrated including fluorochromes with emission spectra in close proximity to each other.

Exceptional Sensitivity and Resolution

Sensitivity redefined using state-of-the-art optics and low-noise electronics.

Extract autofluorescence and improve resolution of highly autofluorescent samples.

New Levels of Flexibility

No need to reconfigure optical filters for different fluorochromes.

Use any commercially available fluorochrome excited by the onboard lasers.

Choose from a variety of sample input and collection devices including 5 and 15 mL tubes for input and 96-well plates, 1.5 and 5 mL tubes for collection.

Seamless Sorting Experience

Automated drop delay, sort monitoring, and clog detection for a reliable sorting experience.

Comprehensive sort reports automatically record settings used from every sort.

Assay transferability from the Cytek Aurora system or conventional flow cytometers.

Predefined and Custom Sort Modes

Select one of Cytek's predefined sort modes or create a custom defined sort mode to meet the needs of each user's sorting application.

Purity

Isolate the population of interest with little to no contaminants from other populations

Enrich

Prioritize retrieving a high number of the target population with reduced sort purity

Multiway

Intended for 4- or 6-way sorting for efficient drop deflection

Single Cell

Isolate single cells into 96-well plates

Mixed

A combination of Purity and Enrich modes

Custom

Adjust the sort decision settings to meet your application needs

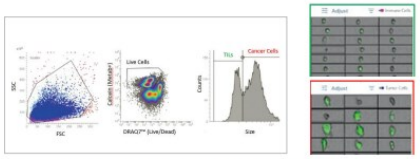

Label-free identification of TILs and cancer cells based on size

Label-free sorting

Minimize sample preparation and sort precious, sensitive and transiently expressing cells using image-enabled FSC, SSC and light loss detectors to enable accurate cell characterization without fluorescent antibody labeling.

Fluorescent localization

Reveal the spatial context of fluorescent signals hidden in flow cytometry. Track the subcellular movement of a protein across organelle boundaries within the cell, such as the NFκB translocation from the cytoplasm to the nucleus.

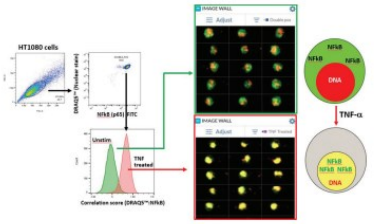

Configurations				
Number of spectral lasers	3	4	4	5
Number of fluorescent detectors	44	56	66	78
Total detectors	52	64	74	86
Lasers				
Ultraviolet laser (349 nm)			●	●
Violet laser (405 nm)	●	●	●	●
Blue laser (488 nm)	●	●	●	●
Yellow-green laser (561 nm)		●		●
Red laser (638 nm)	●	●	●	●

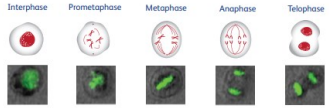

Cell cycle analysis

Flow cytometry methods only rely on a single indicator of DNA content for cell cycle classification, which is incomplete. Image feature analysis can provide insight into DNA distribution information to differentiate the phases of the cell cycle.

Cell-cell interaction

Reveal the spatial context of cells using image feature analysis to identify combinations of engaged cells. Distinguish between two cells that are coincident (passed through the interrogation point in close proximity) and true doublets (cells that are actually touching each other). Further image analysis can reveal receptor accumulation at the site of the cell-cell synapse (active synapse).

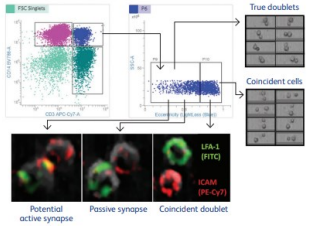

Cell sorting - trendy

- Snadná obsluha
- Šetrná manipulace
  - On-chip technologie
- Velikost ↓ a bezpečnost ↑
- Microfluidic-based cell sorting
- Spectral cell sorting
- Image-based sorting

- Buoyancy Activated Cell Sorting (BACS™)
  - metoda, která používá částice s nízkou hustotou (mikrobubliny) pro flotační separaci.

Elektronika a data

File size considerations

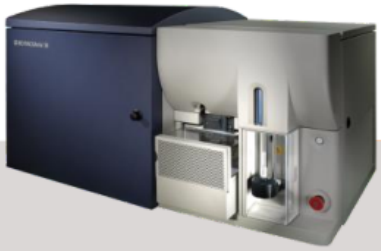

FCS data
- Saved for selected channels only
- H/W optional
- 10,000 events → ~2 MB for an 8-color experiment

Data management is vitally important for spectral and imaging cytometers

FCS data
- Saved for all channels
- A/H/W/TTP always saved
- 10,000 events → ~17 MB for **any** experiment

Image files
- All imaging features saved for selected imaging channels
- Larger cells will generate larger image files
- 10,000 events → ~1.5 GB for a PBMC experimen

Sběr dat

- Data jsou sbírána jako "list" hodnot, pro každý "parametr" a pro každou "event" (buňku)
- každé měření z každého detektoru je označeno jako "parameter"

Flow Cytometry Standard data file format. FCS 3.1
http://www.isac-net.org/images/stories/documents/Standards/fcs3.1_normativespecification_20090813.pdf

Spidlen, J. *et al. Cytometry. Part A : the journal of the International Society for Analytical Cytology* ***77, 97-100, (2010).***

Properties:150717_DU145 Ctrl.fcs

Help

OK

Date:17-JUL-2015
System:Windows XP 5.1
Cytometer:FACSAriaII SORP (FACSAriaII)
File:150717_DU145 Ctrl.fcs
File URI:file:/C:/Users/user/Desktop/install/Infinicyt/150717_DU145%20Ctrl.fcs
---
$BEGINANALYSIS: 0
$BEGINDATA: 4148
$BEGINSTEXT: 0
$BTIM: 13:25:01
$BYTEORD: 4,3,2,1
$CYT: FACSAriaII SORP (FACSAriaII)
$DATATYPE: F
$DATE: 17-JUL-2015
$ENDANALYSIS: 0
$ENDDATA: 6055267
$ENDSTEXT: 0
$ETIM: 13:28:55
$FIL: 150717_DU145 Ctrl.fcs
$INST: IBP
$MODE: L
$NEXTDATA: 0
$OP: fedr
$PAR: 19
$SRC: 150717
$SYS: Windows XP 5.1
$TIMESTEP: 0.01
$TOT: 79620
APPLY COMPENSATION: TRUE
AUTOBS: TRUE
CREATOR: BD FACSDiva Software Version 6.1.3
CST BASELINE DATE: 03_24_2015 12:52:48 PM
CST BEADS LOT ID: 91725
CST SETUP DATE: 03_25_2015 03:01:55 PM
CST SETUP STATUS: SUCCESS WITH WARNING
CYTNUM: P5Y500001
CYTOMETER CONFIG CREATE DATE: 05_13_2013 01:32:45 PM
CYTOMETER CONFIG NAME: RF_85u 45 psi_SORP Aria_5-laser (2uv-6v-3b-5yg-3r)
EXPERIMENT NAME: DU145_POPRO1_LDYellow_AF488_AF594_PE_APCCy7
EXPORT TIME: 17-JUL-2015-14:30:11
EXPORT USER NAME: fedr
FJ_FCS_VERSION: 3
FSC ASF: 0.57
GUID: dc7612a3-65af-4520-bc0f-51d53273ebea
LASER1ASF: 0.86
LASER1DELAY: 0.00
LASER1NAME: Blue
LASER2ASF: 0.86
LASER2DELAY: -38.47
LASER2NAME: Red
LASER3ASF: 1.02
LASER3DELAY: 77.49
LASER3NAME: UV
LASER4ASF: 0.63
LASER4DELAY: 45.00
LASER4NAME: Violet
LASER5ASF: 0.83
LASER5DELAY: -76.49
LASER5NAME: YG
P10BS: 602
P10DISPLAY: LOG
P10MS: 0
P11BS: 38
P11DISPLAY: LOG
P11MS: 0
P12BS: 5
P12DISPLAY: LOG
P12MS: 0
P13BS: 1118
P13DISPLAY: LOG

Compensation Matrix

	Alexa Fluor 594-A	DAPI (405nm)-A	Alexa Fluor 647-A	PE-A	Alexa Fluor 488-A	APC-Cy7-A	Qdot 605-A
Alexa Fluor 594-A	100	0,42	1,53	1,94	0,02	0,32	9,95
DAPI (405nm)-A	1,1	100	0,27	0,05	0,01	0,08	0,96
Alexa Fluor 647-A	2,45	22,87	100	0,1	0,08	15,14	0,85
PE-A	440,67	0	0,14	100	8,03	0,03	32,23
Alexa Fluor 488-A	-0,01	0,09	0,01	0	100	0	0,05
APC-Cy7-A	0,01	0,04	2,67	0	0,05	100	0,01
Qdot 605-A	0	41,05	0	0	2,34	0	100

Parameters and Stains

Parameter ($PnN)	Stain ($PnS)	Range ($PnR)	Bits ($PnB)	Decades ($PnE)	Gain ($PnG)	Voltage ($PnV)	Derived From
FSC-A		262144	32	0,0	1.0	280	
FSC-H		262144	32	0,0	1.0	280	
SSC-A		262144	32	0,0	1.0	210	
Alexa Fluor 594-A		262144	32	0,0	1.0	460	
Alexa Fluor 594-H		262144	32	0,0	1.0	460	
DAPI (405nm)-A		262144	32	0,0	1.0	650	
DAPI (405nm)-H		262144	32	0,0	1.0	650	
DAPI (405nm)-W		262144	32	0,0	1.0	650	
Alexa Fluor 647-A		262144	32	0,0	1.0	538	
Alexa Fluor 647-H		262144	32	0,0	1.0	538	
PE-A		262144	32	0,0	1.0	330	
PE-H		262144	32	0,0	1.0	330	
Alexa Fluor 488-A		262144	32	0,0	1.0	366	
Alexa Fluor 488-H		262144	32	0,0	1.0	366	
APC-Cy7-A		262144	32	0,0	1.0	700	
APC-Cy7-H		262144	32	0,0	1.0	700	
Qdot 605-A		262144	32	0,0	1.0	410	
Qdot 605-H		262144	32	0,0	1.0	410	
Time		262144	32	0,0	0.01		
Comp-Alexa Fluor 594-A		262144					
Comp-DAPI (405nm)-A		262144					
Comp-Alexa Fluor 647-A		262144					
Comp-PE-A		262144					
Comp-Alexa Fluor 488-A		262144					
Comp-APC-Cy7-A		262144					
Comp-Qdot 605-A		262144					

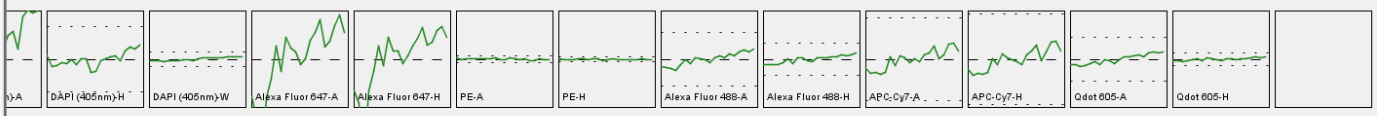

Data Acquisition - Listmode

Event	*Param1 FS*	*Param2 SS*	*Param3 FITC*	*Param4 PE*
1	50	100	80	90
2	55	110	150	95
3	110	60	80	30

Creation of a Voltage Pulse

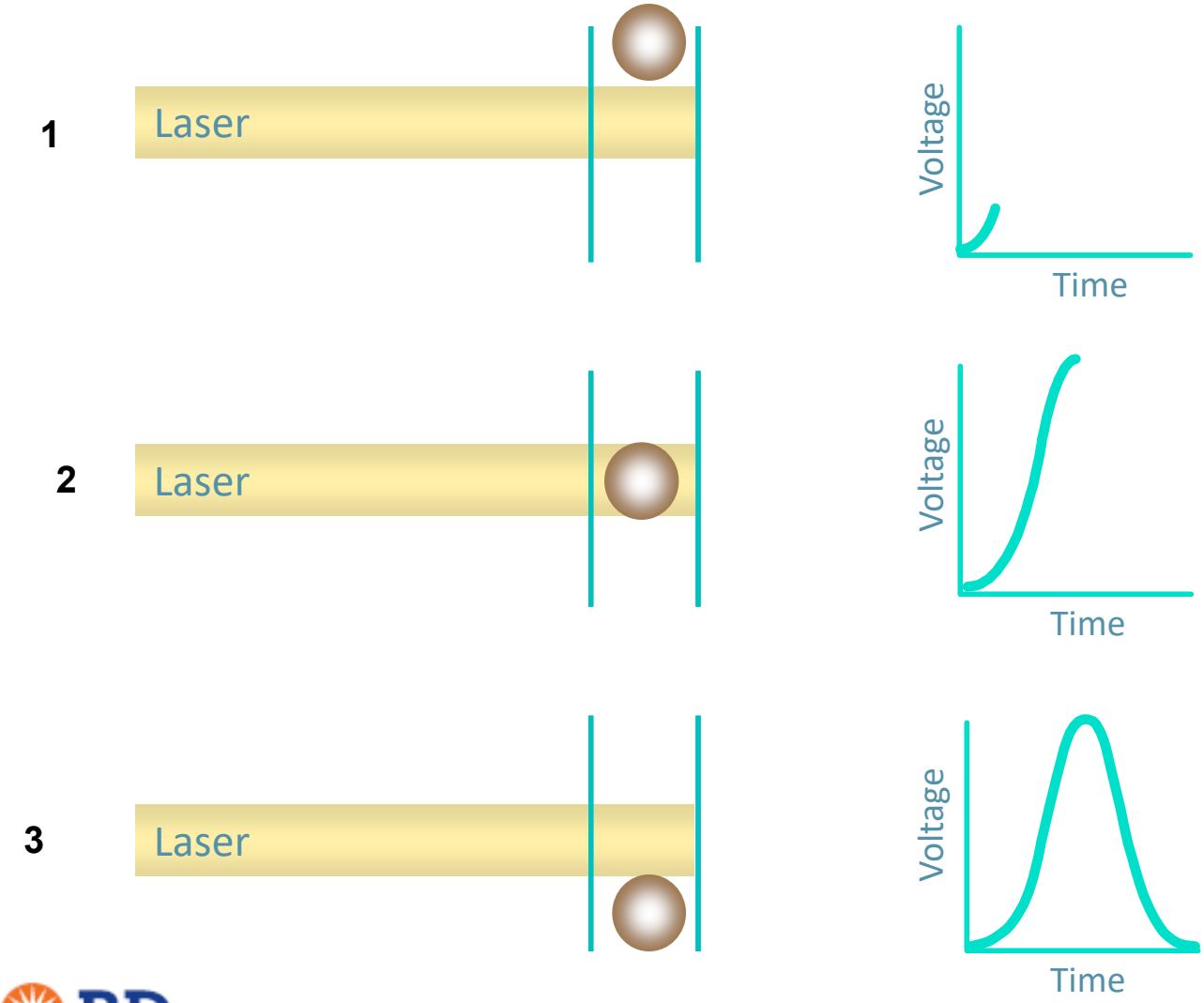

BD

Height, Area, and Width

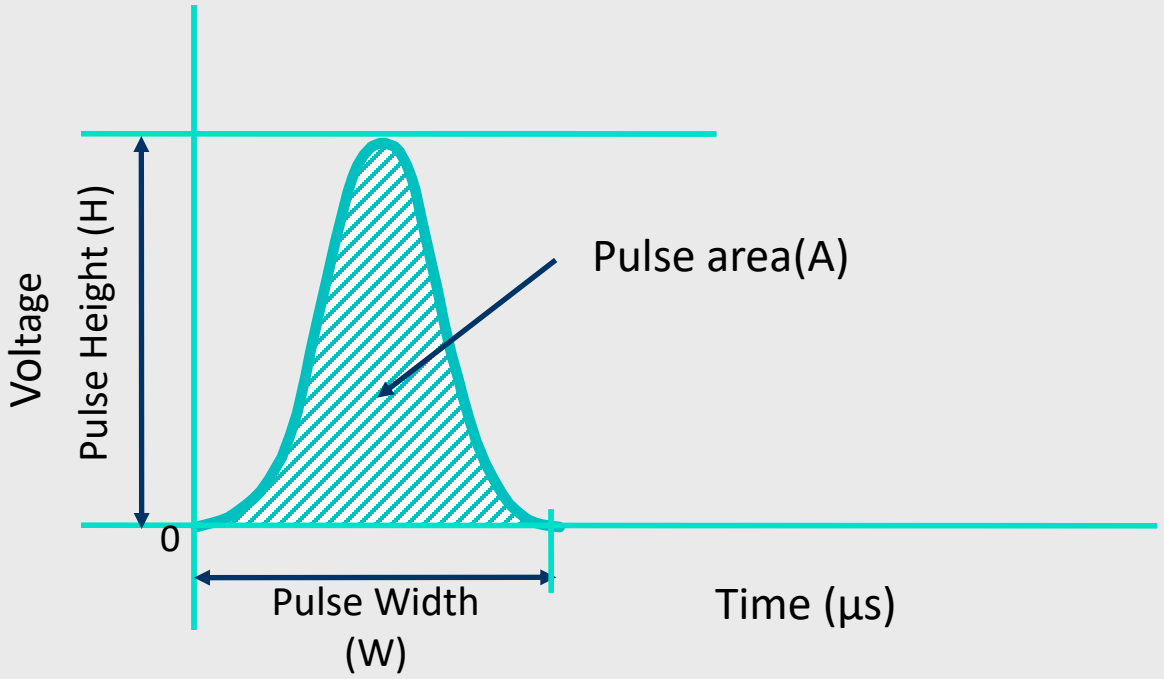

Signal processing

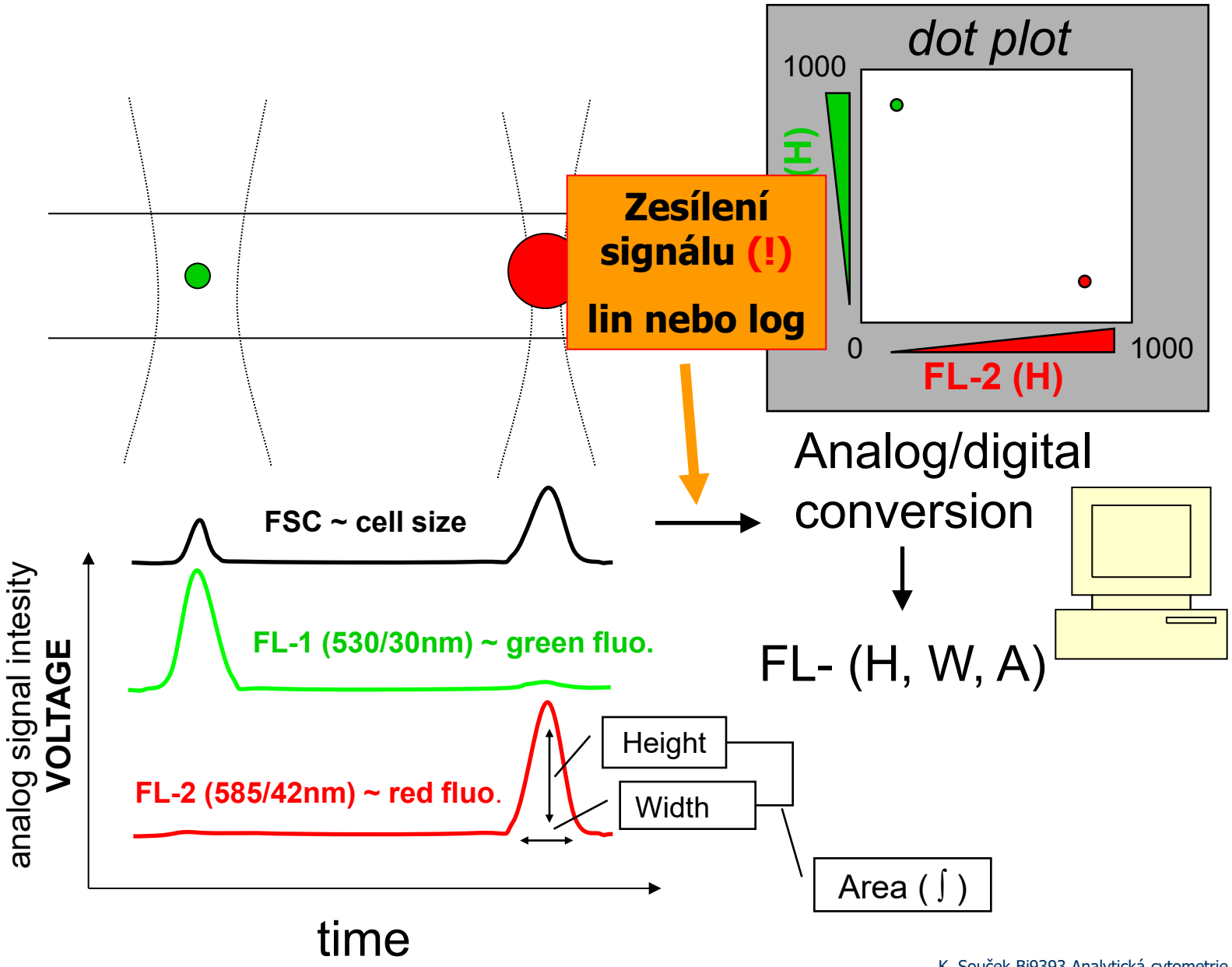

Analog to Digital Converter

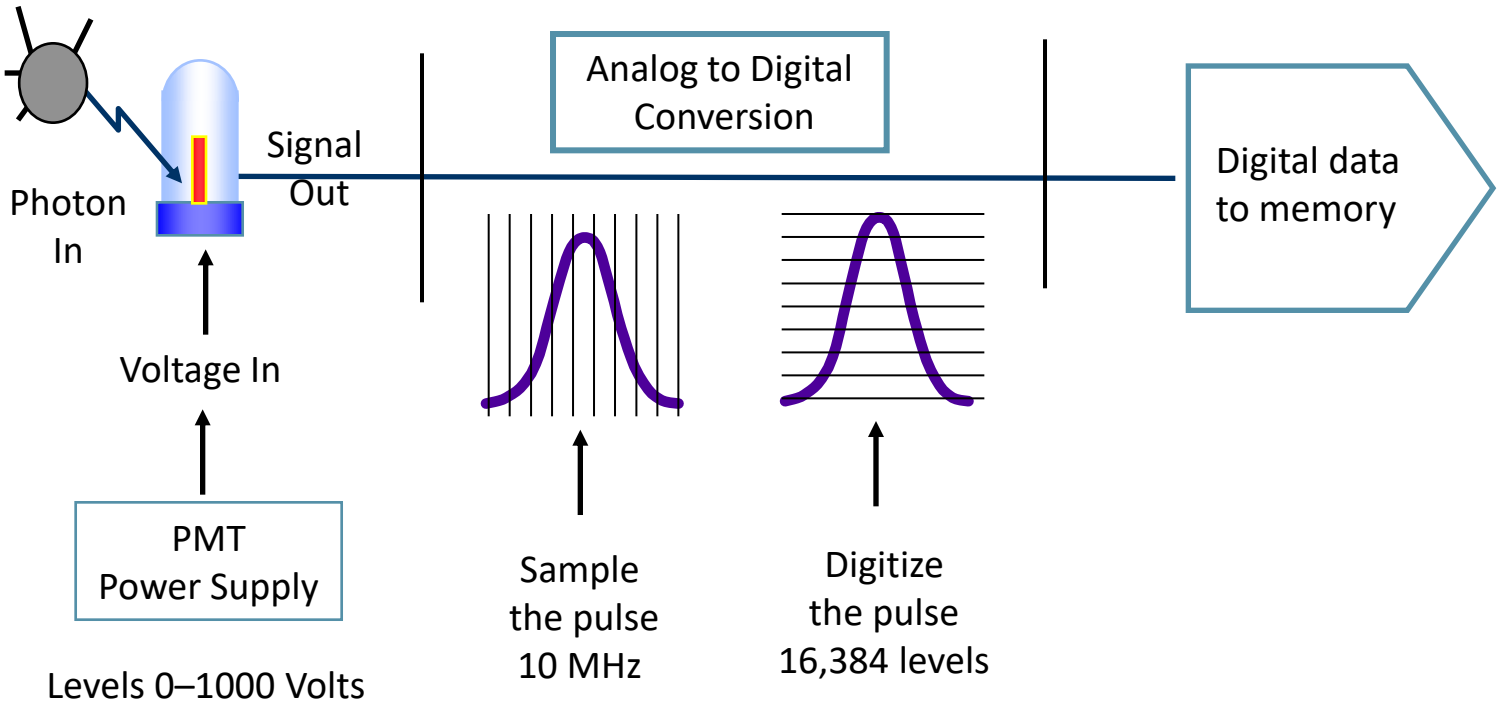

Parameters

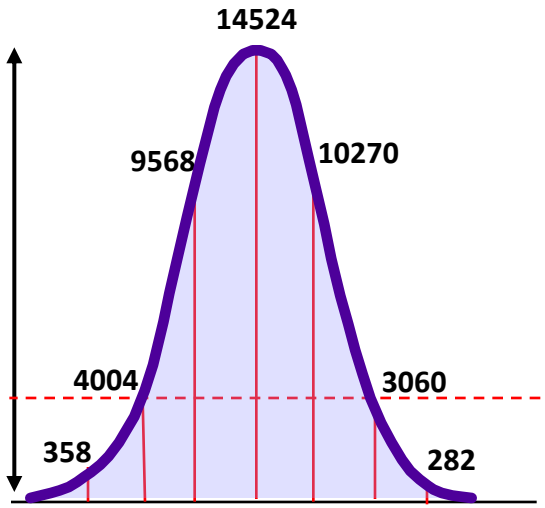

- Area: Sum of all height values
- Height: Maximum digitized value
  X 16
- Width: Area/Height X 64K

Data is displayed on 262,144 scale

$2^8 = 256$
$2^{10} = 1024$
.
.
.

AD převodníky

Počet bitů	# kanálů	rozlišení
8	256	39.1 mV
10	**1024**	**9.77 mV**
12	4096	2.44 mV
14	16384	610 μV
16	65536	153 μV
18	**262144**	**38.1 μV**
20	1048576	9.54 μV
22	4194304	2.38 μV
24	16777216	596 nV

Full scale measurement range = 0 to 10 volts
ADC resolution is 12 bits: 212 = 4096 quantization levels
ADC voltage resolution is: (10-0)/4096 = 0.00244 volts = 2.44 mV

Logaritmické zesílení & dynamický rozsah

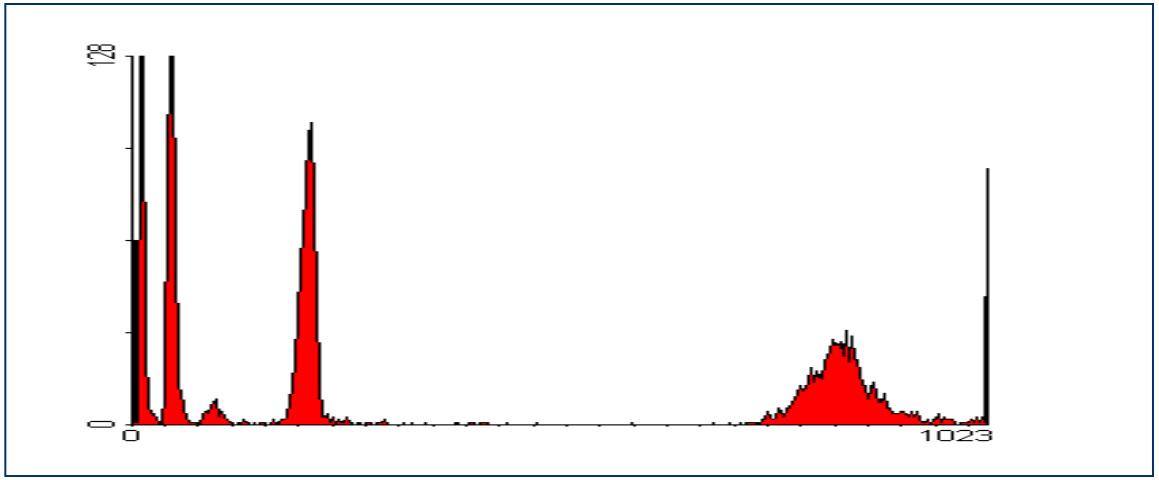

lin

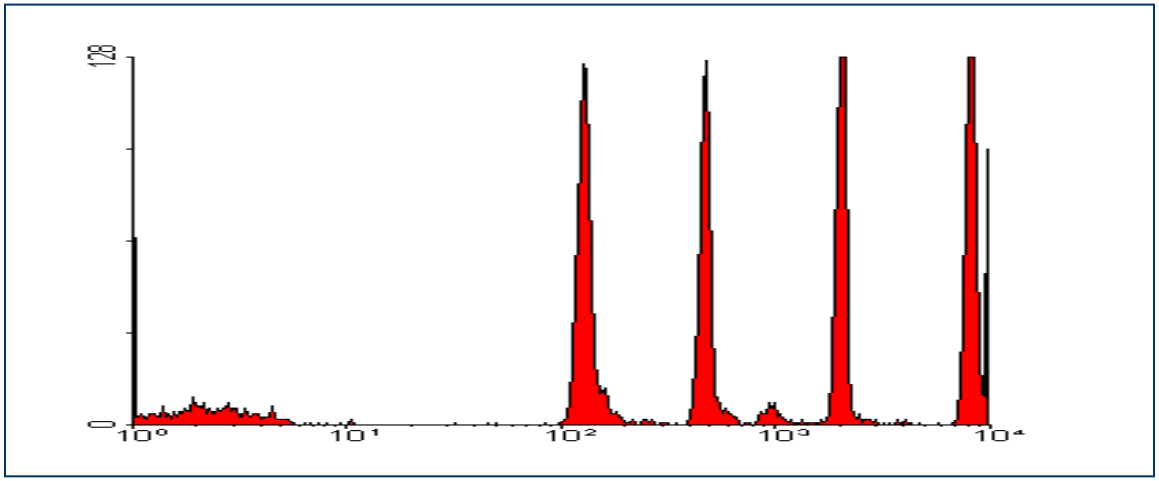

log

upraveno podle J.P.Robinson

Charakteristiky pulsu

- Pulsy detekované na průtokovém cytometru jsou analogové jevy detekované pomocí analogových zařízení
- Tyto pulsy trvají několik mikrosekund
- Pokud nemůžeme digitalizovat tento puls v reálném čase musíme kombinovat analog-digitalní zpracování pulsu
- běžně trvalo několik mikrosekund digitalizovat puls – to nebylo dostatečně průchodné pro vysokorychlostní sběr dat
- Nové – plně digitální systémy mohou digitalizovat puls přímo pomocí MHz frekvence

Analýza dat

- Zobrazení dat
  - histogram
  - dot plot
  - isometric display
  - contour plot
  - chromatic (color) plots
  - 3 D projection
- Gating

Způsoby pro zobrazení dat

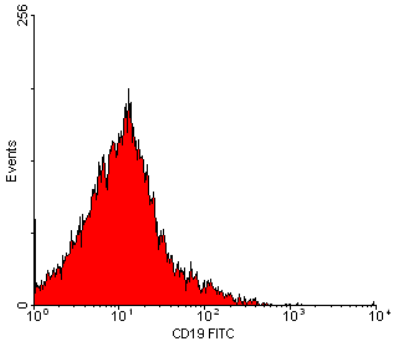

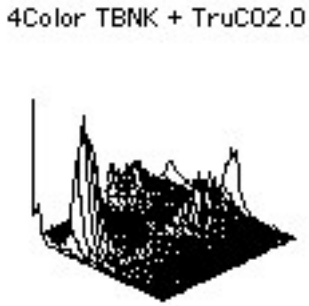

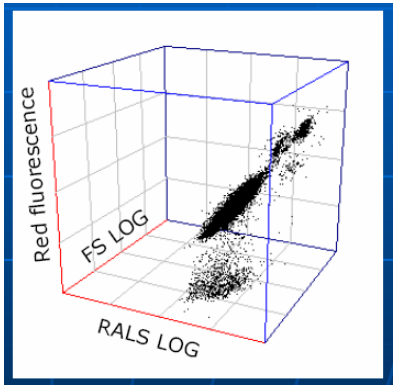

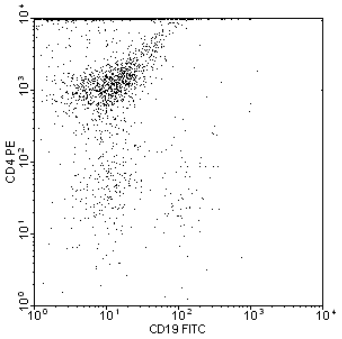

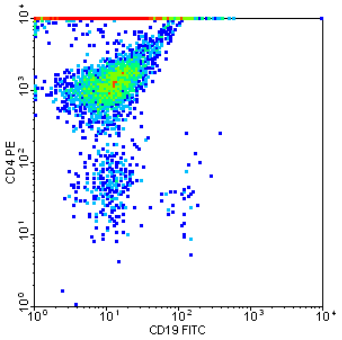

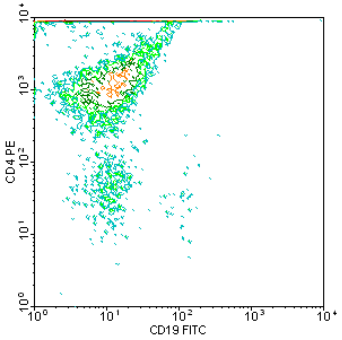

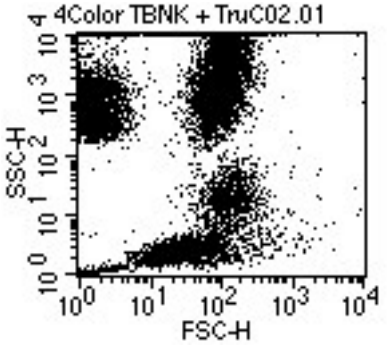

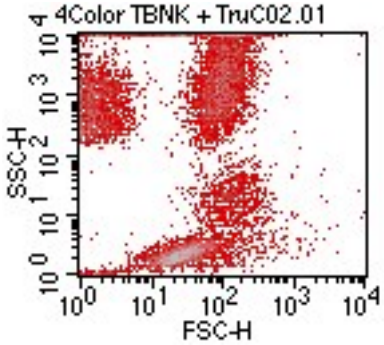

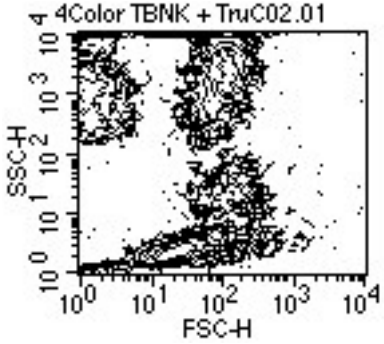

Shrnutí

- Světlo, fluorescence
- Optické systémy
- Fluidní systémy
- Sorting
- Signál, data – základní princip

Na konci dnešní přednášky byste měli:

1. znát základní principy rozptylu světla a
2. fluorescence;
3. vědět jaké zdroje světla se využívají v průtokové cytometrii;
4. a jakým způsobem je detekováno;
5. znát základní principy fluidních systémů a laminárního proudění.
6. Znát základní princip zpracování a vizualizace dat